UNIVERSITY OF
LIVERPOOL

Characterisation of the Metastasis-Inducible Calcium-binding S100P protein on cell activity

Thesis submitted in accordance with the requirements of the University of Liverpool for the degree of Doctor in Philosophy

by

Valéry Kossi Wodadje ATTIGNON

December 2010

I must thank first and foremost my supervisors Roger Barraclough and Philip Rudland for all their guidance and inspiration throughout my studies.

Many thanks to all my colleagues for their company, useful discussions and delicious cakes.

Table of Contents

S100P is a member of the S100 family of small regulatory calcium-binding proteins, which has been shown to play a role in the metastatic phase of cancer. Intracellular overexpression of S100P under physiological conditions has been correlated to metastasis and poor overall survival in breast cancer patients. The mechanism of the Metastasis-Inducing Calcium-binding protein, S100P in metastasis has not yet been fully elucidated.

Investigation of the role of metastatic S100P was divided into three parts, investigating the effects of intracellular S100P on cell activity such as cell motility, the expressions of other genes, and the effect of extracellular S100P on intracellular signalling processes. Several analyses such as motility assays, gene expression using microarrays, quantitative real-time PCR and SiRNA, changes in intracellular signalling induced by addition of extracellular S100P have been performed. These experiments were carried out using an expression system developed in our laboratory consisting of a human S100P cDNA inserted in a tetracycline-inducible vector transfected into non-metastatic benign rat mammary tumour-derived cells (Rama 37), and human cervical carcinoma cells (HeLa).

Results observed after microarray hybridisation showed 5 upregulated genes and 3 downregulated genes, after intracellular overexpression of S100P in rat mammary tumour cells. Further analysis on upregulated gene knock-down using SiRNA on one selected up-regulated gene, the microtubule associated serine/threonine kinase 1 (Mast1) helped defining S100P's role on gene expression. Extracellular addition of S100P has been shown to increase cell motility suggesting alternative cell motility stimulation via a cell surface receptor. Extracellular S100P has been shown to activate intracellular phosphorylation of a member of Serine/Threonine-specific protein kinase family: Akt and Extracellular signal-Regulated Kinases: Erk 1/2 through the Receptor for Advanced Glycosylation End-Product (RAGE).

Results enabled the Metastasis-Inducing Calcium-binding protein mechanisms to become clearer so that S100P could represent a potential target for novel diagnostic and therapeutic applications.

List of Figures

List of Tables

µg - Micrograms

µg/mL - Micrograms per millilitre

µL - Microlitre

µM - Micromolar

µm - Micrometre

APS - Ammonium persulfate

BSA - Bovine serum albumin

cDNA - Complementary DNA

CO_2 - Carbon dioxide

DMSO - Dimethyl sulfoxide

ECL - Enhanced chemiluminescence

ERK1/2 - Extracellular signal-regulated kinases 1/2

FBS - Foetal bovine serum

FCS - Foetal calf serum

FDR - False discovery rate

g - Grams

h - Hour

HRP - Horseradish peroxidase

kDa - Kilodalton

M - Molar

MAPK - Mitogen-activated protein kinase

min - Minute

mg - Milligrams

mg/mL - Milligrams per litre

µg/mL - Micrograms per litre

mL - Millitre

mm - Millimetre

mM - Millimolar

NaOH - Sodium hydroxide

nm - Nanometre

nM - Nanomolar

PBS – Phosphate-buffered saline

PDZ - Post synaptic density protein (PSD95), Drosophila disc large tumour suppressor (DlgA), zonula occludens-1 protein (zo-1)

PI3K - Phosphoinositide 3-kinases

PTEN - Phosphatase and tensin homolog

RAGE - Receptor for advanced glycation endproduct

rpm - Revolutions per minute

SEM - Standard error of means

SDS - Sodium dodecyl sulphate

SDS - PAGE - sodium dodecyl sulphate polyacrylamide gel electrophoresis

TBE - Tris borate EDTA

TBST- Tris-buffered saline Tween-20

TEMED - N,N,N',N'-tetramethylethylenediamine

Chapter 1

INTRODUCTION

1.1. S100 protein family

1.1.1. History

S100 proteins are small, acidic proteins (9–14 kDa) found exclusively in vertebrates (Schafer and Heizmann, 1996). The first member was identified in 1965 by Moore who identified a subcellular fraction from bovine brain "S100" named because the constituents were soluble in 100% saturated ammonium sulphate at neutral pH (Moore, 1965). With at least 25 members found to date in humans, the S100 proteins constitute the largest subfamily of the EF-hand proteins (Table 1.1). Of these, 21 family members (S100A1-S100A18, trichohylin, filaggrin and repetin) have genes clustered at chromosome locus 1q21, while other S100 proteins are found at chromosome loci 4p16 (S100P), 5q14 (S100Z), 21q22 (S100B) and Xp22 (S100G).

1.1.2. Structure

S100 proteins show 25-65% identity to one another at the amino acid sequence level and contain two distinct helix-loop-helix calcium-binding motifs known as EF-hand, flanked by conserved hydrophobic residues and separated by a linker region. The sequences of the linker region and the C-terminal extension are the most variable parts of the S100 protein sequences from one S100 protein to another (Schafer and Heizmann, 1996). All S100 proteins, with the exception of S100G (calbindin D9k), are organised as tight symmetric, antiparallel homodimers or heterodimers, with the non-covalent interface between the two monomers being formed mostly by hydrophobic amino acid residues (Heizmann et al., 2002). Each monomer is composed of a classic EF-hand near the C terminus, common to all EF-hand proteins, and a pseudo EF-hand, near the *N*-terminus that has been found exclusively in S100 and S100-like proteins (Donato, 2001; Santamaria-Kisiel et al., 2006; Zhou et al., 2006) (Figure 1.1).

Approved gene Symbol (gene name)	Synonyms	Gene location
S100A1	S100αα	1q21
S100A2	CaN19, S100L	1q21
S100A3	S100E	1q21
S100A4	CAPL, p9Ka, 42A, pL98, mts1, metastasin, calvasculin, 18A2, murine placental calcium protein, fibroblast-specific protein (fsp)	1q21
S100A5	S100D	1q21
S100A6	CACY, 2A9, PRA, CaBP 5B10, calcyclin, Siah-1-interacting protein (SIP)	1q21
S100A7 (isoform a-c)	psoriasin, PSOR1, BDA111, CAAF2	1q21
S100A7A	S100A15, S100A7L1, NICE-2, S100A7f	1q21
S100A7L2 (S100A7-like2)	S100A7b	1q21
S100A7L3 (S100A7-like3)	S100A7P1 (S100A7-pseudogene 2), S100A7d	1q21
S100A7L4 (S100A7-like4)	S100A7P2, S100A7e	1q21
S100A8	MRP-8, p9, calgranulin A (CAGA); CP-10 (murine), L1 light chain, CGLA	1q21
S100A9	MRP-14, p14, calgranulin B(CAGB), L1 heavy chain, BEE22, CGLB	1q21
S100A10	CAL12, CLP11, P11, p10, 42C, calpactin light chain, annexin II ligand, calpactin I, light polypeptide, ANX2LG, CAL1L, GP11	1q21
S100A11	calgrizzin, S100C, MLN70 (metastatic lymph node gene 70 protein), protein S100-C	1q21
S100A12	CaBP in Amniotic fluid-1 (CAFF1), P6, calgranulin C (CAGC), calgranulin-related protein (CGRP), MRP-6, CaBPcornea-associated antigen (COAg); extracellular newly identified RAGE-binding protein (EN-RAGE), neutrophil S100 protein	1q21
S100A13		1q21
S100A14	S100A11P, S100A11 pseudo gene, BCMP84, S100A15,S114; breast cancer membrane protein 84	1q21

Approved gene Symbol (gene name)	Synonyms	Gene location
S100A16	aging-associated gene 13 protein (AAG13), DT1P1A7, MGC17528, S100F	1q21
S100A17	trichohyalin-like 1 protein, (CHHL1), THHL1; S100A17; basalin; TCHHL1	1q21
S100B	S100β	21q22
S100P		4p16
S100Z		5q14
Repetin		1q21
S100G	Calbindin 3 (CALB3); calbindin D9K (CABP9K)	Xp22

***Table 1.1* S100 Family nomenclature and synonyms**

The EF hand is a helix-loop-helix structural domain, first described by Kretsinger and Nockolds (Kretsinger and Nockolds, 1973) found in a large family of calcium-binding proteins consisting of an alpha-helix (E), loop and a second alpha-helix (F). The majority of S100 proteins have two distinct EF-hands that bind Ca^{2+} ions with different affinities (Baudier et al., 1984; Strynadka and James, 1989). The pseudo EF-hand found between the helix 1 and helix 2 in the N-terminal region has a lesser affinity than the canonical EF-hand found in the C-terminal region between helix 3 and helix 4. Most S100 proteins undergo a large conformational change upon Ca^{2+} binding to the canonical EF-hand and this exposes a large hydrophobic pocket which was first seen in early studies of S100A and S100B (Baudier and Gerard, 1983). Calcium binding to the pseudo EF-hand does not cause any conformational changes in helices 1 and 2. During the significant conformational change, Ca^{2+} binds the canonical EF hand, reorienting helix 3 from almost parallel with helix 4 in the apo form to almost perpendicular (~90° reorientation). This change in helix 3 instead of helix 4 is a unique characteristic of S100 proteins compared to other EF-hand proteins. S100B has an almost 90° reorientation of helix 3, while other S100 proteins such as S100A4 have a less drastic effect (~60°) and S100P experiences no change at all (Lee et al., 2004; Malashkevich et al., 2008; Zhang et al., 2003).

1.1.3. Functions

S100 proteins are expressed in a tissue and cell-specific fashion (Donato, 2001), mostly detected in the cytoplasm and in some cases in the nucleus of normal cells. For example, S100A1 and S100A2 are found in the cytoplasm and nucleus, respectively of smooth-muscle cells (Mandinova et al., 1998), whereas S100P is located in the cytoplasm of placental tissue (Becker et al., 1992; Emoto et al., 1992). It is thought that S100 proteins predominantly serve as a calcium trigger or sensor proteins that, upon calcium dependent activation, regulate the function and/or subcellular distribution of certain target proteins and peptides (Donato, 2003; Ravasi et al., 2004; Santamaria-Kisiel et al., 2006).

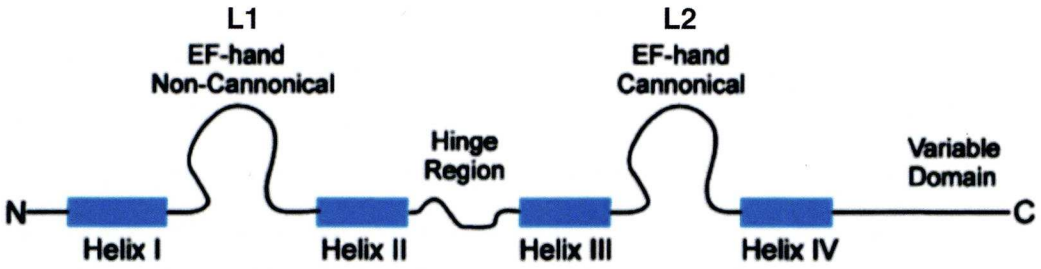

***Figure 1.1* Schematic representation of the secondary structure of a S100 protein.**

Each Ca^{2+}-binding loop (L1 and L2, in the N- and the C-terminal half, respectively) is flanked by α-helices (helices I and II, and helices III and IV for L1 and L2, respectively). A linker region (hinge region) connects helix II–III. Helix IV is followed by a C-terminal extension. The hinge region and the C-terminal variable domain extension display the least amount of sequence similarity between family members (Donato, 1999; Kligman and Hilt, 1988; Schafer and Heizmann, 1996).

When they are present extracellularly, some members of the S100 protein family can act as leukocyte chemoattractants, macrophage activators and modulators of cell proliferation in cultured cells (Cornish et al., 1996; Devery et al., 1994; Hiratsuka et al., 2006; Lau et al., 1995; Yen et al., 1997). Extracellular functions have been mainly described via a multiligand cell surface receptor for advanced glycation end-products (RAGE), a member of the immunoglobulin superfamily of cell surface molecules, which is expressed on leukocytes and endothelial cells and has been to shown to be a receptor for S100A1, S100B (Huttunen et al., 2000), S100A8, S100A9 (Ehlermann et al., 2006), S100A12 (Hofmann et al., 1999), and S100P (Arumugam et al., 2004), and activating downstream signalling pathways. Intracellular functions include regulation of protein phosphorylation and enzyme activity, calcium homeostasis, regulation of cytoskeletal components (Fano et al., 1989; Kriajevska et al., 1998; Sorci et al., 2000) and regulation of transcription factors (Baudier et al., 1995). A number of members of the S100 family have also been shown to play a role in modulating proliferation, some, like S100A1, have been shown to inhibit cell proliferation (Zimmer et al., 1998). Most of the S100 family members have a role in modulating cytoskeletal dynamics, exhibiting direct interaction with tubulins, intermediate filaments, actin, myosin and tropomyosin (Davies et al., 1993; Santamaria-Kisiel et al., 2006). These processes have been implicated in mediating metastasis (Davies et al., 1993; Donato, 2003; Kriajevska et al., 1998) and are implicated in actin polymerisation and the subsequent formation of membrane protrusions that are required for chemotaxis. Remodelling of the actin cytoskeleton is indeed important for motility and chemotaxis of cancer cells, which in turn influence the metastatic capability of these cells. These functions could implicate S100 proteins in a variety of pathologies and gradually their role in carcinogenesis is beginning to be unravelled. It is clear that some S100 proteins may act as tumour promoters and others may act as tumour suppressors, and there is exquisite tissue specificity in their actions (Salama et al., 2008).

1.1.4. S100s, Cancer and Metastasis

Cancer is a general term used to describe a group of more than two hundred diseases sharing common characteristics (Hanahan and Weinberg, 2000). Properties known as the "Hallmark of Cancer" acquired by most human tumours are: self-sufficiency in growth signals, insensitivity to growth-inhibitory signals, evasion of

apoptosis, limitless replicative potential, sustained angiogenesis, and tissue invasion and metastasis (Hanahan and Weinberg, 2000). Each of these physiological novel capabilities acquired during tumour development represents the successful breaking of an anti-cancer defence mechanism applied by cells and tissues. In most cases, tumours are benign, meaning that they are not cancerous. They may cause health problems depending on their size and location, but do not have the ability to infiltrate surrounding tissue (invasion) or to spread to distant organs (metastasis), a synonym of malignant cancer progression. The usual organ targets of cancer cell metastasis are the lung, brain, bone and liver, often leading to the cause of patient death (Cancer Research UK), as very few patients with metastatic cancer are currently curable (IARC, 2010).

Cancer is a major worldwide health problem, seeing the total number of diagnosed cases and deaths is increasing, with a projection of new estimated cases to jump from 11.3 million in 2007 to 15.5 million in 2030 (Source World Health Organisation), combined with a projected 45% increase in death from 2007 to 2030 (from 7.9 million to 11.5 million deaths) (IARC, 2010). The leading cause of this increase is an increasing and ageing global population, but takes into consideration the expected decline in death rates for some cancers in highly resourced countries.

The most frequent types of cancer worldwide (in order of the number of global deaths) are:

- Among men: lung, stomach, liver, colorectal, oesophagus and prostate
- Among women: breast, lung, stomach, colorectal and cervical.

In females, breast cancer has the highest incidence rate in the world (1,400,000 cases) and in the UK (45,700 cases) (IARC, 2010). Breast cancer is the most common female cancer in the UK. Breast Cancer patients' prognosis depends on several factors e.g. human epidermal growth factor receptor (HER)-2 (Slamon et al., 1987) or the transcription and translation factor Y-box binding protein-1 (YB-1) (Wu et al., 2006), but the later the stage of the disease at diagnosis, the lower the survival rate. Women diagnosed before the occurrence of metastasis have 5 year survival rates varying from 99% to 44% from early to late stage and grade and the 5 year survival rates drop down to 14% after apparition of distant metastasis (Cancer monthly, The Source for Cancer Treatment Results).

Several studies to understand cancer and mechanisms of metastasis and involved proteins have been performed, and the presence of some members of the S100 protein family have been correlated with metastasis. S100A4, one of the most studied

proteins of the S100 family, has been characterised as a metastasis-associated protein (Davies et al., 1993). The association with a high metastatic capacity was first described for rodent tumour cell lines that had a high level of S100A4 protein and mRNA expression (Ebralidze et al., 1989). Further research then reported that transfection of rat (Davies et al., 1993), or human cells (Grigorian et al., 1996) with S100A4 cDNA, when is expressed as protein (Davies et al., 1993), can introduce a metastatic phenotype in non-metastatic rat mammary tumour cells (Rama 37) (Davies et al., 1993; Grigorian et al., 1996). When transfected cells overexpressing S100A4 were injected subcutaneously, it resulted in tumour development with a significant reduction in the latent period (~50%) and the appearance of metastases in the lungs and lymph nodes. Cells overexpressing S100A4 exhibited increased invasive characteristics, such as penetrating connective tissue and invading adjacent skeletal muscle (Davies et al., 1993), whereas inhibition of S100A4 expression in metastatic cells can revert cells to a less metastatic phenotype (Maelandsmo et al., 1996). S100A4 is not tumorigenic itself, since it failed to develop tumours in transgenic mice overexpressing S100A4 protein (Ambartsumian et al., 1996; Davies et al., 1996), but acts as a metastasis inducer in a given tumorigenic background.

The association between S100A4 expression and metastasis observed in animal studies has led to a number of studies of S100A4 as a prognostic marker in human cancers. A study, over a period of 14-20 years evaluated 349 invasive human breast cancer specimens for expression of S100A4 and other variables. This study showed that patients with carcinoma positively stained for S100A4 were highly correlated with patients' death (Platt-Higgins et al., 2000; Rudland et al., 2000). In addition to breast cancer, S100A4 has been shown to be a prognostic marker in a number of other human cancers, including oesophageal-squamous cancers (Ninomiya et al., 2001), non-small cell lung cancers (Kimura et al., 2000), primary gastric cancers (Yonemura et al., 2000), malignant melanomas (Andersen et al., 2004), prostate cancers (Saleem et al., 2005), thyroid carcinomas (Zou et al., 2004), bladder cancers (Davies et al., 2002) and pancreatic carcinomas (Rosty et al., 2002). Different studies have then been performed to determine the mechanistic functions of S100A4 in several different facets of tumour progression, including motility, invasion, angiogenesis and apoptosis. Motility and invasion have been studied using several transfected cell lines. These have shown that S100A4 stimulates cell motility (Davies et al., 1993; Jenkinson et al., 2004) via an interaction with non-muscle myosin IIA (Kriajevska et al., 1994). Matrix

Metalloproteinases (MMPs) have been also implicated with an essential role in cell migration up-regulated by S100A4 (Schmidt-Hansen et al., 2004).

Other members of the S100 family such as S100B, S100A7, S100A8, S100A9 and S100P, have also been studied and have been related to metastasis and poor patient prognosis. S100B has been significantly associated with melanoma (Schultz et al., 1998), increasing serum level of S100B are associated with tumour stage (Bonfrer et al., 1998), and there is a high expression in metastatic melanomas (Heizmann, 2004; Schultz et al., 1998). The level of expression of S100B reflected patient prognosis (Hauschild et al., 1999a; Hauschild et al., 1999b; Schultz et al., 1998), and S100B serum levels have been correlated with patient survival, distinguishing three different risk groups depending on S100B levels (< 0.3 μg/l, 0.3-0.6 μg/l and > 0.6 μg/l in a 643 melanoma patients cohort (von Schoultz et al., 1996). S100B is also implicated in the regulation of tumour-suppressor p53 oligomerisation (Fernandez-Fernandez et al., 2005; van Dieck et al., 2009). S100A7 is up-regulated in skin (Alowami et al., 2003), bladder (Celis et al., 1996), and in breast cancers (Al-Haddad et al., 1999; Leygue et al., 1996; Moog-Lutz et al., 1995). S100A7 has been associated with cell migration and invasion in tumour breast cells (Krop et al., 2005). S100A7 nuclear expression has been significantly associated with poor patient prognosis in a cohort of 100 head and neck squamous cell carcinoma (HNSCC) patients over samples from patients with oral displastic lesions (Tripathi et al., 2010). The heterodimer S100A8-A9 has also been implicated in metastatic process in several types of cancers such as prostate (Hermani et al., 2006) or Lewis lung carcinomas (LLC) (Hiratsuka et al., 2006), but most interestingly has been shown to increase the motility of lung cancer cells by a p38 MAPK-mediated activation of tumour cell pseudopodia (Hiratsuka et al., 2006).

A recent study has demonstrated that transfection of a vector expressing S100P into a benign non-metastatic rat mammary cell line caused a threefold increase in local muscle invasion and a significant induction of metastasis in up to 75% of tumour-bearing animals (Wang et al., 2006). A study of S100P immunohistochemistry in 303 breast cancer patients clearly indicated that the survival of patients with S100P-positive carcinomas was significantly worse by about seven fold than for those with carcinomas negatively stained for S100P. There is also a significant correlation between intensity of immunohistochemical staining of the carcinoma cells for S100P and decreased patient survival (Wang et al., 2006).

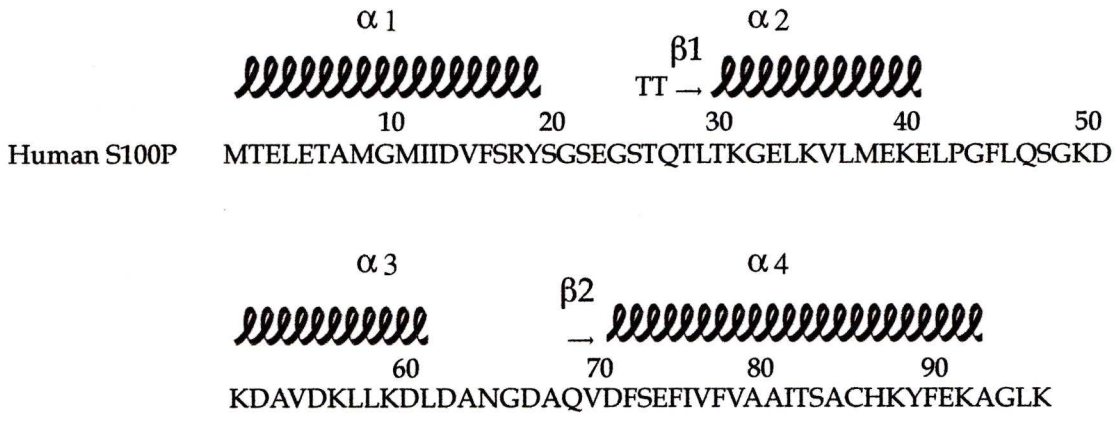

***Figure 1.2* Human S100P protein sequence.**

Human S100P protein Sequence (NP_005971, NCBI Pubmed). The S100P monomer structure contains four helices; namely, helix I (residues 3–18), helix II (residues 30–40), helix III (residues 53–61), and helix IV (residues 71–92). In S100P, the two calcium-binding loops contain two short, antiparallel β-strands formed by residues 27–28 and 68–69, respectively (Zhang et al., 2003).

1.2 S100P

1.2.1. Structure

S100P is a 95-amino acid, 10.4 kDa member of the S100 family, first isolated in 1992 from human placenta (Becker et al., 1992; Emoto et al., 1992). S100P protein structure has 2 distinct EF hand motifs separated with a hinge (L41-V54) region (Figure 1.2) and contains four helices; namely, helix 1 (residues 3-18), helix 2 (residues 30-40), helix 3 (residues 53-61), and helix 4 (residues 71-92). The two calcium-binding loops contain two short, anti-parallel β-strands formed by residues 27–28 and 68–69, respectively (Figure 1.3 A). Ca^{2+}-binding loops of the two EF-hands acquire a Ca^{2+}-bound-like conformation by Hydrogen bonds between the two β-strands. S100P exists in solution as a homodimer which is formed by hydrophobic interactions between subunits along the *N*-terminal helix 1 and the *C*-terminal helix 4 of subunits through anti-parallel packing (Figure 1.4 B). Two metal-binding sites are located in the *C*-terminal and *N*-terminal loops of each monomer, with different calcium binding affinities, a high affinity in the C-terminal loop and a low affinity at the N-terminal loop (Gribenko and Makhatadze, 1998). These C and N-terminal sites can also bind other divalent ions. The C-terminal site can bind Zn^{2+} (with relatively low affinity), and the N-terminal site can bind Mg^{2+}. In response to calcium binding, the C-terminal domain undergoes refolding that exposes its hydrophobic region and thereby facilitates interactions of S100 proteins with target molecules that mediate a spectrum of extracellular and intracellular effects.

Biochemical properties and crystal structure of S100P show significant similarities to other S100 proteins. S100P is structurally similar to S100B, which is consistent with 44% identity of the amino acid sequence alignment, as well as S100A7 and calbindin, despite their low level of amino acid sequence identity (25% comparing with S100A7 and no significant similarities comparing with calbindin) (Zhang et al., 2003).

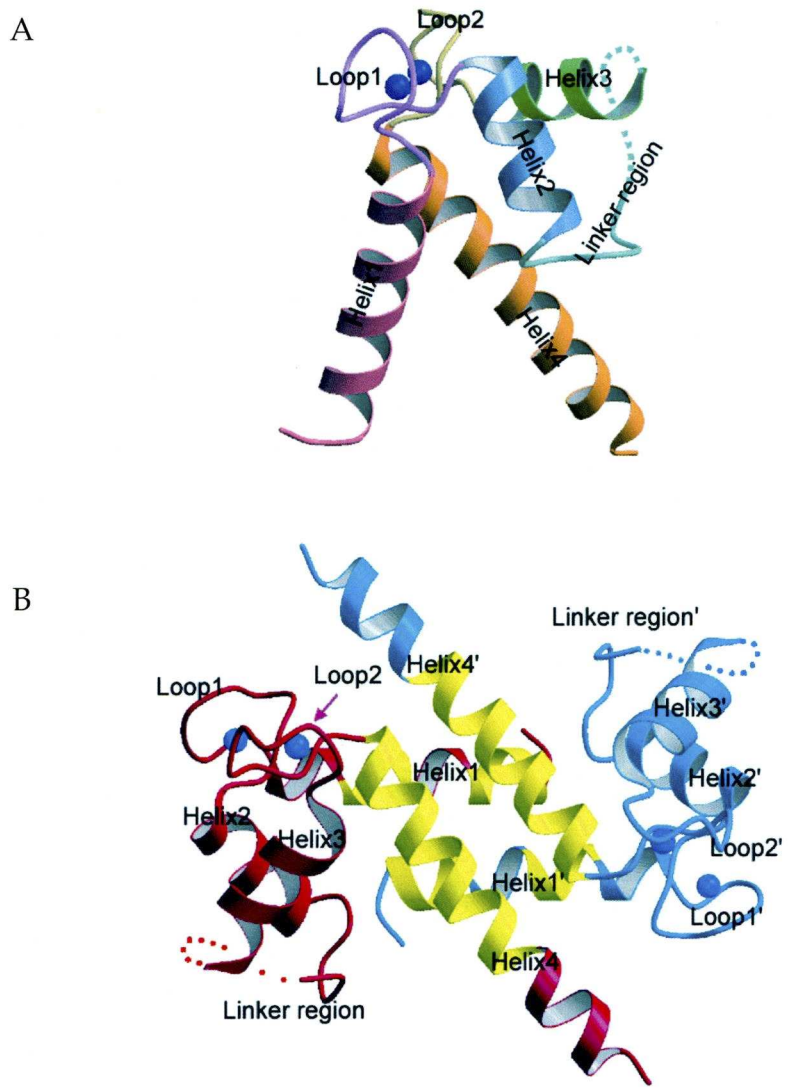

Figure 1.3. **3-Dimensional structure of S100P monomer and dimer**

(A) *S100P monomer. Calcium ions are in blue. Helices 1, 2, 3 and 4 are shown in flesh, lilac, pale-green and orange, respectively. Loops 1 and 2 are shown in pink and khaki. The linker region is in sky-blue, part of which is invisible and marked with a broken line.*

(B) *S100P homodimer. Two monomers are shown in red and blue respectively. The blue spheres are calcium ions. Amino acid residues 46-51 in the linker region are invisible, and are indicated by a broken-line. Regions of contact between the subunits are marked in yellow.*

(Zhang et al., 2003).

1.2.2. S100P in Cancer, Role and Function

There is considerable increasing evidence that S100P plays a role in cancer. The gene for S100P has been found to be highly expressed in several forms of cancer, including pancreatic (Iacobuzio-Donahue et al., 2002), prostatic (Averboukh et al., 1996), colon (Bertram et al., 1998), breast (Guerreiro Da Silva et al., 2000), oesophagus (Sato et al., 2002), and lung cancers (Diederichs et al., 2004).

- Pancreatic cancer

Abnormal expression of S100P has been consistently detected in pancreatic tumours. Overexpression was observed to be specific to pancreatic cancer cells, as it was not detected in samples of an inflammatory disease with similar peculiarities to pancreatic tumours, chronic pancreatitis (Logsdon et al., 2003). The specificity for cancer cells was confirmed in microdissected pancreatic cancer tissues and isolated primary cultures of cancer and stromal cells (Ohuchida et al., 2006). S100P is one of the most common genetic alterations in pancreatic cancer (Crnogorac-Jurcevic et al., 2003; Deng et al., 2008; Dowen et al., 2005; Iacobuzio-Donahue et al., 2002; Logsdon et al., 2003; Missiaglia et al., 2004; Ohuchida et al., 2006), and has been detected in 90% of pancreatic tumours (Arumugam et al., 2005), suggesting that S100P is an important factor in pancreatic cancer progression, since it has been observed to stimulate proliferation, survival, motility, and invasiveness of these cells (Arumugam et al., 2005). Specificity of S100P overexpression in cancer suggested its use as a histological marker for the disease, and as it has also been proposed to be a marker of pre-malignacy. S100P's role in tumour progression has been supported by the detection of S100P expression in the early stages of preneoplastic epithelial neoplasms (PanIN) with an expression level increase in invasive adenocarcinoma (Dowen et al., 2005). Mechanisms responsible for the induction of S100P gene expression during tumorigenesis are not fully understood.

S100P is secreted from pancreatic cell lines, and extracellular S100P was found to act extracellularly through the RAGE receptor and activate extracellular-signal-regulated kinases 1 and 2 (Erk 1/2), members of the mitogen activated protein kinase family (MAP Kinases), and NFκB signalling pathways in pancreatic cell lines, which increased cell proliferation, migration, survival and tumour growth (Arumugam et al.,

2004; Arumugam et al., 2005). These two pathways are constitutively active in most pancreatic cancer cell lines (Wang et al., 1999). S100P was also found to be secreted extracellularly and act as an autocrine loop involving S100P and RAGE. Thus inhibition of the S100P RAGE interaction with cromolyn (disodium 1,3-bis [(2-carboxylatochromon-5-yl)oxy]-2-hydroxy- propane), an anti-allergy compound (Berman et al., 1975) that has previously been shown to bind specifically to other members of the S100 protein family (S100A1, S100A12, S100A13) (Okada et al., 2002; Oyama et al., 1997; Shishibori et al., 1999), decreased S100P-mediated increases in cancer cell growth, survival, and invasiveness *in vitro*. Moreover the effects of S100P on cell signalling, cell proliferation, and cell survival were blocked by agents that interfered with the RAGE receptor when extracellular S100P was added to the fibroblastic cell line, NIH3T3 (Arumugam et al., 2004). Furthermore siRNA-based knockdown of endogenous S100P mRNA, and thus silencing of endogenous S100P, reduced tumour cell migration *in vitro* (Hamada et al., 2009). Moreover reduction in growth, survival and invasiveness *in vitro* led to a decrease in tumour volume by more than 80% after 6 weeks, and reduced peritoneal dissemination and distant metastasis to liver and lung. Compared with the control siRNA-bearing cells silencing also sensitised cancer cells to chemotherapeutic drugs, since overexpression of S100P affected the rate of tumour growth *in vivo* and resistance of pancreatic cancer cells to 5-fluorouracil chemotherapy (Arumugam et al., 2005).

- Prostate cancer

Prostate glands homeostasis is androgen-dependent, and an unbalanced decrease of androgen in normal prostate cells has been shown to promote normal cells to a metastatic stage (Averboukh et al., 1996). Moreover S100P expression has been shown to be regulated by androgen. Thus the expression of the S100P gene was abolished after 30 h of hormone deprivation in LN-Cap-FGC prostate cancer cells, but was then restored within 50 h by the addition of synthetic androgen (Averboukh et al., 1996). Furthermore expression of S100P mRNA has been shown to be highly elevated in prostate cancers using tissue microarray, with the highest frequency of S100P protein expression seen in metastatic prostate cancer (Mousses et al., 2002). Overexpression of S100P has also been described in PC3 prostate cancer cells. This promotes cell growth and proliferation in these human prostate cancer cells *in vitro* and *in vivo* and reduced

apoptosis *in vitro,* suggesting a promoting and aggressive role for S100P in cancer. These observations were confirmed by inhibition of cell growth after S100P gene silencing (Basu et al., 2008).

- Colon cancer

S100P is highly expressed in nonpolypoid adenomas, which have distinct characteristics compared with ordinary polypoid adenomas and have been are associated with an increased risk relative to polypoid adenomas of harboring high-grade dysplasia and progressing to an invasive tumour (Kita et al., 2006; Richter et al., 2003). S100P was shown to be expressed at greater levels in colon cancer than matched normal tissue . S100P also stimulated colon cancer cell growth, migration and exogenous S100P stimulated both ERK1/2 phosphorylation and NFκB activity *in vitro,* through the RAGE receptors (Fuentes et al., 2007).

- Breast Cancer

Breast cancer is the most common cancer among women, and several tissue analyses revealed an implication of S100P in breast cancer. It has also been shown that S100P overexpression is associated with immortalisation of human breast epithelial cells *in vitro* and early stages of breast cancer development *in vivo* (Guerreiro Da Silva et al., 2000). Moreover S100P has been shown to be absent in normal breast tissue, but can be detected in typical and atypical hyperplasias, and in *in situ* and invasive ductal carcinoma, indicating a strong association between S100P overexpression and cancer tumour progression (Guerreiro Da Silva et al., 2000). A positive correlation between S100P and high risk breast premalignant lesions has suggested that S100P is involved in the very early stages of breast carcinogenesis (Schor et al., 2006).

Previous studies in our laboratory have shown that S100P protein can induce metastasis in a rat mammary cell system and its presence in cancer cells is associated with a poor outcome in breast cancer patients (Wang et al., 2006). Thus subcutaneous injection of Rama 37 cells overexpressing S100P into the rat mammary fat pad region, produced primary tumours with significantly higher muscle invasiveness compared to cells transfected with vector alone. They also metastasised unlike the vector alone. Metastases were observed in lungs, and axillary lymph nodes. Immunohistochemical

staining confirmed intracellular staining for S100P was located in both nuclei and cytoplasm of these resultant tumours/metastases. There was no staining for S100P in the primary tumours of the rats injected with parental cells not expressing S100P (Wang et al., 2006). Further immunocytochemical staining of human breast carcinomas showed predominantly nuclear with some cytoplasmic staining for S100P. Unlike the other S100 protein associated with metastasis, S100A4, which was found predominantly in the cytoplasm (Rudland et al., 2000), the overall survival for patients with carcinomas stained positively for S100P was highly significantly worse than for patients with carcinomas classified as negatively stained (Wang et al., 2006), These results are comparable to those with two other predominantly cytoplasmically located metastasis-inducing proteins, S100A4 (Rudland et al., 2000) and osteopontin (Rudland et al., 2002), with a strong decrease of overall patient survival with positively stained tumours. Thus, both S100P and S100A4 showed the same ability to induce metastasis in the same mammary cell system and to be associated with poor outcomes of breast cancer patients. However it may be that the mechanism may be different since S100P was seen in the nucleus suggesting an additional transcriptional role for S100P induction of metastasis.

- Other cancers

S100P has been also reported to be expressed in ovarian tumours and to be associated with a worse patient prognosis (Surowiak et al., 2007). S100P is overexpressed in gastric cancer (Liang et al., 2007; Shyu et al., 2003). Furthermore, increased levels of S100P have been shown to be correlated with decreased survival in patients with lung cancer (Beer et al., 2002; Diederichs et al., 2004).

1.2.3. Regulation of S100P expression

S100P transcription and protein tissue expression, observed by several microarray and immunohistochemical studies, correlate with characteristic features of the malignant phenotype. S100P expression has been shown to be controlled by androgen and IL-6 via the androgen receptor (Averboukh et al., 1996; Hammacher et al., 2005), since S100P mRNA is up-regulated in the presence of androgen and IL-6 in prostate cancer cell lines. Moreover microarray analysis of breast cancer cell lines

showed that overexpression of the proto-oncogene ERBB2 (HER2/neu) correlated with S100P up-regulation (Mackay et al., 2003).

Furthermore upregulation of S100P has been associated with hypomethylation of CpG pairs in the 5'UTR (untranslated region also known as leader sequence) of the S100P mRNA in prostate cancers (Wang et al., 2007), in pancreatic cancer (Sato et al., 2004) and in cervical carcinoma cells (Jakubickova et al., 2005). CpG dinucleotides are statistically underrepresented in the genome, but are found concentrated at the expected frequencies in C + G rich regions, termed CpG islands, that frequently coincide with promoter or gene-regulatory regions (Doerfler, 1983). In the healthy genome, most CpG islands are unmethylated, and the associated genes which are expressed (Bird, 2002) are mostly methylated (Baylin et al., 2000). Abnormal global hypomethylation can lead to the activation of pro-metastatic genes. One such example is, S100A4, expression of which has been shown to be increased in hypomethylation conditions (Rosty et al., 2002). The S100P gene has been identified as a target for hypomethylation during cancer progression, with 35 CpG sites and 6 predicted transcription factor binding sites identified in the S100P promoter region. Thus S100P expression is up-regulated 12 fold in cell lines from prostate cancer specimens over normal cell lines derived from radical prostatectomy specimens, with S100P hypomethylated in 50% of the tumour-derived cell lines (Wang et al., 2007)

Another study revealed that the bone morphogenetic protein 4 (BMP4), a member of the transforming growth factor-beta (TGFβ) superfamily (Wozney et al., 1988), induced transcription of S100P in a pancreatic duct epithelial cell line (Hamada et al., 2009), although a regulatory element mediating this transactivation was not identified.

1.2.4. Targets for interaction of S100P

The metastasis-inducing effects of S100P may be mediated by both intracellular and extracellular protein functions. Thus S100P binding to the RAGE receptor stimulated the extracellular signal-regulated kinases (ERK)-1/-2 and nuclear transcription factor NFκB. There are possible downstream mechanisms leading to cell proliferation, migration, survival and tumour growth (Arumugam et al., 2004; Arumugam et al., 2005; Fuentes et al., 2007). These effects can be blocked by agents, which interfere with RAGE, suggesting that S100P may act in an autocrine manner via

RAGE. S100P has been shown to interact intracellularly with, and partially activate the protein, ezrin (Koltzscher et al., 2003), a membrane cytoskeleton crosslinker protein of the ezrin/radixin/moesin (ERM) family which has been implicated in metastasis (Akisawa et al., 1999). Ezrin modulates the state of actin filaments via direct linkage between actin filaments and the plasma membrane (Bretscher et al., 2002), although the underlying mechanism is not fully understood. The S100P binding protein Riken (S100PBPR) has been described to bind S100P (Dowen et al., 2005). S100P is also capable of interacting with and to form heterodimers with other members of the S100 family, namely S100Z (Gribenko et al., 2001), S100A1(Wang et al., 2004) and S100A6 (Whiteman et al., 2007).

1.2.5. Subcellular localisation and tissue distribution of S100P

The S100P subcellular localisation has been described as nuclear/ supranuclear, cytoplasmic or membranous and differs depending on the cell/tissue and experimental settings (Parkkila et al., 2008; Sato and Hitomi, 2002). This may reflect the functional state of the protein and its actual interactions. S100P has been shown to translocate to the cell periphery upon binding to ezrin, as a dimer-specific S100P ligand (Koltzscher et al., 2003), whereas binding to S100PBPR was identified to occur in the cell nucleus (Dowen et al., 2005). These studies suggest that S100P localisation is a dynamic process, requiring dimerisation, since the F15A mutated S100P is unable to dimerise and is also incapable of translocation (Koltzscher et al., 2003).

1.2.6 S100P possesses an unknown nuclear mode of action for metastasis

Literature strongly supports the significant role of S100P during the development and progression of different cancers (Bartling et al., 2007; Diederichs et al., 2004; Guerreiro Da Silva et al., 2000; Hammacher et al., 2005; Mousses et al., 2002; Ohuchida et al., 2006; Schor et al., 2006), with a crucial vital role for metastasis induction (Wang et al., 2006). S100P may have intracellular effects on cell function, since S100P can interact with intracellular molecules including ezrin (Koltzscher et al., 2003), and may be influenced by the complement of proteins expressed by a specific cell. On the other hand the nuclear localisation of S100P raises the question of a

potential role in gene expression (Figure 1.4), but any mechanistic links with metastasis are unknown. Furthermore preliminary experiments by Dr G. Wang have shown that adding large amount of S100P to the outside of Rama 37 cells causes a redistribution of the cytoskeleton (unpublished observation). However, the functions of this protein in the nuclear, cytoplasmic, and extracellular compartments are not known. A better understanding of the molecular and cellular events triggered by S100P and this functional analyses could potentially contribute to the development of novel diagnostic and therapeutic strategies for this metastasis-inducing protein.

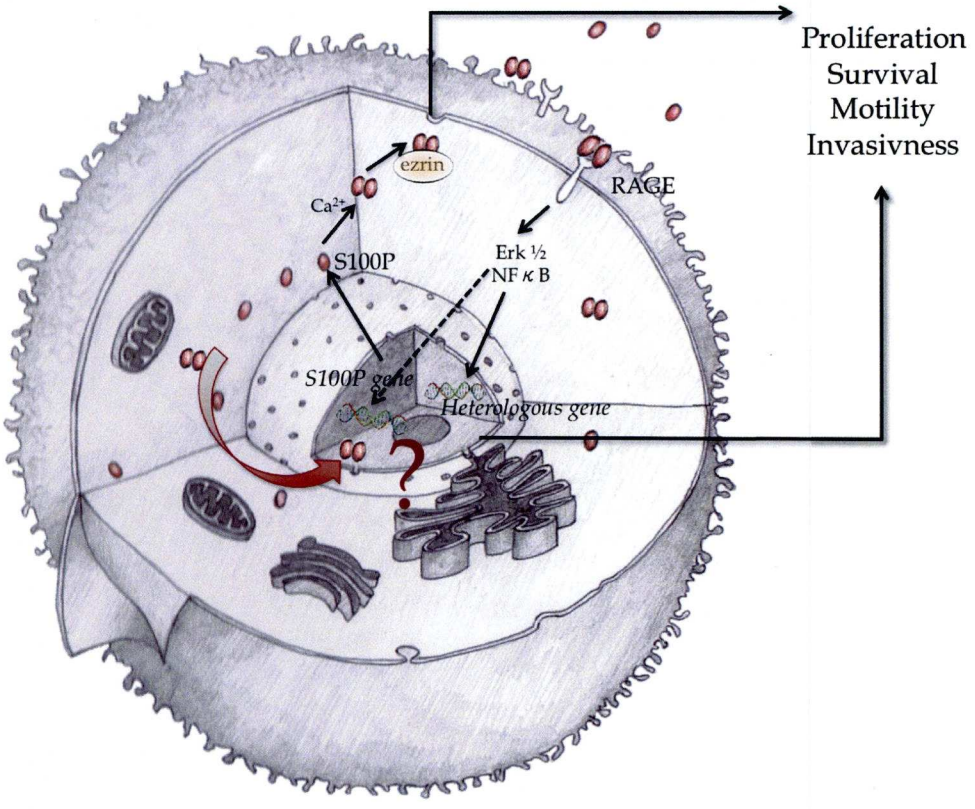

***Figure 1.4* Diagrammatic illustration of the occurrence of S100P in a tumour cell**

S100P protein is expressed in an inactive "apo" state and triggered by calcium ions to form active homodimers (Gribenko et al., 1998; Gribenko et al., 2002; Lee et al., 2004). These can operate either in an intracellular manner or as extracellular signalling molecules (Arumugam et al., 2004). In the cytoplasm, binding to ezrin leads to activation of ezrin, which is molecule implicated in metastasis, moreover binding to S100PBPR translocates S100P into the nucleus (Dowen et al., 2005; Koltzscher et al., 2003). Secreted forms of S100P can also bind to the extracellular RAGE receptor and activate Erk/ MAPK pathway to influence gene expression (Arumugam et al., 2004; Fuentes et al., 2007).

1.3. Aim of Project

The primary aim of the project is to understand the mechanisms whereby S100P induces metastasis in cancer cells. The project is divided into three parts, investigating the effects of 1) intracellular S100P on cell activity such as cell motility; 2) the effect of intracellular S100P on the expressions of other genes; and 3) the effect of extracellular S100P on intracellular signalling processes.

Firstly, the effects of increased intracellular S100P on cell motility were analysed using an inducible system constructed in the rat mammary cell line Rama 37.

Secondly, changes in up-regulation and down-regulation of the expression of genes after induction of S100P were analysed using microarrays.

Thirdly, changes in intracellular signalling induced by the addition of extracellular S100P were analysed.

Chapter 2

Materials and Methods

2.1. MATERIALS

2.1.1. Chemicals and Biochemicals

Chemicals	Suppliers
2-mercaptoethanol (thioethylene glycol)	Sigma-Aldrich, USA
2-Propanol (Isopropanol)	Sigma-Aldrich, UK
Acrylamide / Bis-Acrylamide (30% w/v)	Sigma-Aldrich, UK
Acetic acid	Fisher Scientific, UK
Agarose	Sigma-Aldrich, UK
Ammonium persulphate (APS)	Sigma-Aldrich, UK
Chloroform	VWR, France
Dimethylsulfoxide (DMSO)	Sigma-Aldrich, UK
Ethanol	VWR, France
Formamide , deionized	Sigma-Aldrich, UK
Glycerine	VWR, France
Glycine	AnalaR, UK
Glycerol	VWR, France
Goat IgG Purified Immunoglobulin	Sigma-Aldrich, UK
Hydrochloride acid (HCl)	VWR, France
Methanol	Fisher Scientific, UK
Milk powder	Marvel, UK
Propan-2-ol	Fisher Scientific, UK
Phenol	VWR, France
Power Sybr Green PCR Master Mix	Applied Biosystems, UK

Chemicals	Suppliers
Protease Inhibitor Cocktail	Sigma-Aldrich, UK
Sodium chloride (NaCl)	VWR, France
Sodium dodecyl sulfate (SDS)	Fisher Scientific, UK
Sodium hydroxide (NaOH)	VWR, France
SYBR Safe DNA gel stain	Invitrogen, UK
TEMED	Bio-Rad Laboratories, UK
Tris-Base	Fisher Scientific, UK
Triton X-100	Sigma-Aldrich, UK
Trizol reagent	Invitrogen,UK
Tween-20	Sigma-Aldrich, UK

2.1.2. Kits

Kit	Supplier
M-MLV Reverse Transcriptase	Promega, UK
SuperSignal® West Pico Chemiluminescent Substrate Kit	PIERCE, USA
REASTAIN Quick-Diff Kit Staining Solutions	REAGENA, Finland
RNeasy Mini Kit	Qiagen, UK
Quantitect® Reverse Transcription	Qiagen , UK

2.1.3. Other Materials

Name	Supplier
3MM Paper	Whatman ,UK
ABI PRISM™ optical adhesive covers	Applied Biosystems, UK
DNA mass standard (1 kb DNA ladder)	Invitrogen, UK
Falcon™ 50 mL conical tubes	BD Biosciences, USA
Falcon™ 15 mL conical tubes	BD Biosciences, USA
Immobilin™-P- PVDF , pore size 0.45 µm	Millipore, USA
Microcentrifuge tubes, PCR, clear, 0.5 ml	Eppendorf, UK
Microcentrifuge tubes, PCR, clear, 1.5 ml	Eppendorf, UK
Microcentrifuge tubes, PCR, clear, 2.0 ml	Eppendorf, UK
MicroAmp plates, optical 96-well reaction plate	Applied Biosystems, UK
Superscript random hexamer primers	Qiagen, UK
SeeBlue Plus2 Pre-Stained Standard	Invitrogen, UK
Transwell Permeable Supports	Corning, UK

2.1.4. Solutions

2.1.4.1. Solutions

Solutions	Composition
Tris Buffered Saline (TBS)	50mM Tris 150mM NaCl pH 7.4

Solutions	Composition
Phosphate-Buffered Saline (PBS)	137 mM NaCl 2.7 mM KCl 8 mM Na_2HPO_4 1.5 mM KH_2PO_4, pH 7.4
10% Sodium Dodecyl Sulfate (SDS)	10% (w/v) SDS ddH_20
1x Tris Borate EDTA (TBE)	89 mM Tris-Base 89 mM Boric Acid 2mM EDTA (pH 8)
Coomassie Staining Solution	0.25% (w/v) Coomassie bb G250 50% (v/v) Methanol 10% (v/v) Acetic Acid
Coomassie Destaining Solution	50% (v/v) Methanol 10% (v/v) Acetic Acid

2.1.4.2. Medium and Antibiotics for Cell Culture

Medium and Antibiotics	Composition
Routine Medium	1x DMEM (GIBCO) 50 ng/ml Insulin 50 ng/ml Hydrocortisone 5% (v/v) Foetal Calf Serum (FCS)
Trypsin Solution	0.008%(v/v) Trypsin in Versene 140 mM NaCl 3 mM KCl 8 mM Na_2HPO_4 1.5 mM KH_2PO_4 0.7 mM EDTA pH 7.2
Freezing solution	20% (v/v) FCS 20% (v/v) DMSO DMEM

2.1.4.3. Western Blot Solutions

Western Blot Solutions	Composition
1 x Loading Buffer	125 mM Tris-HCl (pH6.8) 4% (w/v) SDS 20% (v/v) glycerol 0.004% (w/v) bromophenol blue 10% (v/v) 2-mercaptoethanol
1 x SDS-PAGE Running Buffer	25 mM Tris-Base 192 mM Glycine 0.1% (w/v) SDS ddH_20
10% polyacrylamide SDS-PAGE Resolving gel	1.9 ml dd-H_20 1.7 ml 30% (w/v) acrylamide 1.3 ml 1.5M Tris (pH 8.8) 0.05 ml 10% (w/v) SDS 0.05 ml 10% (w/v) Ammonium persulphate 2 µL TEMED
15% polyacrylamide SDS-PAGE Resolving gel	1.1 ml dd-H_20 2.5 ml 30% (v/v) acrylamide 1.3 ml 1.5 M Tris (pH 8.8) 0.05 ml 10% (w/v) SDS 0.05 ml 10% (w/v) Ammonium persulphate 2 µL TEMED

Western Blot Solutions	Composition
5% SDS-PAGE Stacking gel	0.68 ml dd-H_20 0.17 ml 30% (w/v) acrylamide 0.13 ml 1M Tris (pH 6.8) 0.01 ml 10% (w/v) SDS 0.01 ml 10% (w/v) Ammonium persulphate 1 µL TEMED
1 x Transfer Buffer	25mM Tris-Base 192mM Glycine 20% (v/v) Methanol ddH_20
Western Washing Buffer	0.1 % (v/v) Tween in TBS
BSA Blocking Buffer	3% (w/v) BSA in TBS
Milk Blocking Buffer	5% (w/v) Powder Milk in Western Washing Buffer
APS	10% APS (w/v) in ddH_2O
Stripping Buffer	200 mM Glycine, pH2.5 0.05% (v/v) Tween-20

2.1.5. Primers

2.1.5.1. Primers for quantitative real-time PCR

- *Rattus Norvegicus*

Primers	Sense Sequence	Gene Bank Acc Num	Sequence positions	Product size (bp)	Efficiency (%)
GAPDH	5′- AAGGGCTCATGACCACAGTC -3′ 5′- GGATGCAGGGATGATGTTCT -3′	NM_017008	586 - 605 700 - 681	114	98
S100P	5′- GATGCCGTGGATAAATTGCT -3′ 5′- ACTTGTGACAGGCAGACGTG -3′	NM_005980	249 - 268 356 - 337	107	104
Folh1	5′- TTCTCTCCACAAGGGACACC -3′ 5′- CTTCATGACCCGTTCCAGTT -3′	NM_057185	561 - 580 650 - 631	89	95
Mast 1	5′- GAAGAGCGGACCACGTTAAG -3′ 5′- CACTGCGGGGTACATTCTTT -3′	NM_181089	4459 - 4478 4568 - 4547	109	103
Myc Target 1	5′- GTTGACGTCAGAGGGATGGT -3′ 5′- TGGGCAATCTTATTGGGAAG-3′	NM_001106207	1249 - 1268 1341 - 1322	92	94
S100A7a	5′- ATCTTGGGCAAACTGGTGAA -3′ 5′- ACCCTTTCCTTGCAGACTGA -3′	NM_001109471	416 - 435 517 - 498	101	101
Ccnd2	5′- TTCATTGAGCACATCCTTCG -3′ 5′- GGTAGCACACAGAGCGATGA -3′	NM_022267	472 - 491 548 - 567	76	98
Pttg1ip	5′- CTCTGGTGCAACGAGAACAA-3′ 5′- CCTCAAAGTTCACCCAGCAT-3′	NM_001013238	226 - 245 343 - 324	117	97

- Homo Sapiens

Primers	Sense Sequence	Gene Bank Acc Num	Sequence positions	Product size (bp)	Efficiency
GAPDH	5′- CAGCAAGAGCACAAGAGGAA-3′ 5′-TGTGAGGAGGGGAGATTCAG-3′	NM_002046	1131 - 1150 1223 - 1204	92	100
S100P	5′- GATGCCGTGGATAAATTGCT -3′ 5′- ACTTGTGACAGGCAGACGTG -3′	NM_005980	249 - 268 356 - 337	107	103
Folh1	5′-ATTGCAGAGGCTGTTGGTCT-3′ 5′-CTGCTATCTGGTGGTGCTGA-3′	NM_001193473	734 - 753 840 - 821	106	100
Ccnd2	5′-CTTCGCTTCTGGTATCTGGC-3′ 5′-TGTGGAATGTTGTGATGGGA-3′	NM_001759	2258- 2277 2361 - 2342	103	99
Akr7a2	5′-CCAGTCTTGGCCTTAAGCTG-3′ 5′-GAGCAAGGCAGGAAGCTAGA -3′	NM_003689	1164 - 1183 1248 - 1229	84	101
Mast 1	5′- AATTTCTCGATGCCCTCCTT -3′ 5′- GGTGAAGTGCTGGTCAGGAT -3′	NM_014975	159 - 178 259 - 240	100	100
S100A7a	5′- ACCCATGTCATCCCAGAGAG-3′ 5′- CTGCCATAGCAAATCAGCAA-3′	NM_176823	3073 - 3092 3178 - 3159	105	99

2.1.6. SiRNA Sequences

Gene	SiRNA Name	Acc. No	Sense Sequence (5′ → 3′)	Sequence Position
MAST 1	Rn_MAST1_1	NM_181089	5′-CGGUUCUAGCUCUUGAAUATT-3′ 5′-UAUUCAAGAGCUAGAACCGTT-3′	1446-1466 1466 - 1446
MAST 1	Rn_MAST1_2	NM_181089	5′-GCACAGCUUCUAAUAUCUATT-3′ 5′-UAGAUAUUAGAAGCUGUGCGT-3′	1853 - 1873 1873 - 1853
MAST 1	Rn_MAST1_3	NM_181089	5′-GCAUGUUUCGCCGCACCAATT-3′ 5′-UUGGUGCGGCGAAACAUGCTG-3′	60 - 80 80 - 60
MAST 1	Rn_MAST1_4	NM_181089	5′-GCCUCACCACCAACUUAUATT-3′ 5′-UAUAAGUUGGUGGUGAGGCTC-3′	1578 - 1598 1598 - 1578
Negative Control	Ctrl_AllStars_1	n/a	n/a	n/a
BLOCK-IT Alexa Fluor Red Fluorescent Oligo	n/a	n/a	n/a	n/a

All SiRNA Probes were purchased from Qiagen, UK

2.1.7. Antibodies

2.1.7.1. Antibodies used in Western blotting

AB	Antibody to	Produced in	Dilution Buffer	Dilution	Supplier
1°	Akt	Rabbit	3% BSA/ TBST	1:1000	Cell Signaling Technology® UK
1°	Phospho-Akt (Ser473)	Rabbit	3% BSA/ TBST	1:1000	Cell Signaling Technology® UK
1°	MAST 1	Goat	5% Milk/ TBST	1:500	Santa Cruz Biotechnology, USA

AB	Antibody to	Produced in	Dilution Buffer	Dilution	Supplier
1°	Cyclin D2	Rabbit	3% BSA/ TBST	1:1000	Cell Signaling Technology® UK
1°	Anti-human PSMA	Sheep	3% BSA/ TBST	1:1000	R&D Systems, UK
2°	Anti-goat IgG	Rabbit	3% BSA/ TBST	1:15,000	Sigma- Aldrich, USA
2°	Anti-mouse IgG	Rabbit	3% BSA/ TBST	1:20,000	Sigma- Aldrich, USA
2°	Anti-rabbit IgG	Goat	5% Milk/ TBST	1:10,000	Sigma- Aldrich, USA
2°	Anti-sheep IgG	Donkey	3% BSA/ TBST	1:5000	R&D Systems, UK

2.1.7.2. Immunostaining Antibodies

AB	Name	Produced in	Dilution Buffer	Dilution	Supplier
1°	Anti-S100P	Mouse	3% BSA/ TBST	1:1000	BD Transduction Laboratories, UK
2°	Anti-mouse	Donkey	3% BSA/ TBST	1:5000	LifeSpan, UK

2.1.7.3. Other

Name	Supplier
DPX mountant	Merck, UK

2.1.8. Cell Culture

2.1.8.1. Cell lines

Name	System
Rama 37	*Rattus Norvegicus*
HeLa	*Homo Sapiens*

2.1.8.2. Vectors

Vector name	Supplier
pcDNA3.1(+) pcDNA3.1 (-)	Invitrogen, UK
T-REx System	Invitrogen, UK

2.1.8.3. Transfection Reagents

Reagent	Supplier
Hiperfect Transfection Reagent	Qiagen, UK

2.1.8.4. Inhibitors

Inhibitor	Supplier
LY 294002	Calbiochem®, UK
Wortmannin	Calbiochem®, UK
PD 98059	Cell Signaling, UK
Anti-rat RAGE Antibody	R&D Systems,UK

2.1.9. Instruments

Instrument	Supplier
7500 Fast Real Time PCR Systems	Applied Biosystems, USA
Chemidoc Gel documentation system	BioRad, UK
Gel electrophoresis power supply	BioRad, UK
Mastercycler PCR-Machine	Eppendorf, UK
Micro-centrifuge	Eppendorf, UK
NanoDrop ND-1000 Spectrophotometer	NanoDrop Technologies, San Diego, USA
SDS-PAGE Mini-Protean gel apparatus	Biorad Laboratories, UK
Molecular Imager® Gel Doc™ XR	Biorad Laboratories, UK

2.1.10. Software for data handling

Software	Supplier
Quantity three	BioRad, USA
7500 Fast-Time PCR Systems	Applied Biosystems, USA
Sigmaplot	Systat Software, USA
Excel	Microsoft, USA
GelEval	Frogdance Software, UK

2.1. METHODS

2.2.1.TISSUE CULTURE

2.2.1.1. Cell culture

2.2.1.1.a. Cell lines used

The cell lines used during this project were the non-metastatic rat mammary (Rama) 37 cell line obtained from a benign DMBA-induced tumour in a Ludwig OLA strain of Wistar-Furth rats (Dunnington et al., 1983), and a human cell line derived from an epidermoid carcinoma of the cervix (HeLa), the latter consists of highly stable immortalised cancer cells, isolated from a cancer of the cervix of Henrietta Lacks who died of cancer in 1951 (Scherer et al., 1953).

- Rama 37 T-25 cells transfected with inducible system

The rat mammary (Rama) 37 expresses undetectable levels of S100P protein by Western blotting or immunochemistry. An inducible Rama 37 system has been developed in the laboratory (Dr G. Wang); the construct contains a human S100P cDNA regulated by tetracycline regulatory elements consisting of a tetracycline-regulated expression system for mammalian cells: the T-Rex™ System From Invitrogen™. This tetracycline-regulated system uses regulatory elements from the *E. coli* Tn*10*-encoded (Tet) resistance operon (Hillen and Berens, 1994; Hillen et al., 1983). Tetracycline regulation in the T-Rex™ system is based on the binding of tetracycline to the tet repressor and depression of the promoter controlling expression of the gene of interest (Yao et al., 1998). The components of the T-REx(™) system include (cf Appendix Figure A.1 and A.2):

- An inducible expression plasmid for expression of S100P under the control of the strong human cytomegalovirus immediate-early (CMV) promoter and two tetracycline operator 2 ($tetO_2$) sites (pcDNA™4/TO)
- A regulatory plasmid, pcDNA6/TR©, which encodes the Tet repressor (*Tet*R) under the control of the human CMV promoter
- Tetracycline or doxycycline for inducing expression

S100P mRNA and protein can be induced by adding doxycycline to the medium. Inducible expression of S100P cDNA expression plasmid construct is under the control of this antibiotic.

- Rama 37 cells transfected with pcDNA3 (Invitrogen®)

Rama 37 cells were transfected with a pcDNA3 vector (5427bp) inserted with S100P full length cDNA. This vector contain the following elements (cf Appendix Figure A.3):

- Human cytomegalovirus immediate-early (CMV) promoter
- Multiple cloning sites in the forward (+) and reverse (-) orientations to facilitate cloning
- Neomycin resistance gene for selection of stable cell lines
- Episomal replication in cell lines that are latently infected with SV40 or that express the SV40 large T antigen

Rama 37 cells transfected with empty vector were used as negative controls.

- HeLa cells transfected with an inducible system

HeLa cells were transfected with the T-Rex ™ System previously used with Rama 37 cells (Dr Wang).

2.2.1.1.b. Routine culture

Rat mammary epithelial cell lines (Rama 37) and human HeLa cells lines (HeLa) were routinely cultured in Routine Medium. Cells were cultured at 37°C in a humidified atmosphere containing 10% (v/v) carbon dioxide and 90%(v/v) air.

2.2.1.1.c. Routine passaging of cells

All cells were grown to approximately 80% confluence on 10 cm diameter tissue culture dishes in Routine Medium. Medium was aspirated off, dishes were washed three times with 10 ml of PBS, 1 ml of trypsin solution was added and swirled over the surface of the cells. Dishes were incubated at 37°C for 2-5 min to

release the cells from the dish, and when the cells were detached 5 ml of medium was added to the plate and gently aspirated to disperse the cells. Cells suspension from one dish was then aliquoted to five new dishes containing medium (split ratio 1: 5) (Warburton et al., 1982a).

2.2.1.1.d. Freezing cells

Cells were conserved by cryopreservation. Cells were grown to approximately 80% confluence in a 10 cm diameter dish, detached from the dish as previously described, counted in a Z1™ Series COULTER COUNTER® Cell and Particle Counter, and pelleted by centrifugation at 1500g. Cells were resuspended in Freezing Medium to a final density of 2 x 10^6 cells/mL, aliquoted into cryotubes and then placed on dry ice for one h before transfer to a -80°C freezer, then to a -140°C freezer for long term storage (McLellan and Day, 1995).

2.2.1.1.e. Thawing cells

Cryotubes previously stored in a freezer were thawed in a water bath at 37°C and the contents were immediately transferred to a Sterilin tube containing 20 mL Routine Medium supplemented with a further 10% FCS and centrifuged at 1500g in a bench-top centrifuge. The supernatant was removed by aspiration and the pellet resuspended in a suitable volume of Routine Medium supplemented with 15% (v/v) FCS, following which, cells were plated out. Medium was then changed to regular Routine Medium after 24 h (Freshney, 2005).

2.2.1.1.f. Counting cells

Cells were detached as described previously and counted using the Z1™ Series COULTER COUNTER® Cell and Particle Counter. Trypsinised cells were resuspended in Routine Medium and 1 mL of the cell suspension was added to 19 mL of Isoton for counting. The number of cells measured by the Coulter counter is calculated in a volume of 500µL from the 20mL sample, so to calculate the concentration of the 20 mL total volume, the number of cells given by the Coulter counter was then multiplied by 40 to determine the concentration of cell/mL.

2.2.1.1.g. Treatment of cells

- Cell treatment with doxycycline

Prior to induction of S100P in cells transfected with the inducible system, cells were washed three times with PBS, then 10 mL of Routine Medium containing 67.5 nM of doxycycline was added to the cells. Cells were then cultured in normal routine conditions.

- Cell treatment with inhibitors.

Inhibitors used for cell signalling analysis were: Wortmannin (Brian et al., 1957; Hazeki et al., 1996), LY294002 (Vlahos et al., 1994), PD 098059 (Dudley et al., 1995) and Anti-RAGE inhibitors. Cells were washed three times with PBS and pretreated with inhibitor for 30 min prior to starting experiments.

2.2.1.2. Cell migration

- Migration in a Boyden chamber assay

Cell migration assays were performed using the Boyden chamber assay, based on a chamber of two medium-filled compartments separated by a microporous membrane (Figure 2.1). Cells were placed in the upper compartment and were allowed to migrate through the pores of the membrane into the lower compartment (Boyden, 1962). The migratory ability of the cells were measured in a Boyden chamber by passage through a filter membrane of 0.33 cm^2 growth surface area containing 8 μm pores in 24-well polystyrene tissue culture-treated sterile plates (Transwell® Permeable supports, Corning Inc, NY, USA).

Chemotactic-induced migration in response to a FCS concentration gradient was measured by adding 400μL of Routine Medium containing 10% (v/v) FCS to the lower compartment and $8x10^4$ cells in 200μL of Routine Medium, but with 2% (v/v) FCS were added to the upper compartment of the Boyden chamber. After the cells had been incubated for 24 h, the upper side of the filter was wiped with a cotton swab several times to remove cells remaining on the upper surface and to make sure that all cells on that side of the membrane had been removed, and the cells on the lower side of the filter were fixed and stained using the Reastain Quick-

Diff kit (Reagena, Finland), according to the manufacturer's instructions. Membranes were detached from the Transwell® insert and put between a microscope glass slide and coverslip with a drop of PBS. Positively stained cells which went through the membrane were scored looking through an optical microscope (Magnification x 50). Each experiment, which consisted of triplicate wells for each sample, were performed three times.

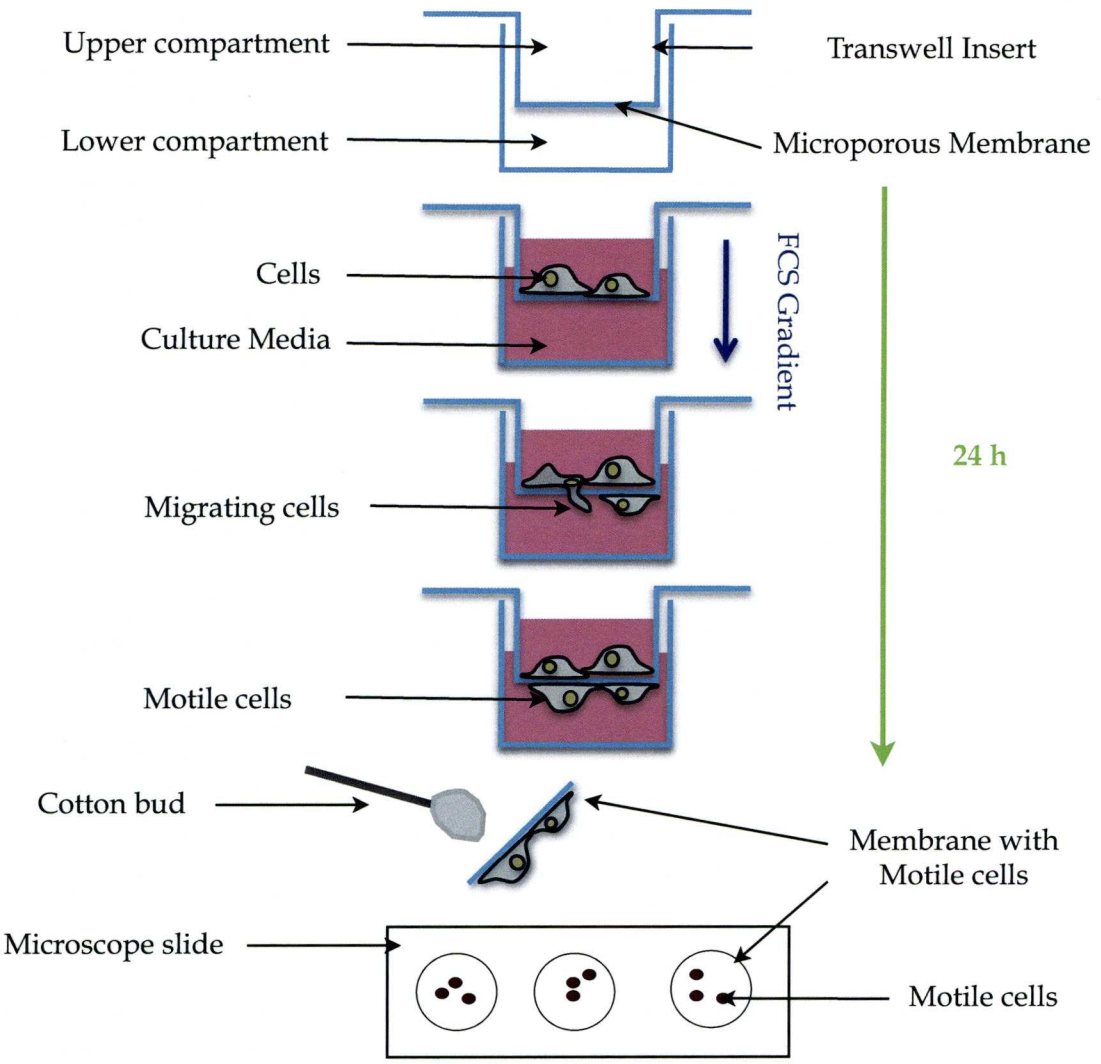

Figure 2.1 Experimental set up for cell migration in the lower compartment of the a Boyden chamber

Cells were added to the upper compartment of the Boyden chamber, and were incubated for 24 h under the experimental condition. Membranes were detached from the Transwell® insert, the upper side of the membrane was gently wiped with a cotton bud, and put between a microscope glass slide and coverslip with a drop of PBS. Positively stained cells which went through the membrane were scored looking through an optical microscope.

2.2.1.3. Characterisation of cell adhesion and proliferation

2.2.1.3.a. Cell adhesion assay

Cells were trypsinised, counted as described previously (Chapter 2: 2.1.1.f.) and resuspended at $4x10^5$ cells/mL in 5 mL. 1 mL of the cell suspension was added to each well of a 24-well plate and at time periods of 0.5, 1, 1.5, 2, 2.5, 3 h, three wells of cells were washed three times with PBS to remove any cells in suspension. Cells adhering to the well were trypsinised and counted using a Coulter counter. Each experiment consisting of triplicate wells, were performed three times.

2.2.1.4 Analysis of cell lines

2.2.1.4.a. Immunohistochemical staining

Cultured cells were washed three times with PBS, trypsined, aliquoted in 1.5 mL Eppendorf tubes and spun down at 800 g. Cell pellets were then treated with three changes of absolute ethanol, each for 2 h at room temperature, followed by one wash with ethanol: 1 , 1 , 1 -trichloroethane (1:1 v/v) for 2 h and one final wash with 1 , 1, 1-trichloroethane for 2 h. Cells were then incubated with four changes of paraffin wax at 60 °C for 2 h, the last incubation being in a vacuum incubator, and finally embedded in fresh wax, and dried overnight at 4 °C. Sections were dewaxed by passage through three changes of xylene for 5 min each, three changes of absolute ethanol for 5 min each, and rehydrated by immersion in water for 5 min. Histological sections of cell pellets, cut at 4 μm, were transferred to 3-aminopropyletriethoxysilane (APES) coated slides (Maddox and Jenkins, 1987) and equilibrated with PBS (Ca^{2+}, Mg^{2+} free, PBS) (Warburton et al., 1982b).

Indirect immunocytochemical staining was carried out using an enhanced HRP labelled polymer system (DAKO EnVision + System, peroxidase (DAB) (Dako Ltd, Ely, UK). Endogenous peroxidase activity was blocked using blocking agent supplied with the Envision Kit before slides were incubated with 1% (w/v) BSA / PBS for 30 min at room temperature. Monoclonal anti-S100P (BD Biosciences, Cowley, Oxford) was then used at a dilution of 1:50 in 1% (w/v) BSA/PBS for approximately 2 h at room temperature in a moist chamber. Indirect immunohistochemical staining was then carried out using the reagents prepared according to the manufacturer's instructions. The sections were then washed in

running tap water before being counterstained in Mayers' haemalum. They were then dehydrated through graded ethanol and xylene and were mounted in DPX mountant (Heras et al., 1995).

2.2.1.4.b. Immunofluorescence

S100P was detected in cells by immunofluorescence as previously described (Rudland et al., 1989; Wang et al., 2000). Cells were grown to confluence and plated at 50% confluence in an eight-well chambered slides (Lab-Tek®) until approximately 60% confluence was reached. Cells were washed three times with PBS and once with methanol, prior to fixing with methanol for 15 min at -20°C. The cells were washed one more time with PBS and incubated for approximately 1 h with an appropriate dilution of primary antibody diluted in 0.5% (w/v) BSA. The slides were then washed three times in PBS, for 3 min each, and incubated with the relevant fluorescein isothiocyanate (FITC) conjugated secondary antibody at an appropriate dilution for 1 h. The slides were washed with PBS as before, and mounted using non-fluorescing aqueous mountant (Hydromount) (Johnson et al., 1982).

2.2.2. PROTEIN BLOTTING TECHNIQUES

2.2.2.1. Protein extraction

For Western blotting, total cellular protein was isolated from cell lines. Cells were grown to 70%-80% confluency in a 10 cm Petri dish, washed three times with PBS buffer, scraped and collected with 100μL of 2x loading buffer (0.125M Tris-HCl pH 6.8, 4% SDS (w/v), 20% glycerol, 0.004% bromophenol blue) in 1.5 mL tubes on ice. Samples were sonicated on ice with 20 discontinuous pulses of 50% duty cycle setting at an output control setting of 2, on an ultrasonic generator (type 7533A, DAWE®, England, UK). Cell lysate was centrifuged for 10 min at 10,000g. Samples of protein from cell lines in gel loading buffer were heated to 98°C for 10 min, cooled on ice for 1 min, and were then separated by electrophoresis on polyacrylamide-SDS gels.

2.2.2.2. Denaturing polyacrylamide gel electrophoresis (SDS-PAGE)

Protein samples in loading buffer were run for 1 h until the dye reached the bottom of the resolving gel for Tris-Glycine SDS PAGE electrophoresis gels. Polypeptides from different cell lines were analysed on different percentage polyacrylamide resolving gels depending on the size of protein to be detected, using 4% (w/v) acrylamide stacking gels in the Bio-Rad miniprotein system with 0.75 or 1 mm spacers, as described previously (Sambrook and Russell, 2001).

2.2.2.3. Coomassie blue staining of separated polypeptides after SDS-PAGE

Proteins were visualised after SDS-PAGE by submerging the gel in Coomassie blue-staining solution (50% (v/v) methanol, 10% (v/v) acetic acid, 0.25% (w/v) Coomassie blue) at room temperature for at least 3 h with gentle agitation. The gel was then destained by incubation in several changes of destaining solution (10% (v/v) methanol, 5% (v/v) acetic acid) for up to 15 h (Sambrook and Russell, 2001).

2.2.2.4. Western blotting

Blotting of proteins onto an immobilon-P polyvinyldifluoride (PVDF) membrane (Millipore, Bedford, USA) pre-soaked in methanol and rinsed in water, was carried out using a Bio-Rad semi-dry transfer apparatus for 1 h at 150 mA in a blotting buffer (20 mM Tris-base, 150 mM glycine, 20% ethanol, 0.1% SDS) (Burnette, 1981).

The PVDF membrane was blocked for 1 h at room temperature with defatted milk in Blocking Buffer, washed twice for 5 min with Washing Buffer and incubated at 4°C overnight with primary antibody diluted in 5% (w/v) powdered milk in Blocking Buffer. Subsequently, to remove unbound primary antibody, the membrane was washed as before and incubated at room temperature with the secondary antibody diluted in Blocking Buffer for 1 h on an orbital shaker.

Proteins bound to horseradish peroxidase-conjugated secondary antibody were detected by the Supersignal West Pico Chemiluminescent Substrate (Pierce Biotechnology, Inc., Perbio Science, Framlington Northumberland, U.K.) according to the manufacturer's instructions. 1 mL of chemiluminescent reagents A and B were combined and placed on the blotted dry membrane for 8 min before autoradiography. The latter process involved exposures for 1 to 30 min on Fuji RX film. Western blots were scanned, and protein amount quantified using GelEval software.

2.2.2.5. S100P immunoprecipitation

Culture medium was taken from treated or untreated cell culture plates of growing cells and centrifuged at 1500 g in a bench-top centrifuge to remove dead cells. The primary S100P antibody was added to the sample, placed in centrifuge tubes, and left on a tube rotator at 4°C overnight. The following day protein A/G agarose beads were washed three times with 100 µL PBS before use, and were added to the sample of culture medium and antibody and left on a rotating wheel at 4°C for 1 h to capture the immune complexes. Tubes were centrifuged for 30 seconds at 4°C, and the supernatant was carefully completely removed. The beads were washed three times with 500 µL of cold Lysis Buffer. In order to minimise background the supernatant was removed completely after each wash. After the last wash 100 µL of two times electrophoresis Sample Buffer was added to the samples which were boiled for 5 min, vortexed briefly, and boiled for 5 more min. Samples were then subjected to the Western blotting protocol, as described in Section 2.2.4.

2.2.3. MANIPULATION OF DNA

Agarose gel electrophoresis

Agarose was dissolved in 1x TBE buffer (described in section I. 4 .a.) at the required concentration (0.6 - 2%(w/v) by heating in a microwave oven. After cooling for a few minutes at room temperature, SYBR Safe DNA Stain was added to agarose gels to a final concentration of 1 µL/mL and the gel was set in 4 to 6 mm deep gel casts in Perspex trays of varying sizes (4x 4 cm to 20x 20 cm). Once set, the gels were placed in appropriately sized tanks and submerged in 1 x TBE buffer. To

increase the density of each DNA sample a 1: 2 volume of 2 x Loading Buffer was added to each sample (described in Section 1.4.3.). Electrophoresis conditions ranged from 60 - 120 V for 30-120 min (Sambrook and Russell, 2001).

2.2.4. MANIPULATION OF RNA

2.2.4.1. Isolation of RNA

Total RNA was extracted from approximately 2 x 10^6 cells with TRIZOL® Reagent (Invitrogen, U.K.) according to the manufacturer's protocol. Cells were washed three times with PBS and lysed directly in a 10 cm diameter culture dish by adding 3 mL of TRizol Reagent, as described previously (Chomczynski and Sacchi, 1987). The cell lysate was passed several times through a sterile pipette tip and transferred into a 1.5 mL Eppendorf tube. Homogenised samples were incubated for 5 min at room temperature to permit the complete dissociation of nucleoprotein complexes. 0.2 mL of chloroform was then added per 1 mL of TRizol Reagent and tubes were shaken vigourously by hand for 15 s and incubated at room temperature for 3 min. Samples were centrifuged at 10,000 g for 15 min at 4°C. Following centrifugation, the aqueous phase containing RNA was transferred to a fresh tube and the RNA was precipitated by mixing with isopropyl alcohol (0.5 mL per 1 mL of TRizol Reagent) and standing at room temperature for 10 min before being centrifuged at 10,000 g for 10 min at 4°C. The supernatant was removed from the RNA pellet which formed at the bottom of the tube, and the pellet was washed once by adding 75% (v/v) ethanol. Samples were mixed by vortexing and centrifuged at 7,000 g for 5 min at 4°C. The RNA pellet was briefly air-dried for 5 min and dissolved in 50µL RNase-free water by passing the solution a few times through a pipette tip, and incubated for 10 min at 58°C.

2.2.4.2. RNA clean-up

Total RNA was purified using the RNeasy Total RNA Mini Kit (Qiagen, UK) as described by the manufacturer to remove contaminating phenol. RNA samples were adjusted to a volume of 100µL with RNase-free water, and 350µL of Buffer RLT (Lysis buffer supplied by RNeasy Kit containing 25-50% (w/v) guanidine thiocyanate) was added. Samples were mixed, 250µL ethanol (96-100%)

was added to the diluted RNA and mixed well by pipetting. Samples were transferred to an RNeasy Mini spin column, placed in a 2 mL collection tube, and centrifuged for 15 s at 13,500 g. The flow-through was discarded and 500µL of Buffer RPE (Membrane bound RNA washing buffer supplied by Qiagen) was added to the RNeasy spin column and centrifuged for 15 s at 9,000 g to wash the spin-column. The flow-through was discarded and 500µL of Buffer RPE was added once more to the RNeasy spin column and centrifuged for 2 min at 13,500 g to wash the spin column. The RNeasy spin column was then placed in a new 1.5 mL collection tube, and 30µL of RNase-free water was added directly to the spin column, and the mixture was centrifuged for 1 min at 9,000 x g to elute the RNA.

2.2.4.3. Determination of RNA concentration

The ratio of the optical densities from RNA samples measured at 260 and 280 nm in a spectrophotometer (Molecular Devices, SPECTRA® Max plus), was used to evaluate nucleic acid purity, and total RNA concentrations were determined by the absorbance at 260 nm. The A_{260}/A_{280} ratio of pure RNA is between 1.7 and 2 depending on base composition. At a wavelength of 260 nm, the extinction coefficient for a single-stranded RNA is 38 $(\mu g/mL)^{-1}$ cm^{-1}. Thus, an optical density (OD) of 1 corresponds to 38 µg/mL for single-stranded RNA (Alberts, 1994). Concentrations and ratios were then confirmed by nanodrop spectrophotometer sample analysis.

2.2.4.4. Microarray analysis of differential mRNA expression

RNA from untreated Rama 37 T-25 cells were compared to that from Rama 37 T-25 cells treated with 67.5 nM doxycycline for 72 h. Three separate experiments were performed and total RNA was prepared from each sample, and used to generate cRNA, which was labelled with biotin using the GeneChip® Two-Cycle Target Labeling kit from Affymetrix. cRNAs were then hybridised to GeneChip Rat Genome arrays (Affymetrix). A GeneChip Test 3 Array, containing a subset of 155 genes from several organisms including mammalian, plants and eubacteria, was run to provide a convenient and accurate quality determination of labelled target RNA, prior the main run on an Affymetrix GeneChip Rat Genome 230 2.0 array. This array

carried 31,024 probe sets representing 28,700 well-substantiated rat genes and was purchased from Affymetrix (UK). The endogenous genes used for this chip were GAPDH, beta-actin, and hexokinase 1. After a successful test, biotin-labelled cRNAs were then hybridised on 6 Affymetrix GeneChip Rat Genome 230 2.0 arrays with the technical assistance of Dr Lucille Rainbow. After washing, the chips were scanned and data were analysed.

- Microarray data analysis

Microarray data analysis was provided by Mr Brian Lane. The raw data (CEL files) from the rat Genome arrays were representing 3 separate RNA preparations of untreated and 3 separate RNA preparations of doxycycline-treated Rama 37 T-25 cell lines, the latter expressing intracellular S100P, were loaded into the R statistical environment (v2.7.0) and processed with the appropriate (Gautier et al., 2004) package of the BioConductor open-source library (Gentleman et al., 2004). Perfect match (PM) and Mis-Match (MM) data were generated and the MAS 5 algorithm was applied to these data to construct an ExpressionSet object which contained single expression data values for each probe in each of the six arrays. These linear-modeling results were subjected to an empirical Bayes moderation of standard error using the limma package for BioConductor (v2.12.0), which allows simultaneous analysis and comparison between many RNA targets to determine differential gene expression (Wettenhall and Smyth, 2004). The model of induced - uninduced gene S100P expression differences generated first a standard linear model with associated p-values indicating the significance of differential expression (DE) for each gene and a Bayesian version of the model, as well as a false discovery rate (FDR) adjustment for multiple testing (Smyth et al., 2003). The false discovery rate (FDR) was proposed by Benjamini and Hochberg (1995) and is defined as the expected proportion of false positive scores among the total number of significant scores. Algorithms based on FDR explore the elimination of false positives and negatives independent of the number of samples being tested (Storey and Tibshirani, 2003). The moderated p-value generated through FDR control sets a threshold for an expected proportion of false positives in the selected gene list (i.e. a p-value threshold of 0.05 should result in less than 5% of the genes on the selected list being false positives). Output included the Bayesian equivalent of a p-value, an

FDR adjusted p-value, the fold-change associated with the gene expression differences and the log-odds of DE associated with each gene. Genes with evidence of DE have log-odds >0, while those with no evidence of DE have log-odds<0 (Bolstad et al., 2003).

- Microarray validation

cDNA was synthesised from the same set of RNA used for the microarrays samples. Levels of individual mRNAs were measured with quantitative real-time PCR. A standard curve was generated for each gene, composed of known serial dilutions of cDNA, in order to establish the relationship between threshold cycle (Ct) and mRNA concentration. Glyceraldehyde-3-phosphate dehydrogenase (GAPDH) mRNA levels were determined for all samples as a reference, and levels of each mRNA were calculated as a ratio of the candidate gene/GAPDH values (Freeman et al., 1999).

2.2.5. POLYMERASE CHAIN REACTION

2.2.5.1. Reverse transcription

Reverse transcription was performed according to the manufacturer's conditions (Promega). Two μg of total RNA isolated from cell lines and cleaned up (as descibed in Section 2.4.2.) were placed in a sterile RNase-free microcentrifuge tube, and mixed with 1μL of Random hexamer and 1μL of a mixed dNTP stock (10mM each dATP, dGTP, dCTP, dTTP) in a total volume of 15μL. Tubes were heated to 70°C for 5 min to melt secondary structure within the template, and thereafter cooled immediately on ice for 1 min to prevent secondary structure from reforming. Tubes were then centrifuged briefly to collect the solution at the bottom of the tube. Samples were then mixed with 5μL 5X Reaction Buffer (250mM Tris-HCl (pH 8.3), 375mM KCl, 15mM $MgCl_2$, 50mM DTT), 50 units of Moloney murine leukemia virus reverse transcriptase (M-MLV) RT, 25 units of recombinant RNasin ribonuclease inhibitor and DEPC-treated nuclease-free water to a final volume 25μl. Contents of tubes were mixed gently by flicking and were then incubated for 30 min at 42°C (Sambrook and Russell, 2001).

2.2.5.2. Polymerase chain reaction

PCR reactions (Sambrook and Russell, 2001) contained DNA template (100 ng), 2 pM forward primer, 2 μM reverse primer, 2 mM dNTP-mix, 1 μL of $MgCl_2$, 2.5 μL of NH4 Buffer (750 mM Tris-HCl pH 8.8, 200 mM $(NH4)_2SO_4$, 0.1 % (v/v) Tween 20), 0.2 units of *Taq* DNA polymerase (Fermantas, UK) and PCR quality H_2O to a final volume of 25 μL. Cycling reactions were composed of primary denaturation stage at 95°C for 5 min; 30 cycles of denaturation at 95°C for 30 sec, an annealing step between 58-62°C (depending on primer annealing temperatures) for 30 sec, an elongation at 72°C for 30 sec, and a final elongation stage 72°C for 5 min. The samples were held at 4°C. A minimum of 5 μL of the PCR reaction was analysed by agarose gel electrophoresis to verify the product size.

2.2.5.3. Quantitative real-time Polymerase Chain Reaction

PCR primers for quantitative real-time PCR experiments were designed with the Primer 3 (v. 0.4.0) design software available online: (http://frodo.wi.mit.edu/primer3/). A Blast search was then performed on the NCBI website (http://blast.ncbi.nlm.nih.gov/Blast/) to ensure the uniqueness of the primer sequences (Altschul et al., 1990). The PCR primers were designed to cross intron–exon boundaries (to allow detection of products of contaminating genomic DNA) for each particular cDNA.

cDNA templates obtained from RNA samples was amplified by using SYBR®Green PCR master mix (Applied Biosystems). The real-time PCRs were performed in a 7500 Fast Real-Time PCR System (Applied Biosystems, USA) under the following conditions: 95°C for 5 min, followed by 40 cycles at 95°C for 30 sec, 60°C for 30 sec, and 72°C for 30 sec.

Melting curve analyses were performed following the qPCR. The specificity of the amplicons was confirmed by the presence of a single peak. A standard curve, consisting of a dilution series of cDNA, was used to determine the efficiency of the PCR reaction. Standard curves were generated using a ten-fold serial dilution of a cDNA pool, and these enjoyed a linear correlation coefficient (R^2) of 0.991-0.999. Based on the slopes of these standard curves, the estimated PCR amplification efficiencies were calculated from the slope

of the standard curve using the following formula E = 10^[(-1/R) -1]*100. Efficiencies were ranged from 94% to 102% (cf Primers table in section 2.1.5.1).

Calculation of efficiency and relative quantification was normalised to that of the reference gene (GAPDH) and was carried out using the standard curve method (Freeman et al., 1999). Individual samples were always measured in triplicate to ensure reliability.

2.2.5.4. SiRNA

Small Interfering RNA (SiRNA) were purchased from Qiagen and sequences are displayed in Table 2.1.6 SiRNA transfection was performed using HiPerfect Reagent according to the Qiagen protocol. On the day of transfection, 6 x 10^4 cells were seeded per well of a 24 well plate in 0.1 mL of Routine Medium. Cells were incubated under normal growth conditions. 5nM SiRNA was diluted in 100 µL culture medium without serum. After mixing by vortexing, 3 µL of HiPerFect transfection reagent were added to the diluted SiRNA and vortexed for 10 s. Samples were incubated for 5-10 min at room temperature to allow formation of transfection complexes. Complexes were added, drop-wise onto the cells and the plate was swirled gently to ensure uniform distribution of the transfection complexes. Cells were then incubated with the transfection complexes under normal growth conditions. After 3 h, 400 µL of Routine Medium was added and the cells were incubated and gene silencing monitored.

To visualise SiRNA transfection efficiency, fluorescein-labelled, double-stranded RNA duplex (BLOCK-IT™ Fluorescent Oligos, Invitrogen ™) were transfected with SiRNA probes (sequences displayed in Section 1.6.). Fluorescence was visualised after 12 h with a fluorescent microscope to visualise the transfection efficiency.

Knockdown of MAST1 using SiRNA probes was compared to control probes, AllStars Negative Control SiRNA, a validated negative control SiRNA from Qiagen. This SiRNA has no homology to any known mammalian gene. It has been validated using Affymetrix GeneChip arrays and a variety of cell-based assays and shown to have minimal nonspecific effects on gene expression and phenotype (presented in "data for AllStars Negative Control SiRNA", Qiagen).

2.2.5.5. Statistical analysis

All Statistical differences between groups were conducted using a Student's t-test. Data presented for migration assays, cell staining, and gene expression fold change are in the mean and standard deviation (S.D.) of triplicate experiments performed three times. *P* value of less than 0.05 was considered a statistically significant difference. Statistical calculation were performed using Sigmaplot X and Excel software.

Chapter 3

Identification of S100P as a Protein Associated with Increased Cell Migration

3.1. Introduction

Tumour-cell invasion and metastasis is conventionally understood as the process whereby individual cells detach from the primary cancer, enter lymphatic vessels or the bloodstream and seed in distant organs (Gabriel, 2007). The ability to migrate is a prerequisite for a cancer cell to escape the primary tumour and enter the circulation, and is highly dependent upon the ability of tumour cells to undergo directional migration (Bailly et al., 1998). The tumour cell responds to stimuli in the microenvironment that signals its detachment from the primary tumour mass, invasion through the extracellular matrix and migration towards a blood vessel (Wyckoff et al., 2000). It is a complex mechanism, and studies have associated some of the S100 protein family members with metastasis and provided evidence suggesting an influential role in metastasis promotion through a number of different processes (Salama et al., 2008) such as interactions with matrix metalloproteinases (Bjornland et al., 1999), transcription factor regulation (Grigorian et al., 2001), and migration (Takenaga et al., 1994a), as well as acting as chemoattractants (Devery et al., 1994).

One member of the S100 family, the metastasis inducer S100A4, has been shown to increase cell migration, and eight calcium-dependent intracellular targets of S100A4 have been identified to date: tropomyosin (Takenaga et al., 1994b), heavy chain of non muscle myosin IIA (Ford and Zain, 1995; Kriajevska et al., 1998; Kriajevska et al., 1994), protein p37 (Dukhanina et al., 1997), S100A1 (Tarabykina et al., 2000; Wang et al., 2000), p53 (Grigorian et al., 2001), methionine aminopeptidase 2 (Endo et al., 2002), the cell signalling associated liprin beta1 (Kriajevska et al., 2002) and CCN3 a member of a family of small cysteine rich secreted proteins (Li et al., 2002).

Several observations support a role of S100P in invasive growth and metastasis in cancers. During embryogenesis, S100P is expressed in trophoblasts of the placenta and, in the adult, it is weakly present in normal tissues but expressed in several cancer types (Parkkila et al., 2008), such as those of breast (Wang et al., 2006), pancreas (Logsdon et al., 2003), or lung (Beer et al., 2002), and it has been associated with poor patient prognosis in breast (Wang et al., 2006), and lung (Beer et al., 2002; Diederichs et al., 2004).

An increase in S100P protein expression has been correlated with increasing grade of pancreatic intraepithelial lesions (Ohuchida et al., 2006), and to increase cell migration and invasiveness and to be associated with high levels of tumour growth and metastasis (Arumugam et al., 2005). S100P was also associated with a hormone-refractory and metastatic phenotypes in prostate cancers (Hammacher et al., 2005). In breast cancer, increased level of S100P was associated with immortalisation and tumour progression (Guerreiro Da Silva et al., 2000; Schor et al., 2006) and poor patient prognosis (Wang et al., 2006). Moreover immunostaining of tumours overexpressing S100P showed the strongest expression in the cell nuclei (Parkkila et al., 2008; Wang et al., 2006).

Cell migration is necessary for developmental morphogenesis, tissue repair and regeneration, and has an important role in tumour metastasis. The regulation of cell migration is important, and activation of metastasis-inducing elements such as S100P stimulate the metastatic dissemination of tumour cells from their primary location to lymph or blood vessels. Two different types of cell movement are commonly described, namely random and directional movement. Random movement occurs in the absence of a stimulus, and is characteristically multi-directional with cells lacking directional persistence; this results in their moving back and forth, in circles or remaining stationary with occasional protrusions and retractions. In contrast, directional motility is usually initiated in response to a signal, one common example is chemotaxis in which cells migrate towards a source of growth factor or other chemical stimulus. Directional movement is characteristically persistent, with cells becoming polarized and subsequently migratory in straight paths toward the stimulus. One of the initial steps in cell movement is the protrusion of the cell membrane, which is driven by localised actin polymerisation (Rodriguez et al., 2003). Microtubules, one of the major components of the cytoskeleton are also essential for cell migration and cell polarisation (Goode et al., 2000).

To study the intracellular effects of S100P in tumour cells, inducible Rama 37 and HeLa cell systems have been developed in our laboratory (Dr G. Wang) to allow the regulation of the intracellular production and level of S100P. The system involved transfecting two expression plasmids into the target cells. One contains a modified tetracycline repressor under human immediate-early (CMV) promoter control (Lamartina et al., 2003) and the other, the S100P coding region cloned

downstream of a tetracycline regulatory element (Figure A.1) (Wang et al. submitted for publication). The resulting rat mammary Rama 37 T-25 cell line and HeLa A-9 cell lines originate from clones transfected with the inducible system. Rama 37 pcDNA3-e (empty vector) and Rama 37 pcDNA3-S100P cell line clones constitutively expressing S100P were used to examine the role of S100P in cellular activities associated with the metastatic process (Figure A.2). Rama 37 cells were chosen as the *in vitro* model, because they express a very low amount of endogenous S100P, which is undetectable by Western blotting and results were analysed and correlated to the human system using HeLa cells for similar reasons.

3.2. Results

3.2.1. Induction of S100P protein

When Rama T-25 cells were treated with doxycycline, production of intracellular S100P was induced from the transfected inducible vectors. To confirm the induction of S100P in stable transfected cell lines, in which S100P production could be induced by doxycycline treatment, intracellular proteins were extracted from doxycycline-treated and control untreated cells and subjected (as described in Materials and methods Section 2.2.1.1.g.) to Western blot analysis. Analysis showed that the maximum level of S100P protein was obtained with 67.5 nM doxycycline for Rama 37 T-25 and 112.5 nM doxycycline treatment for HeLa A-9 cells for 48 h (Figure 3.1 and Figure 3.2).

A

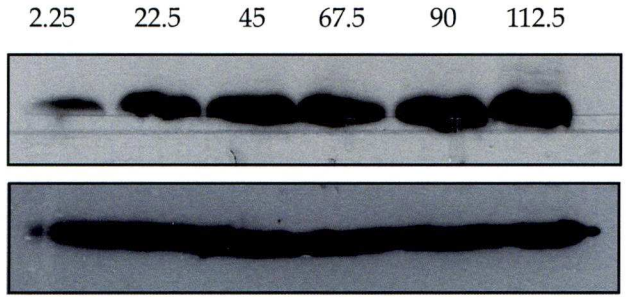

B

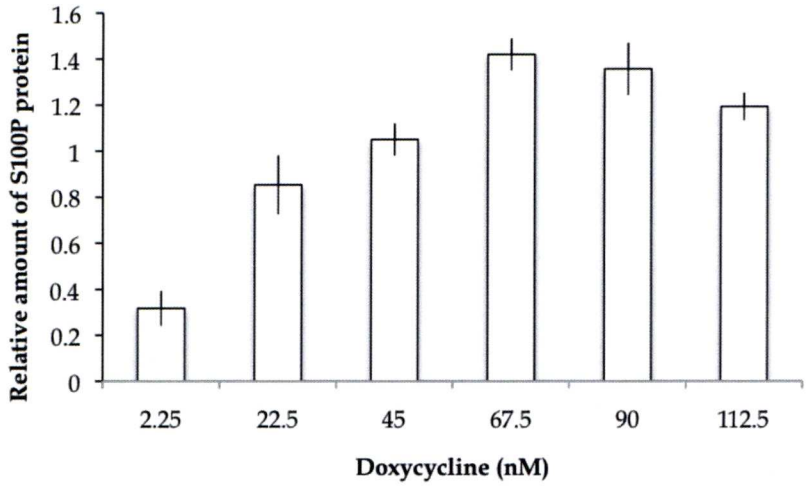

C

Doxycycline (nM)	2.25	22.5	45	67.5	90	112.5
Relative amount of S100P (Mean)	0.32	0.85	1.05	1.42	1.36	1.19
Standard deviation (S.D.)	0.08	0.13	0.07	0.08	0.11	0.06

Figure 3.1 **The effect of doxycycline concentration on the relative amount of intracellular S100P in inducible Rama 37 T-25 cells**

A. *Western Blot analysis showing a representative experiment of intracellular expression of S100P and β-actin in inducible Rama 37 T-25 cells with concentrations of doxycycline shown.*

B. *Histogram showing the relative amount of intracellular S100P proteins compared to β-actin proteins detected by Western Blot. Error bars represent the standard deviation calculated from three separate blots.*

C. *Table showing the relative amount of intracellular S100P extracted from induced Rama 37 T-25 cells with concentration of doxycycline shown, and the standard deviation calculated from three separate blots.*

A

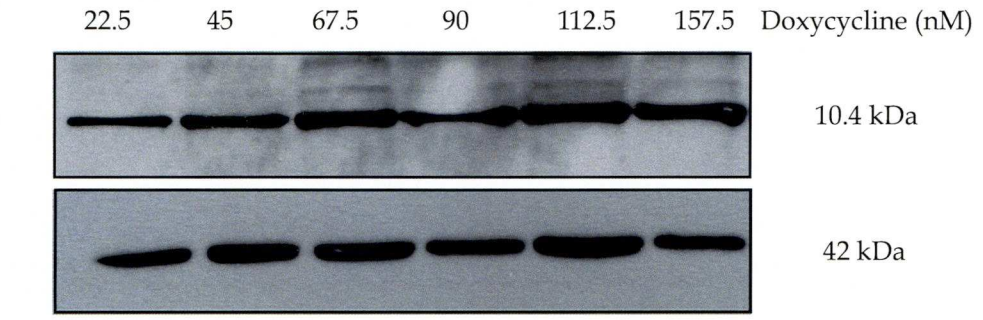

B

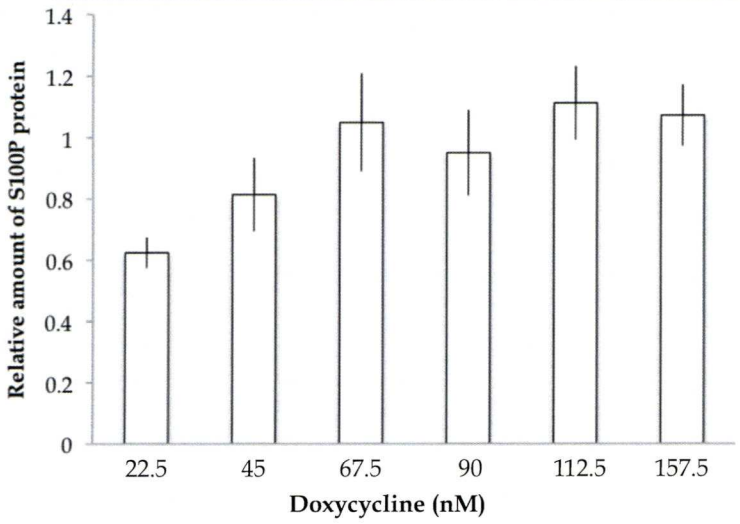

C

Doxycycline (nM)	22.5	45	67.5	90	112.5	157.5
Relative amount of S100P (Mean)	0.62	0.81	1.05	0.95	1.11	1.07
Standard deviation (S.D.)	0.05	0.12	0.16	0.14	0.12	0.1

***Figure 3.2* The effect of doxycycline concentration on the relative amount of intracellular S100P in inducible HeLa A-9 cells**

A. *Western Blot analysis showing a representative experiment of intracellular expression of S100P and β-actin in inducible HeLa A-9 cells with concentrations of doxycycline shown.*

B. *Histogram showing the relative amount of intracellular S100P proteins compared to β-actin proteins detected by Western Blot. Error bars represent the standard deviation calculated from three separate blots.*

C. *Table showing the relative amount of intracellular S100P extracted from induced Rama 37 T-25 cells with concentration of doxycycline shown, and the standard deviation calculated from three separate blots.*

When Rama 37 T-25 cells were treated with 67.5 nM of doxycycline, and extracts of the cells subjected to Western blotting, the results showed a single band on the gel at the expected molecular weight for S100P of 10.4 kDa within 24 h of adding doxycycline (Figure 3.3 A). The same band was visible up to 96 h of doxycycline treatment. Quantitation of 3 separate Western blotting experiments showed a significant, 5-fold increase in the intracellular S100P/β-actin ratio up to 72 h (Figure 3.3 B), $p < 0.0001$ (Student's t-test, comparison between 72 h of doxycycline treatment and untreated cells).

Thereafter, between 72 and 96 h, there was no further significant increase in the S100P/β-actin ratio, which remained at 5 fold ($p = 0.835$, Student's t-test comparison between 72 h and 96 h of treatment). Conversely, when the Rama 37 T-25 cells were not treated with doxycycline, there was no significant increase in the S100P/β-actin ratio between zero and 96 h of induction ($p = 0.694$, Student's t-test).

A

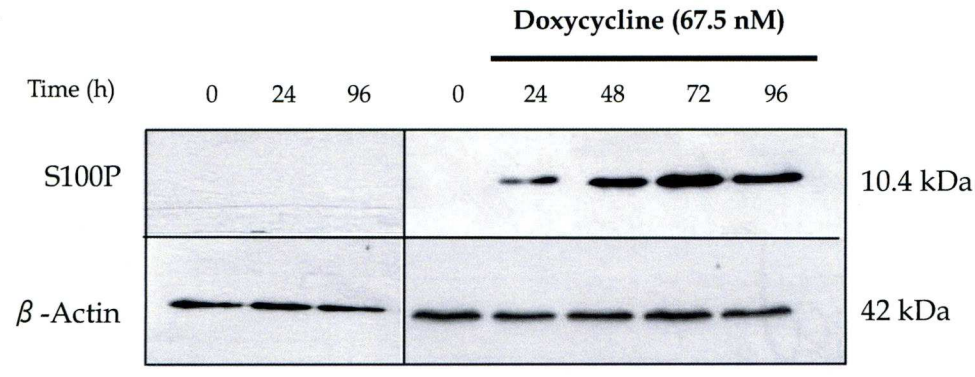

B

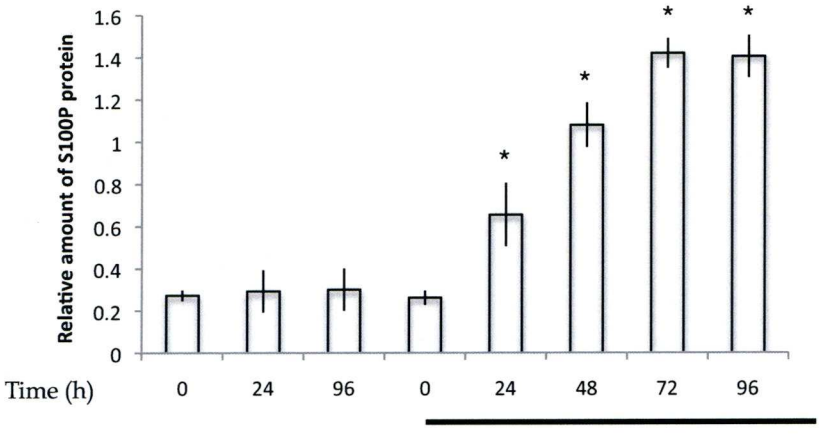

C

	Untreated cells			Doxycycline (67.5 nM)				
Time (h)	0	24	96	0	24	48	72	96
Relative amount of S100P (Mean)	0.27	0.29	0.30	0.26	0.65	1.08	1.42	1.40
S.D.	0.02	0.1	0.1	0.33	0.15	0.1	0.07	0.1
p value	/	0.56	0.69	/	0.02	0.004	0.0001	0.0001

***Figure 3.3* Stimulation of intracellular production of S100P protein in inducible Rama 37 T-25 cells.**

A. Western Blot analysis showing a representative time course of intracellular expression of S100P and β-actin in inducible Rama 37 cells without treatment with 67.5 nM doxycycline.

B. Bar chart showing the relative amount of S100P proteins compared to β-actin proteins detected by Western Blot

C. Table showing Student's t-test results between cells non-expressing S100P and cells expressing S100P at the time shown. Data show mean ± S.D from three independent experiments ($p < 0.05$).*

Total RNA was harvested from the cells and relative expression levels of S100P mRNA were determined by quantitative real-time PCR (as described in Materials and methods Section 2.2.4). Quantitative real-time PCR experiments confirmed the Western blot observations and revealed an increased level of S100P mRNA expression in Rama 37 T-25 cells treated with doxycycline for 72 h (Figure 3.4). Expression of S100P mRNA was normalised to the transcript of the reference gene GAPDH, and was compared to RNA from non-expressing, S100P-untreated Rama 37 T-25 cells (Figure 3.4 A). These quantitative real-time PCR experiments indicated a 13-fold upregulation of S100P mRNA (Figure 3.4 A). This value is consistent with the 10-fold increase of S100P protein in the inducible Rama 37 cells upon induction.

A constitutive Rama 37 pcDNA3-S100P cells transfected with a constitutive expression vector, pcDNA3, containing S100P cDNA were also analysed by quantitative real-time PCR and Western blotting, then compared to Rama 37 cells transfected with an empty pcDNA3 vector (Rama 37 pcDNA3-e), to determine whether the inducible system is inducing the mRNA and protein to levels similar to the constitutively-transfected cells relative to non-expressing cells. Quantitative real-time PCR analysis of the constitutively-expressing rat cells revealed a significant 17-fold upregulation of relative S100P mRNA (p = 0.002, Student's t-test) and Western blotting revealed a significant 12-fold upregulation of S100P protein (p = 0.001, Student's t-test) relative to empty vector control cells (Figure 3.4). No detectable S100P protein bands were visible by Western blot in empty vector control cells (p = 0.0005, Student's t-test) (Figure 3.4 A-B). Quantitative real-time PCR analysis indicated differences between the inducible system S100P protein mRNA expression and vector constitutively overexpressing S100P, with a stronger staining intensity in cells constitutively expressing S100P. These observations were confirmed by western Blotting (Figure 3.4)

A

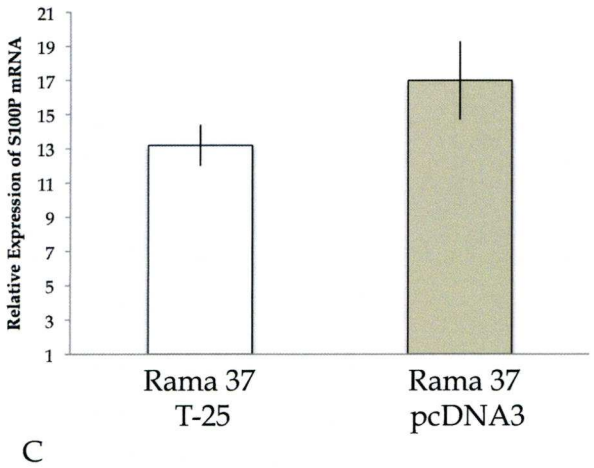

B

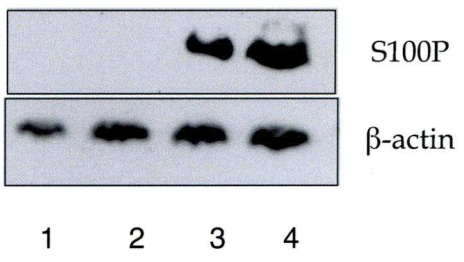

C

	Rama 37 T-25	Rama 37 pcDNA3
Relative amount of S100P mRNA (Mean)	13.2	17
S.D.	13.2	17

	1	2	3	4
Relative amount of S100P protein (Mean)	0.26	0.3	1.44	1.5
S.D.	0.01	0.03	0.09	0.11

***Figure 3.4* S100P mRNA and protein expression in Rama 37 cells**

A. *Quantitative RT-PCR showing the levels of S100P in transfected Rama 37 cells. Expression levels were measured from cell cultures isolated at 0 h and after cultivation in medium containing doxycycline (67.5 nM) for 72 h. The qPCR result were first normalised to housekeeping gene GAPDH. Finally, this normalised expression was compared to untreated cells (for Rama 37 T-25) and cells transfected with empty pcDNA3 vector for Rama 37 cells transfected with pcDNA3, constitutively overexpressing S100P.*

B. *Western Blot analysis showing intracellular expression of S100P and β-actin in transfected Rama 37 cells.*

1: Rama 37 cells transfected with pcDNA3 Empty vector.

2: Rama 37 T-25 cells transfected with the T-Rex Inducible system with S100P cDNA but not treated with doxycycline.

3: Rama 37 T-25 cells induced to express S100P by treatment with doxycycline (67.5 nM) for 72 hours.

4: Rama 37 cells transfected with S100P cDNA in pcDNA3.

C. *Table showing the relative amount of intracellular S100P extracted from induced Rama 37 T-25 cells with doxycycline for 72 h and for Rama 37 cells transfected with S100P cDNA in pcDNA3. Standard deviation were calculated from three separate qPCR experiment and three separate blots.*

To find out whether the human inducible system behaved in the same way as the rat inducible system, the induction of S100P was carried out on the HeLa A-9 cells. QPCR experiments showed a significant 10-fold upregulation of S100P mRNA after 72 h of 112.5 nM doxycycline treatment ($p= 0.001$, Student's t test) (Figure 3.6 C), which shows that the human inducible system behave similarly to the rat inducible system, with a similar fold induction of mRNA.

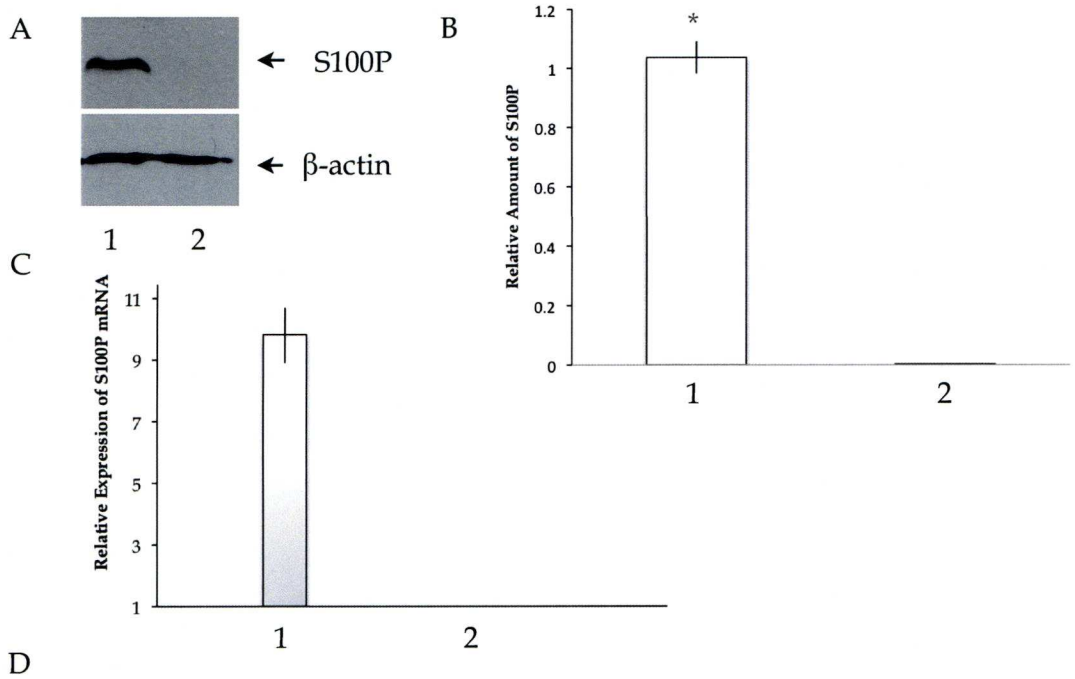

	1	2
Relative amount of S100P protein (Mean)	1.04	0.03
S.D	0.05	0.00006
Relative amount of S100P mRNA (Mean)	9.8	1
S.D.	0.9	0.1

Figure 3.5. **Stimulation of intracellular production of S100P protein in inducible HeLa A-9 cells.**

A. Western Blot analysis showing intracellular expression of S100P and β-actin in transfected HeLa A-9 cells (1) with or without (2) a 72 h of 112.5 nM doxycycline treatment.

*B. Histogram showing the relative amount of S100P protein compared to β-actin protein detected by Western Blot in transfected HeLa A-9 cells (1) with or without (2) a 72 h of 112.5 nM doxycycline treatment (Student's t-test, * $p < 0.05$).*

C. Quantitative RT-PCR showing relative expression levels of S100P mRNA in HeLa A-9 cells after and before 72 h of doxycycline treatment. Expression levels were measured from cell cultures isolated at 0 h and after cultivation in doxycycline (112.5 nM) treated medium for 72 h. The results were first normalised to the housekeeping mRNA for β-actin. Finally, expression was compared to untreated HeLa cells transfected with T-Rex inducible system).

3.2.2. Intracellular S100P stimulates cell migration in vitro

3.2.2.1. Rat mammary cells

To investigate potential effects of S100P on rat mammary cell migration, chemotactic analyses *in vitro* were performed with cells overexpressing intracellular S100P. Migration was measured using cells over a 24 h period in Boyden chambers (as described in Materials and methods Section 2.2.1.2.). Assays were first performed with pcDNA3-S100P cells using Rama 37 pcDNA3-e as a control. Results showed a significant increase in migration of cells overexpressing S100P (8.6%) (Figure 3.6) compared to S100P-negative Rama 37 pcDNA3-e cells (2.7 %; p = 0.00017, Student's t test).

Further analysis of the effects of S100P on cell migration were carried out with Rama 37 cells transfected with the inducible system. Migration was determined over the time periods of 0-24 h or 48-72 h of doxycycline treatment. Cells were seeded in the Boyden chamber at time 0 h or at 48 h. 24 h of doxycycline treatment is the time period which I have shown by Western blotting to produce an appreciable quantity of S100P (Figure 3.7) in the Rama 37 T-25.

Cell migration assays showed a higher percentage of migrating cells in the periods 0-24 h and 48-72 h in the presence of doxycycline and induction of S100P (Figure 3.7 A) than in the absence of the inducer. 24 h after addition of doxycycline, cell migration increased 4.6 fold compared to cells not exposed to doxycycline. There was also an increase 72 h after addition of doxycycline over those cells not treated with doxycycline, but it was less 3.9 fold. This reduction in doxycycline enhancement of migration is due to a slight increase in the number of migrating cells in the uninduced culture at later times of culture. The difference in migration in 24 h between doxycycline-treated and non-treated controls is highly significant at either time (p = 0.005 at 24 h and 0.002 at 72 h, Student's t-test, Figure 3.7 B).

A

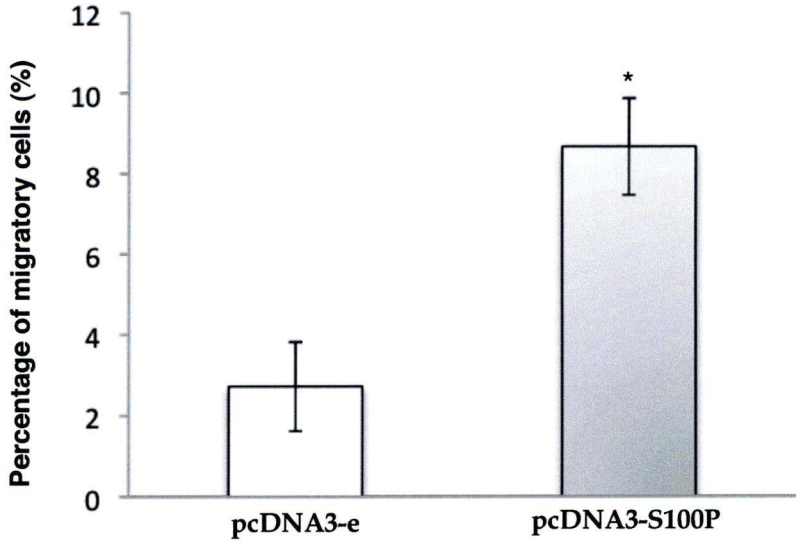

B

	pcDNA3-e	pcDNA3-S100P
Mean of Motile cells (%)	2.7	8.6
S.D	1.1	1.2
p value	P = 0.00017*	

***Figure 3.6* Stimulation by intracellular S100P of migration in the Rama 37 cell lines constitutively overexpressing S100P.**

A. *Histogram showing the mean percentage of migratory cells constitutively overexpressing intracellular S100P (grey bar), and cells non expressing S100P (white bar). Data show the mean +/- Standard Deviation (S.D.) from three separate experiments.*

B. *Table showing Student's t-test results between cells non-expressing S100P and cells expressing S100P (* $p < 0.05$).*

A

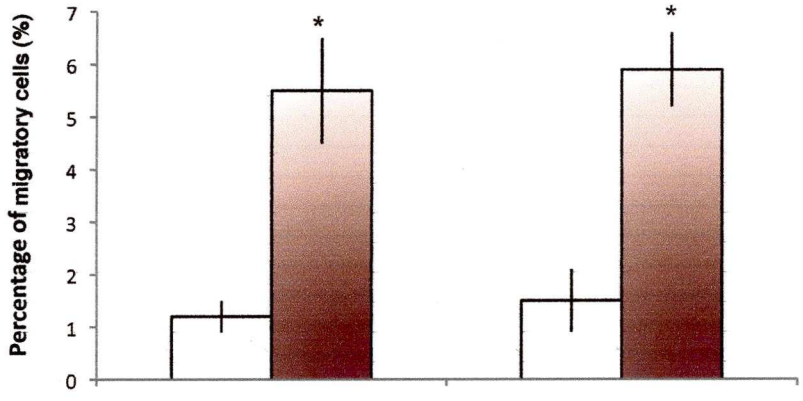

B

	24h		72h	
Doxycyline (67.5 nmol)	-	+	-	+
Mean of motile cells (%)	1.2	5.5	1.5	5.9
S.D	0.3	1	0.6	0.7
***p* value**	0.005 *		0.002 *	

***Figure 3.7* Stimulation by intracellular S100P of migration in Rama 37 T-25 cell lines.**

A. *Histogram showing the mean of percentage of migratory cells treated with 67.5 nM doxycycline (red bars) for 24 h and 72 h, and untreated cells (white bars). Data show the mean +/- Standard Deviation (S.D.) from three separate experiments.*

B. *Table representing Student's t–test results between untreated and doxycycline-treated cells (* $p < 0.05$).*

3.2.2.2. Human cells

Effects of S100P on human cell migration were investigated with HeLa A-9 cells transfected with the inducible system. As previously described, migration was determined over a 24 h period of doxycycline treatment starting at 0 h or 48 h. The percentage of migrating cells at 24 h and 72 h increased compared to untreated cells 24 h and 72 h after addition of doxycycline and induction of S100P (Figure 3.8 A). 24 h after addition of doxycycline, cells have significantly increased their migration 2.8-fold compared to cells not exposed to doxycycline, and 72 h after addition of doxycycline there was still a 2.8-fold increase of treated cells over those left untreated. The migration difference between doxycycline-treated and non-treated controls is highly significant at either time ($p= 0.003$ at 24 h and 0.002 at 72 h, Student's t-test, Figure 3.8 B).

A

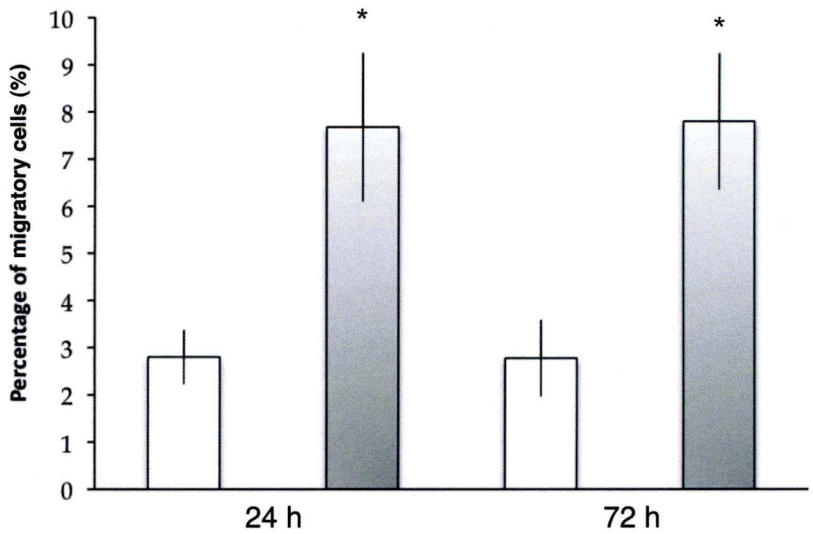

B

	24 h		72 h	
Mean of Motile cells (%)	2.8	7.7	2.8	7.8
S.D	0.6	1.6	0.8	1.5
p value	p= 0.03*		p= 0.02*	

***Figure 3.8* Stimulation by intracellular S100P of migration in HeLa cell lines overexpressing S100P.**

A. *Histogram showing the mean of percentage of migrating cells overexpressing intracellular S100P (grey bar) after 72 h of doxycycline treatment (112.5nM), and untreated cells not expressing S100P (white bar). Data show the mean +/- Standard Deviation (S.D.) from three separate experiments.*

B. *Table showing Student's t–test results between cells non-expressing S100P and cells overexpressing S100P (* $p < 0.05$).*

3.2.3. Intracellular Distribution of S100P

Overexpression of S100P has been detected in several cancers such as breast (Guerreiro Da Silva et al., 2000), colon (Birkenkamp-Demtroder et al., 2005), prostate (Averboukh et al., 1996), pancreatic (Logsdon et al., 2003) and lung (Diederichs et al., 2004). This protein has also been functionally implicated in carcinogenic processes such as cellular immortalisation (Guerreiro Da Silva et al., 2000). The role of S100P implication could be dependent on its subcellular location. Nuclear, cytoplasmic, and extracellular location of S100P is evident in the vast majority of S100P expressing cells (Arumugam et al., 2004; Fuentes et al., 2007; Wang et al., 2006). Thus, in this section, the subcellular distribution of S100P following its induction with doxycycline in the T25 cells has been examined.

3.2.3.1. Subcellular distribution of induced S100P

Intracellular localisation and level of S100P in Rama 37 cells was examined by immunohistochemistry to show the subcellular distribution of S100P protein expression at the microscopic level (as described in Materials and methods Section 2.2.1.4.a.). The immunostaining corroborated the Western blot data, whereby the level of S100P protein in cells treated with doxycycline was much higher than that in untreated cells (Figure 3.9). In untreated Rama 37 T-25, few cells showed the presence of detectable S100P (Figure 3.9 A a). In Rama 37 T-25 cells treated with doxycycline (67.5 nM), intracellular S100P was detected from 24 h up to at least 96 h (Figure 3.9 A b-e), consistent with the Western blotting data (Figure 3.2). 63% of total cells after 24 h, increasing to 80% after 48 h, 89% after 72 h and decreasing to 78% at 96 h (Figure 3.9 B).

Quantification of the intracellular distribution of S100P between cytoplasm and nucleus in the T-25 cells (Figure 3.9 B) revealed that in untreated cells, after 48 h, 5% of the cells showed the presence of S100P in the cytoplasm and 5% S100P in the nucleus, but this staining might be due to non-specific antibody staining or to a minimum of S100P protein undetectable by Western blotting. In contrast, when T-25 cells were treated with doxycycline, S100P was present in the cytoplasm of 52% of cells at 24 h, 30% at 48 h, 48% at 72 h and only 34% at 96 h of S100P induction (Figure 3.9 B). Nuclear S100P staining was significantly detected after 24 h of

treatment, but only in less than 10% of total cells ($p = 0.021$, Student's t-test between nuclear staining of untreated cells and cells treated with doxycycline (67.5 nM) for 24 h). However, the proportion of nuclear staining cells increased to 50% at 48 h ($p = 0.0002$, Student's t-test, compared between cell treated for 24 and 48 h and remained at more than 40% ($p < 0.0001$, Student's t-test, comparison between cells treated for 72h and 96 h) at both 72 h and 96 h of doxycycline treatment. In contrast to the nuclear staining, the proportion of cells exhibiting cytoplasmic staining of S100P, highly significantly increased to 50% of cells at 24 h ($p = 0.0002$, Student's t-test between cytoplasmic staining of untreated cells and treated with doxycycline (67.5 nM) for 24 h) but then significantly decreased to only 30% at 48 h ($p = 0.001$, Student's t-test), and then significantly increased again to 50% of cells ($p < 0.0002$, Student's t-test), and after 96 h of treatment, the number of cells with S100P cytoplasmic staining once again significantly decreased to less than 40% ($p= 0.0002$, Student's t-test) (Figure 3.9 B).

In the above analysis, cells stained for both cytoplasmic and nuclear were classified as nuclear stained, since a translocation of S100P to the nucleus was observed. The presence of S100P going to the nucleus raises the question of a potential role in gene expression. When cells were untreated, nearly all cells were unstained at any time, but after treatment even if there were still a high proportion of unstained, it decreased during the time course, 38% after 24 h ($p < 0.0001$, Student's t-test), 20% at 48 h ($p < 0.0001$, Student's t-test), and a minimum of 11% at 72 h ($p <0.0001$, Student's t-test). After 96 h of treatment there was a slightly higher level with 20% of cells unstained ($p < 0.0001$, Student's t-test).

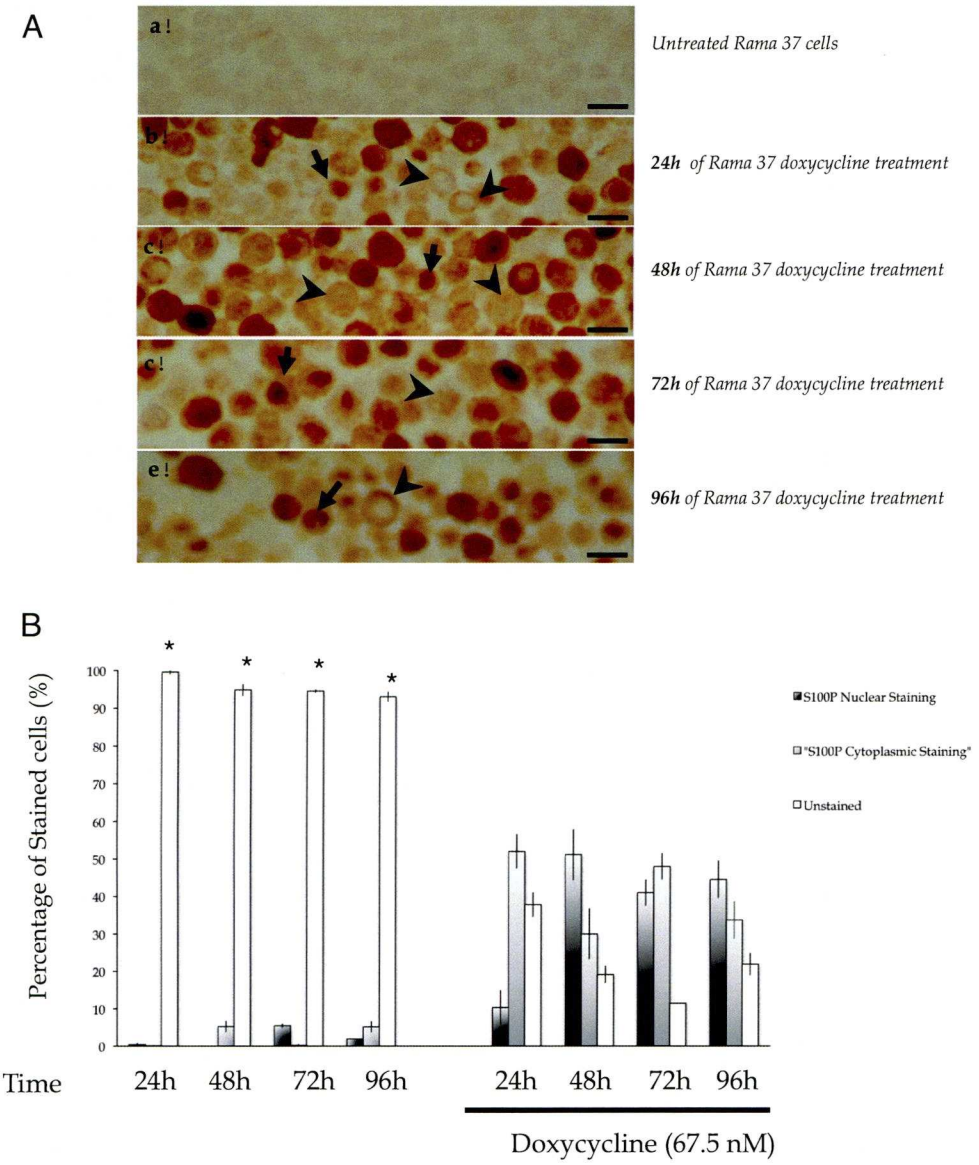

***Figure 3.9* Intracellular S100P protein expression in inducible Rama 37 T-25 cells detected by immunohistochemistry.**

A. *Imunocytochemical staining for S100P of inducible Rama 37 T-25 cells for untreated cells and treated cells for 96 h with 67.5 nM of doxycycline. The stain was cytoplasmic (arrowheads) and nuclear (arrows).*

(Magnification: x40; Bar 12 μm.)

B. *Histogram representing percentage of cells after S100P immunohistochemical detection. White bars show unstained cells, black bars show an S100P nuclear cell staining, and grey bars show a cytoplasmic S100P cell staining.*

($p < 0.05$)*

S100P was additionally detected by immunofluorescence to compare the presence of intracellular S100P after activation of the inducible system by treatment with doxycycline in Rama 37 cells (67.5 nM) and HeLa cells (112.5 nM) (Figure 3.10). No S100P was detected before treatment (Figure 3.10 A_1), and S100P was detected in Rama 37 T-25 treated cells for 72 h (Figure 3.10 A_2) with 35% of S100P nuclear staining ($p < 0.0001$, Student's t-test analysis between untreated cells and treated cells for 72 h with doxycycline (67.5 nM)) and 55% of cytoplasmic staining ($p < 0.0001$, Student's t-test analysis between untreated cells and treated cells for 72 h with doxycycline (67.5 nM)). Results accorded with previous observations (Parkkila et al., 2008; Rehbein et al., 2008; Sato and Hitomi, 2002; Tong et al., 2010; Wang et al., 2006; Whiteman et al., 2007). More types of cell lines were analysed by immunofluorescence in order to find out whether the presence of nuclear S100P was just a feature of the inducible Rama 37 cell lines. Rama 37 cell lines constitutively expressing S100P were examined for nuclear and cytoplasmic S100P. In Rama 37 pcDNA3-e cells, no intracellular S100P was detected (Figure 3.10 B_1) but was detectable in 90% of Rama 37 pcDNA3-S100P cell cultures constitutively expressing S100P. Staining analysis revealed 30% of nuclear staining ($p < 0.0001$, Student's t-test analysis between S100P expressing and non-expressing cells) and 60% of cytoplasmic staining ($p < 0.0001$, Student's t-test). The proportion of nuclear staining is consistent with that of 44% obtained using the inducible Rama 37 system after the same period of 72 h.

Human HeLa A-9 cells transfected with the inducible systems were also analysed by immunofluorescence, and again untreated cells did not reveal any S100P (Figure 3.10 C_1). Immunofluorescence was apparent after treatment (Figure 3.10 C_2), although at an apparently lower level than in the pCDNA-3 and T25 cells, with 40% of unstained cells after 72 h of doxycycline treatment (112.5 nM), 15% of nuclear staining and 45% of cytoplasmic staining. In summary, intracellular expression of S100P could be induced in the two entirely independent cell lines transfected with a S100P cDNA inserted in an inducible system sensitive to doxycycline.

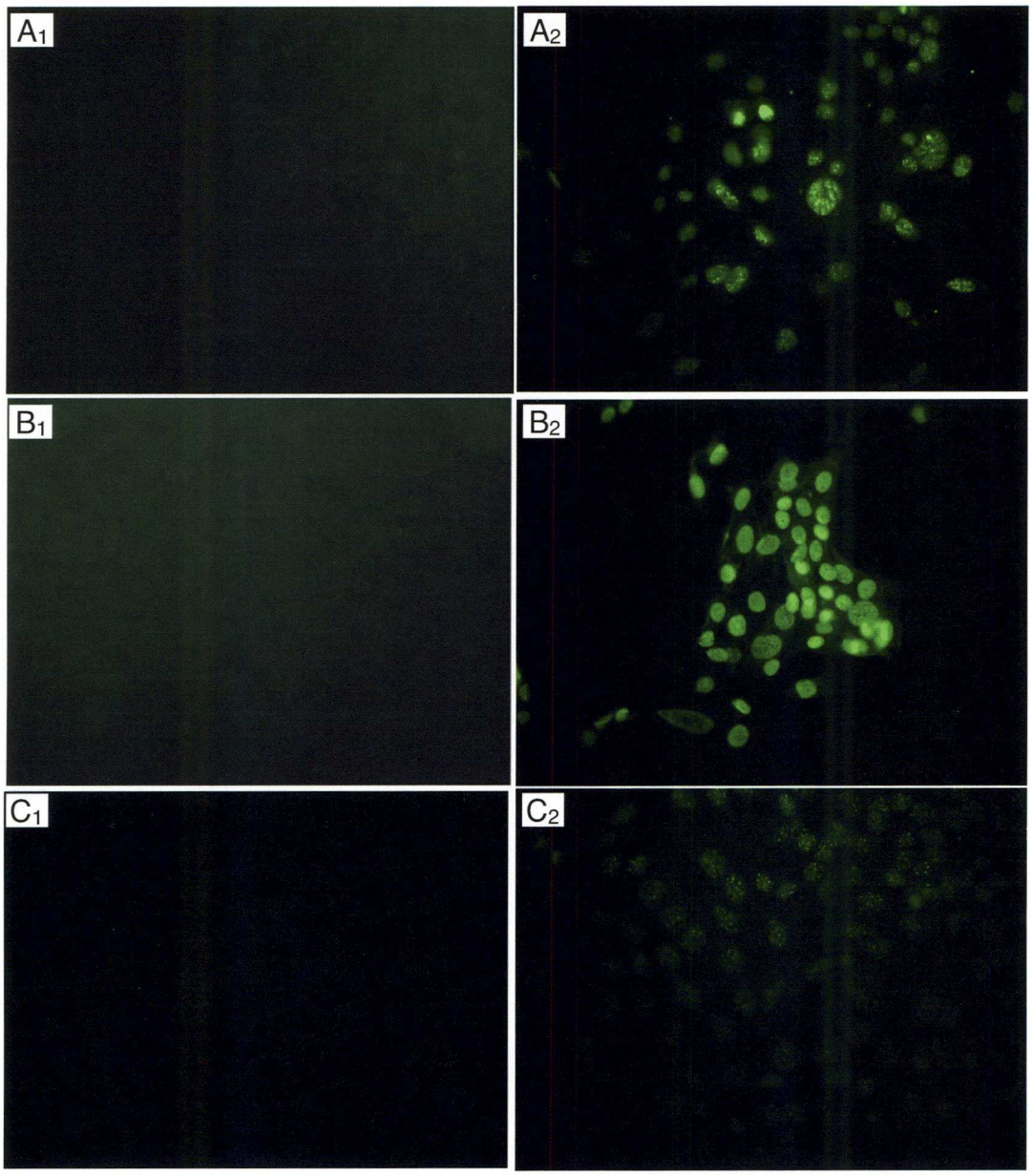

Figure 3.10 **Immunofluorescence microscopy showing expression of intracellular S100P protein.**

A. Immunofluorescence for S100P in Rama 37 cells transfected with the inducible system.

A_1. Untreated Rama 37 cells.

A_2. Rama 37 cells treated for 72 h with doxycycline (67.5 nM) to activate intracellular S100P production.

B. Immunofluorescence for S100P in Rama 37 cells transfected with a pcDNA3 vector.

B_1. Rama 37 cells transfected with a pcDNA3 vector only

B_2. Rama 37 cells transfected with a pcDNA3 containing a S100P cDNA sequence.

C. Immunofluorescence for S100P in HeLa cells transfected with the inducible system.

C_1. Untreated HeLa cells

C_2. HeLa cells treated for 72 h with doxycycline (112.5 nM) to activate intracellular S100P production.

(Magnification: x50)

Observations confirmed the ability of S100P to translocate to the nucleus. Different degrees of translocation have been observed between Rama 37 cells, and HeLa cells showing higher nuclear S100P presence in rats cells rather than Human cells. All these observations combine to suggest that S100P might have a potential nuclear function. Furthermore these observations will be important to help us understand and characterise the intracellular effects of S100P.

3.2.4. Discussion

Literature indicates that S100P is an active constituent of cancer phenotype (Birkenkamp-Demtroder et al., 2005; Parkkila et al., 2008), associating an over-expression of S100P with tumour progression and development (Arumugam et al., 2005; Basu et al., 2008; Diederichs et al., 2004), and most importantly, S100P stimulates health degradation by inducing tumour cells to metastasise (Wang et al., 2006). Distant metastasis is the primary cause of death in cancer patients, and an important step in the metastatic process is the migration of tumour cells into surrounding host tissue.

To characterise the properties of S100P protein I used cells transfected with a single inducible transgene vector that confers site-specific expression after doxycycline induction. IIn this study I have suitably checked for any leakiness, which was not significant and the uninduced cells did not stimulate cell migration. Doxycycline is 6-deoxy-5-oxy tetracycline antibiotic, synthesized from oxytetracycline by a series of sequential steps that produce methacycline and eventually doxycycline (Nelson, 1998). Reports have described that doxycycline produces some effects on cancer cells *in vitro* and *in vivo* (Fife and Sledge, 1995; Fife and Sledge, 1998). It inhibited cell proliferation and apoptosis induction and tumours growth in breast carcinoma cells (Fife et al., 1994). It inhibited cell proliferation, apoptosis induction and tumours growth in breast carcinoma cells (Fife et al., 1994), but low concentrations have been described not to have any effect on cancer cells (Onoda et al., 2006; Sourdeval et al., 2006).

My investigations clearly demonstrate that overexpression of intracellular S100P significantly stimulates cell migration in the rat mammary (Rama 37 T-25) and human cervical cancer cell lines (HeLa A-9). This demonstrates a direct role for

S100P in one crucial aspect of metastasis: cell migration. I first observed cytoplasmic staining for S100P after induction of S100P, and staining for S100P in the nuclei is strongly detected after three days of intracellular expression. My observations showed, as previously reported (Wang et al., 2006; Whiteman et al., 2007), that when S100P is over-expressed in cells, it is translocated to the cell nucleus. I therefore speculate that for invasive carcinomas overexpressing S100P, S100P transcription is somehow activated and elevated S100P protein mediates the invasive phenotype. Therefore, in the next chapter I focused on S100P's intracellular influence on gene transcription using DNA chip microarrays to compare gene expression between S100P non-expressing and overexpressing Rama 37 T-25 cells. This study is followed up by quantitative real-time PCR and SiRNA silencing of any promising upregulated gene that maybe involved in cell migration.

Chapter 4

Epigenetic Modification / Regulation by Overexpression of S100P

4.1. Introduction

Literature indicates that S100P is an active constituent of the cancer phenotype (Birkenkamp-Demtroder et al., 2005; Parkkila et al., 2008), associating an overexpression of S100P with tumour progression and development (Arumugam et al., 2005; Basu et al., 2008; Diederichs et al., 2004), and most importantly, S100P stimulates health degradation by inducing tumour cells to metastasise (Wang et al., 2006). Distant metastasis is the primary cause of death in cancer patients, and an important step in the metastatic process is the migration of tumour cells into surrounding host tissue.

Initially, S100P was isolated from trophoblast cells, in the placenta, which strongly express S100P. However S100P is weakly expressed in adult tissues, including heart, lung skeletal muscle, spleen and leucocytes, but is highly expressed in neoplasmic tissues (Parkkila et al., 2008). S100P has been shown to induce metastasis in rats and to be associated with tumour metastasis aggressiveness and worst patient prognosis in several types of cancer including breast and pancreatic (Arumugam et al., 2005; Wang et al., 2006). Therefore several observations support a role of S100P in invasive growth and metastasis of cancers. Immunostaining of tumours overexpressing S100P demonstrated a strong presence of nuclear S100P, raising the question of a potential role on gene expression associated to its potential metastasis-promoting functions.

My studies in Chapter 3 have indicated a significant association of S100P expression and cell migration, and a strong expression of nuclear S100P. The hypothesis to be tested in this chapter is whether the nuclear S100P affects the expression of other genes. To study this, I have used the transfected inducible Rama 37 T-25 cell line to allow the analysis of variations in gene expression arising from a change in only one parameter, namely, the increased expression of intracellular S100P. In order to identify possible target genes of S100P, oligonucleotide microarray technology was employed to highlight genes that were differentially expressed between Rama 37 cells treated with doxycycline for 72 h and untreated cells. The aim of these studies is to identify genes in which mRNA expression was significantly changed between cells expressing S100P and cells not expressing S100P. Microarray findings would be backed up by qPCR studies and an up-regulated induced gene by overexpression of S100P will be suppressed by its specific SiRNA

to assess its potential to regulate cell migration potentially associated to cell migration.

4.2. Results

4.2.1. Identification of genes associated with S100P overexpression by DNA chip microarray

To identify genes associated with the stimulation of cell migration by S100P, I compared gene expression between induced Rama 37 T-25 cells overexpressing S100P and uninduced Rama 37 cells not expressing S100P by oligonucleotide microarrays. To capture subtle differences and to avoid confounding factors I used cells transfected with the inducible system and studied cells the same treated cells with doxycycline and non-treated cells.

Microarray data analysis with the Bayesian statistics at a p value < 0.05 (as described in Chapter 2 2.4.4.), yielded a list of 55 up-regulated (Table 4.1a-b) and 45 down-regulated genes (Table 4.2a-b). After False Discovery Rate (FDR) analysis to explore the elimination of false positives and negatives independent of the number of samples being tested (Storey and Tibshirani, 2003), the adjusted p value < 0.05 revealed a list reduced to only 7 differentially expressed genes, 5 were up-regulated and 3 down-regulated with at least a 3-fold difference in expression between non-expressing uninduced and induced overexpressing S100P Rama 37 T-25 cells. All the up-regulated genes have been associated with cancer progression. Folate Hydrolase 1 (Folh1), also known as Prostate-specific Membrane Antigen (PSMA), a type II glycoprotein, which is highly overexpressed in prostate cancer (Noss et al., 2002; Sweat et al., 1998) is associated with poor patient prognosis (Perner et al., 2007), and is implicated in endothelial cell invasion and angiogenesis by modulating integrin signalling (Conway et al., 2006).

Akr7a2 (aldo-keto reductase family 7, member A2) is a dimeric succinic semialdehyde (SSA) reductase, previously characterised as aflatoxin aldehyde reductase (Schaller et al., 1999), which has been reported to be highly expressed in renal (O'Connor et al., 1999) and pancreatic cancers (Cui et al., 2009) and has been proposed as a potential biomarker candidate for pancreatic cancer (Cui et al., 2009).

Cyclin D2 (Ccnd2) protein regulator of the Cyclin dependent kinases CDK (G_1 to S phase cell cycle transition (Morgan, 1997) known to be important in cell proliferation (Ando et al., 1993). Overexpression has been correlated with gastric cancer progression and poor patient prognosis (Takano et al., 1999).

AffyProb ID	EntrezGene UID	Fold Change	P value	adj p val	B	Gene Symbol	Gene name
1392570_at	299196	1.7	0.000865	0.4529	-0.36	Abcd4	ATP-binding cassette, sub-family D (ALD), member 4
1380853_at	311926	1.7	0.001173	0.4736	-0.56	Lrp1b	low density lipoprotein-related protein 1B (deleted in tumors)
1378122_a_at	117259	1.7	0.000837	0.4488	-0.34	Sfrs10	splicing factor, arginine/serine-rich 10 (transformer 2 homolog, Drosophila)
1368124_at	171109	1.7	0.001476	0.5100	-0.72	Dusp5	dual specificity phosphatase 5
1372104_at	316516	1.7	0.000958	0.4581	-0.43	Tmbim1	transmembrane BAX inhibitor motif containing 1
1389923_at	294318	1.8	0.001319	0.4970	-0.64	Btbd9	BTB (POZ) domain containing 9
1392968_at	NA	1.9	0.001435	0.5070	-0.70		
1375285_at	691799	2.1	0.000708	0.4078	-0.24	Il17d	interleukin 17D
1390954_at	314897	2.3	0.000672	0.3942	-0.21	Ppm1h	protein phosphatase 1H (PP2C domain containing)
1394514_at	83635	2.3	0.001302	0.4970	-0.63	Gmeb2	glucocorticoid modulatory element binding protein 2
1388145_at	25602	2.3	0.000442	0.3248	0.04	Tnxa	tenascin XA
1369762_at	25517	2.4	0.001338	0.4970	-0.65	Pou1f1	POU class 1 homeobox 1
1384077_at	NA	2.4	0.001001	0.4592	-0.46		
1385575_at	298182	2.4	0.000251	0.2554	0.34	Tyrp1	tyrosinase-related protein 1
1377445_at	29182	2.7	0.000244	0.2554	0.35	Cdh22	cadherin 22
1382733_at	NA	2.7	0.000065	0.1554	0.91		
1396040_at	78957	2.8	0.000222	0.2554	0.39	Shank1	SH3/ankyrin domain gene 1
1370484_at	404977	2.8	0.001772	0.5626	-0.84	Olr1468	olfactory receptor 1468
1385794_at	681210	2.8	0.000459	0.3248	0.02	MGC94891	hypothetical protein LOC681210
1391151_at	303631	3.0	0.000661	0.3942	-0.20	Arsg	arylsulfatase G
1395935_at	NA	3.0	0.000212	0.2554	0.42		
1392459_x_at	NA	3.1	0.000630	0.3839	-0.17		
1391468_at	292264	3.3	0.000033	0.1033	1.12	Myct1	myc target 1
1392374_at	64033	3.3	0.000007	0.0436	1.48	Ccnd2	cyclin D2
1377513_at	NA	3.3	0.001208	0.4771	-0.58		
1395484_at	NA	3.5	0.000799	0.4360	-0.31		
1397367_at	689663	3.6	0.000136	0.2229	0.62	LOC689663	hypothetical protein LOC689663

Table 4.1.a **List of up-regulated genes in Rama 37 cells with S100P overexpression evaluated by DNA chip microarray**

AffyProb ID	EntrezGene UID	Fold Change	P value	adj p val	B	Gene Symbol	Gene name
1390008_at	114491	3.6	0.000946	0.4581	-0.42	Cited4	Cbp/p300-interacting transactivator, with Glu/Asp-rich carboxy-terminal domain, 4
1376527_at	NA	3.6	0.000005	0.0377	1.55		
1368731_at	24614	3.6	0.000606	0.3839	-0.14	Orm1	orosomucoid 1
1378432_at	365548	3.7	0.000934	0.4581	-0.41	Pttg1ip	pituitary tumor-transforming 1 interacting protein
1395959_at	NA	3.7	0.000274	0.2662	0.29		
1393323_at	499126	3.8	0.000460	0.3248	0.02	RGD156357	similar to Hypothetical protein MGC30332
1384536_at	NA	3.8	0.001215	0.4771	-0.58		
1386049_at	691835	3.8	0.001004	0.4592	-0.46	Kctd4	potassium channel tetramerisation domain containing 4
1375668_at	246295	3.9	0.001123	0.4655	-0.53	LOC246295	glycine-, glutamate-, thienylcyclohexylpiperidine-binding protein
1368412_a_at	50677	4.0	0.000412	0.3248	0.08	Ptpro	protein tyrosine phosphatase, receptor type, O
1386404_at	NA	4.1	0.001837	0.5626	-0.87		
1383304_at	60669	4.4	0.000132	0.2229	0.63	Cmklr1	chemokine-like receptor 1
1378306_at	25539	4.4	0.001056	0.4655	-0.49	Sag	retinal S-antigen
1384409_at	362738	4.5	0.001227	0.4771	-0.59	Snx6	sorting nexin 6
1383435_at	245956	4.5	0.000302	0.2795	0.24	Scn3b	sodium channel, voltage-gated, type III, beta
1379587_at	366791	4.7	0.000561	0.3711	-0.10	Rdh5	retinol dehydrogenase 5
1387178_a_at	24250	4.8	0.000196	0.2554	0.46	Cbs	cystathionine beta synthase
1370111_at	54262	5.2	0.000023	0.0806	1.22		
1380471_at	NA	5.2	0.000990	0.4592	-0.45		
1391698_at	353118	5.4	0.000221	0.2554	0.40	Mast1	microtubule associated serine/threonine kinase 1
1383530_at	361625	5.8	0.000124	0.2229	0.66	Nrip3	nuclear receptor interacting protein 3
1389773_at	685479	5.9	0.001835	0.5626	-0.87	S100a7a	S100 calcium binding protein A7A
1381295_at	NA	6.0	0.000407	0.3248	0.08		
1381880_at	NA	6.8	0.000003	0.0335	1.61		
1394650_at	171445	6.9	0.000001	0.0167	1.75	Akr7a2	aldo-keto reductase family 7, member A2 (aflatoxin aldehyde reductase)
1369741_at	50599	7.2	0.000623	0.3839	-0.16	Kcnj3	potassium inwardly-rectifying channel, subfamily J, member 3
1389901_at	29495	7.3	0.001164	0.4736	-0.56	Dlg4	discs, large homolog 4 (Drosophila)
1387363_at	85309	7.6	0.000001	0.0167	1.73	Folh1	folate hydrolase

Table 4.1.b **List of up-regulated genes in Rama 37 cells with S100P overexpression evaluated by DNA chip microarray**

AffyProb ID	EntrezGene UID	Fold Change	P value	adj p val	B	Gene Symbol	Gene name
1376197_at	363595	1.6	0.0014	0.500	-0.67	Tcf7	transcription factor 7, T-cell specific
1380614_at	NA	1.7	0.0014	0.500	-0.67		
1379904_at	680465	1.7	0.0016	0.538	-0.79	Trappc6a	trafficking protein particle complex 6A
1370330_at	246212	1.8	0.0011	0.465	-0.53	Sipa1l1	signal-induced proliferation-associated 1 like 1
1367950_at	29726	1.9	0.0004	0.309	0.15	Slc22a5	solute carrier family 22 (organic cation transporter), member 5
1384000_at	364712	1.9	0.0011	0.465	-0.53	Sox4	SRY-box containing gene 4
1381518_at	NA	1.9	0.0011	0.465	-0.52		
1382555_at	NA	2.0	0.0015	0.516	-0.74		
1398121_at	NA	2.0	0.0016	0.538	-0.78		
1375940_a_at	300317	2.1	0.0007	0.409	-0.26	RGD1311154	similar to hypothetical protein FLJ12242
1392940_at	291022	2.1	0.0009	0.453	-0.37	Ptpdc1	protein tyrosine phosphatase domain containing 1
1384304_at	NA	2.2	0.0017	0.544	-0.81		
1392072_at	29318	2.3	0.0009	0.458	-0.41	Ddt	D-dopachrome tautomerase
1368860_at	29380	2.4	0.0005	0.359	-0.07	Phlda1	pleckstrin homology-like domain, family A, member 1
1383891_a_at	NA	2.4	0.0013	0.497	-0.65		
1383010_at	305589	2.4	0.0003	0.255	0.33	Bcl11a	B-cell CLL/lymphoma 11A (zinc finger protein)
1392534_at	311676	2.6	0.0004	0.325	0.06	Pmepa1	prostate transmembrane protein, androgen induced 1
1377824_a_at	312320	2.7	0.0016	0.538	-0.79	Igf2bp3	insulin-like growth factor 2 mRNA binding protein
1394632_at	681383	2.8	0.0003	0.255	0.33	LOC681383	similar to Protein C10orf11 homolog
1377161_at	NA	2.9	0.0018	0.563	-0.86		
1384261_at	NA	3.5	0.0003	0.255	0.34		
1384347_at	NA	3.6	0.0003	0.302	0.18		

Table 4.2.a **List of down-regulated genes in Rama 37 cells with S100P overexpression evaluated by DNA chip microarray**

AffyProb ID	EntrezGene UID	Fold Change	P value	adj p val	B	Gene Symbol	Gene name
1396459_at	57233	3.8	0.0005	0.358	-0.05	Isl2	insulin related protein 2 (islet 2)
1370457_at	286916	3.9	0.0001	0.133	0.99	Testin	testin gene
1380502_at	361096	4.0	0.0007	0.409	-0.26	Zic2	zinc finger protein of the cerebellum 2
1369600_at	170632	4.0	0.0004	0.325	0.07	Fgf11	fibroblast growth factor 11
1370053_at	65040	4.0	0.0001	0.223	0.62	Dlgap1	discs, large (Drosophila) homolog-associated protein 1
1393472_at	NA	4.2	0.0002	0.255	0.38		
1378734_at	114500	4.3	0.0002	0.255	0.37	Gbx2	gastrulation brain homeobox 2
1383015_at	361697	4.6	0.0010	0.463	-0.47	RGD1311490	similar to DKFZP434P1750 protein
1398159_at	84410	4.6	0.0001	0.223	0.69	Klf5	Kruppel-like factor 5
1371053_at	691644	4.8	0.0000	0.052	1.38	Myh8	myosin, heavy polypeptide 8, skeletal muscle, adult
1390837_at	NA	4.9	0.0011	0.465	-0.50		
1392907_at	NA	4.9	0.0015	0.510	-0.71		
1375143_at	64160	5.0	0.0002	0.255	0.51	Basp1	brain abundant, membrane attached signal protein 1
1390916_at	NA	5.1	0.0004	0.325	0.05		
1375978_at	290639	5.1	0.0000	0.070	1.29	Fcho1	FCH domain only 1
1396265_at	296384	5.1	0.0000	0.044	1.45	Znfx1	Zinc finger, NFX1 type containing 1
1388298_at	296313	5.2	0.0015	0.516	-0.74	Myl9	myosin, light chain 9, regulatory
1383016_at	NA	5.4	0.0006	0.384	-0.13		
1369918_at	246043	5.4	0.0000	0.119	1.05	Klrh1	killer cell lectin-like receptor subfamily H, member 1
1381610_at	NA	5.4	0.0001	0.223	0.70		
1397562_at	679474	6.1	0.0003	0.280	0.24	LOC679474	similar to spermatogenesis associated glutamate (E)-rich protein 4f
1379633_a_at	301000	9.0	0.0009	0.458	-0.41	Uba7	ubiquitin-like modifier activating enzyme 7
1367782_at	25278	9.7	0.0014	0.504	-0.69	Cox6a2	cytochrome c oxidase, subunit VIa, polypeptide 2

Table 4.2.b **List of down-regulated genes in Rama 37 cells with S100P overexpression evaluated by DNA chip microarray**

In the first data list containing 55 up-regulated genes, before FDR analysis, I observed potentially interesting genes such as S100A7a an isoform of another member of the S100 protein family (Kulski et al., 2003; Wolf et al., 2003). The microtubule associated serine threonine kinase 1 (Mast1), which is a cytoskeletal associated kinase (Valiente et al., 2005; Walden and Cowan, 1993). The pituitary tumor-transforming 1 interacting protein (Pttg1ip), a protein facilitating nuclear translocation of transcription factor pituitary tumour transforming factor (Pttg1) (Chien and Pei, 2000), and myc target 1 (Myct1) a protein binding the c-Myc oncogene, which is implicated in cell proliferation (Tsuneoka et al., 2002).

Among the list of down-regulated gene, one is involved in muscle contraction, the myosin heavy chain 8 (Myh8). The FCH domain only 1 (Fcho1) is involved in clathrin-coated vesicle formation (Sakaushi et al., 2007), and the Zinc finger, NFX1-type containing 1 (Znfx1), is binding to the X-box motif of major histocompatibility complex (MHC) class II genes.

I decided to analyse this panel of 7 up-regulated gene products, containing 3 significantly differentially expressed genes with adjusted p values less than 0.05 (Folh1, Akr7a2 and CcnD2), and 4 genes with borderline adjusted p values (S100A7a, Mast1, Myct1 and Pttg1ip) and validate them by quantitative real-time PCR (Table 4.3).

Gene symbol	Gene name	GenBank accession No	Locus	Gene Functions	Adj p value < 0.05
Folh1	Folate hydrolase 1	NM_057185	1q32	Prostate-specific membrane antigen	Yes
Akr7a2	Aldo-keto reductase family 7, member A2	NM_134407	5q36	Detoxification of aldehydes and ketones	Yes
Ccnd2	Cyclin D2	NM_022267	4q42	Regulation of cell proliferation	Yes
S100A7a	S100 calcium binding protein A7A	NM_001109471	2q34	Inflammation	No
MAST1	microtubule associated serine/ threonine kinase	NM_181089	19q11	Interaction with syntrophin on the cell surface	No
Myct1	Myc Target 1	NM_001106207	1p11	Binding to Myc oncogene	No
Pttg1ip	Pituitary tumor-transforming 1 interacting protein	NM_001013238	20p12	Pttg1 translocation into nucleus	No

Table 4.3 **List of up-regulated genes in Rama 37 cells after S100P overexpression evaluated by DNA chip microarray.**

4.2.2. Validation of microarray results

Using qPCR I measured the relative transcript levels of differentially expressed mRNA transcripts to validate these observations for an extended list of 7 candidate genes (Folh1, Akr7a2, Ccnd2, S100A7a, Mastl, Myctl and Pttg1ip), which have been shown to be expressed in the literature in different cancer types, and could be a target for investigations within a potential association with the S100P metastasis- promoting protein.

Results showed that S100P was up-regulated 13 fold in Rama 37 cells treated with doxycycline for 72 h compared to untreated controls incubated for the same time (Figure 4.1), confirming the overexpression of intracellular S100P in Rama 37 T-25 cells. Based on the microarray results, it was expected that Folh1 and Akr7a2 would be up-regulated about 7 fold in S100P overexpressed cells, but only a 1.3 -fold change for Folh1 and 4-fold for Akr7a2 compared to control was observed, which was lower than observed by microarray but was still differentially expressed ($P = 0.012$, Student t-test comparison Folh1 relative mRNA between uninduced and induced cell with doxycycline (67.5nM). There were distinct differences in the expression among these genes by qPCR analysis, however validated the microarray results. The following 2 up-regulated genes observed from the extended list by microarray were validated by qPCR. S100A7a and Mastl, were 5.5 and 4.5 fold up-regulated by qPCR in cells treated with doxycycline for 72 h compared to untreated cells, which were not significantly differently expressed in the microarray results. As expected, it was found that after Gapdh normalisation, either of the Nrip3, Myct1 and Pttg1ip showed significant regulation (Figure 4.1).

A

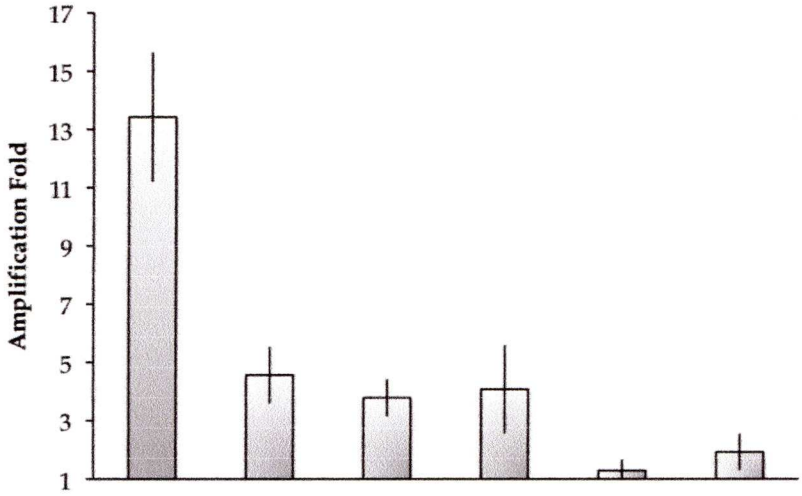

B

Genes	Amplification fold (Mean)	Standard Deviation	*p* value
S100P	13.42	2.2	< 0.0001
Mast 1	4.56	0.9	0.006
Akr7a2	3.79	0.6	0.004
Ccnd2	4.2	1.6	0.031
Folh 1	1.28	0.4	0.004
S100A7a	1.96	0.6	0.034
Pttg1ip	0	/	0.234
Myct 1	0	/	0.384

***Figure 4.1* qPCR validation of differentially expressed genes observed by microarray in Rama 37 transfected cells using the inducible system treated with doxycycline (67.5 nM) for 72 h.**

A. *Relative quantity mRNA level were measured by qPCR in untreated and treated cells for 48 h. Final transcripts data were normalised to GAPDH data. Values shown are mean normalised value ± SD, Student's t-test was performed by comparison between the absence or presence of S100P induction by doxycycline treatment (67.5 nM) for 72 h.*

B. *Table represents fold amplification of analysed genes, with calculated p values between the absence or presence of S100P induction by (67.5 nM) doxycycline treatment for 72 h. Data show the mean +/- Standard Deviation (S.D.) of technical triplicates from three separate biological experiments.*

A

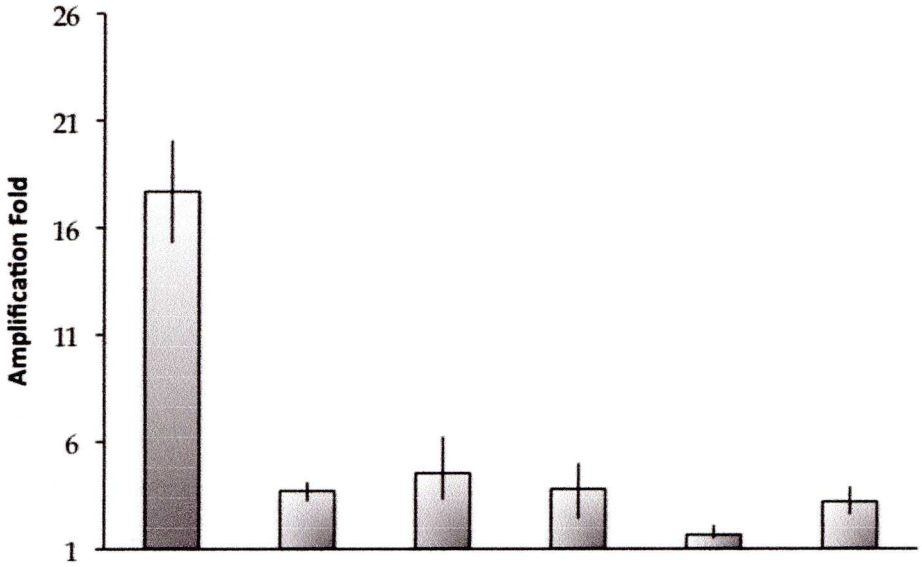

B

Gene symbol	Validated	Mean fold change	Standard Deviation	*p* value
S100P	Yes	17.4	2.4	0.028
Mast1	Yes	3.7	0.4	0.0007
Akr7a2	Yes	4.5	1.7	0.023
Ccnd2	Yes	3.8	1.2	0.016
Folh1	Yes	1.6	0.4	0.007
S100A7a	Yes	3.2	0.7	0.006
Myct 1	No	0	/	0.49
Pttg1ip	No	0	/	0.81

***Figure* 4.2 qPCR analysis of differentially expressed genes observed by microarray in Rama 37 pcDNA3-e and pcDNA3-S100P**

A. *Relative mRNA levels were measured by qPCR between Rama 37 pcDNA3-e, transfected with an empty vector, and Rama 37 pcDNA3-S100P transfected with S100P cDNA. Final transcripts data were normalised to relative GAPDH levels and are represented as amplification fold change of transcripts. Data show the mean +/- Standard Deviation (S.D.) of technical triplicates from three separate biological experiments.*

B. *Mean amplification fold change of analysed genes over GAPDH transcripts. Student t-test comparison between the absence (pcDNA3-e) or presence (pc-DNA3-S100P) of S100P cell intracellular expression: if p< 0.05, validated (Yes), if p> 0.05 not validated (No) (Student's t-test).*

I then used Rama 37 cells constitutively expressing S100P to confirm the differentially expressed genes previously observed, using Rama 37 constitutively overexpressing S100P (pcDNA3-e and pcDNA3-S100P). Similar results were found with significant up-regulation of Folh1 (2 fold change) Akr7a2 (4.5 fold change), and Ccnd2 (4 amplification fold) (Figure 4.2). From the extended list Mast1 (4 fold change) and S100A7a (3 fold change) were shown to be up-regulated, and Nrip3 , Pttg1ip and Myct1 were confirmed in a second cell line not to be differentially expressed.

In summary, of the 3 genes identified from the statistical analysis of the DNA chip microarray data: Folh1, Akr7a2 and Ccnd2, all were validated by qPCR in both transfected Rama 37 cells either transfected with the inducible system or with pcDNA3 vector. 2 other genes, Mast1 and S100A7a have been found up-regulated as well in all S100P-expressing Rama 37 cells tested.

4.2.3. Treatment with Mast1 specific SiRNA decreases *in vitro* cell migration in Rama 37 cells overexpressing S100P

Among the up-regulated genes, Mast1 the gene coding for Microtubule-Associated Serine-Threonine kinase 1, has been confirmed to display the highest fold change in the inducible system. Therefore, Mast1 was chosen for further analysis to investigate whether an increase in cell migration was a direct consequence of the effects of S100P on Mast1. Members of the MAST protein family, composed of 5 members (Mast1-4 and Mast -like) are characterised by the presence of a serine/threonine kinase domain and harbours both a kinase domain and a PDZ scaffolding domain (Walden and Cowan, 1993). PDZ is an acronym combining the first letters of three proteins, post synaptic density protein (PSD95), Drosophila disc large tumour suppressor (DlgA), and zonula occludens-1 protein (zo-1). The PDZ domain is an important interaction module for proteins involved in many intracellular pathways and abnormal activations, and members of the Mast family, specifically, have been shown to bind and stabilise the tumour suppressor phosphatase, PTEN via its PDZ binding domain (Valiente et al., 2005). In rats, Mast1 has been shown to be expressed in several tissues such as heart, brain, spleen, lung, liver, skeletal muscle, kidney and testis (Garland et al., 2008) and is associated with cytoskeleton organisation by its interaction with and β2-syntrophin microtubules.

The role of Mastl in its interaction and mechanism of action in cell migration, is unknown therefore I used Rama 37 constitutively expressing S100P cells to determine whether S100P's influence with Mastl was direct and its role in cell migration.

- Transfection efficiency

Rama 37 pcDNA3-S100P cells were seeded in 24 well plate with Mastl specific SiRNA or scrambled SiRNA transfected along with BLOCK-IT Alexa Fluor Red Fluorescent Oligos, and after cell washing, intracellular fluorescence was observed microscopally to ensure successful probe transfection. After a 12 h incubation with the Hiperfect lipofection solution (Qiagen) more than 90% of both cell lines were stained positive for BLOCK-IT.

- Gene silencing efficiency

Five SiRNA probes sequences were ordered from Qiagen: Rn_Mastl_1, Rn_Mastl_2, Rn_Mastl_3 and Rn_Mastl_4 and the efficacy of SiRNAs against the target Mastl gene, was determined by qPCR of Mastl mRNA. For a better silencing efficiency result, all SiRNA probes were transfected together, and the degradation of target mRNA was tested. The mRNA expression levels were evaluated by qPCR. In order to compare the potency of these SiRNAs, their gene-silencing-activity was assayed using dose-response curves. Prior to transfection, the synthetic SiRNAs were mixed with the Hiperfect transfection reagent and incubated at room temperature to allow the formation of transfection comeplexes, according to the manufacturer's recommendations. Transfections were carried out according to Chap 2. 2.5.3. in 48-well dishes. SiRNA probes were transfected into 6 x 10^4 Rama 37 pcDNA3-S100P cells at concentrations ranging from 1 to 10 nM. After 48 h of incubation at 37°C, cells were harvested and Mastl mRNA levels were assayed (Chap 2. 2.5.4). Stable suppressed expression of Mastl in Rama 37 pcDNA3-S100P cells was observed after 48 h (Figure 4.3), with a 83% of gene knockdown after addition of 5 nM Mastl probes each, and 87% knockdown with 10 nM. No significant Mastl gene expression suppression was observed using an Allstar negative control at any concentrations of Mastl probes.

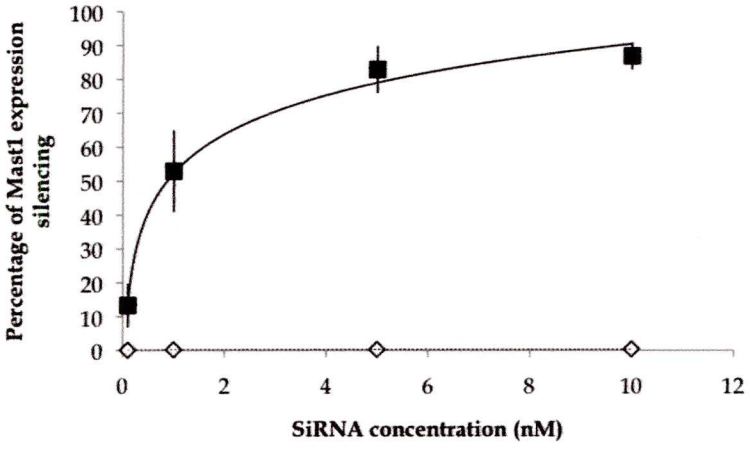

Figure 4.3 **Dose-response curve of SiRNA concentration against percentage of Mast1 mRNA silencing**

The silencing activity of Mast1 was monitored by qPCR (Chap 2.5.3.). mRNA levels were normalised to those of GAPDH mRNA.

SiRNAs were transfected into Rama 37 pcDNA3-S100P cells at various concentrations (1–10 nM) for 48 h represented by black squares for Mast1 oligos and represented by white diamonds for Allstar negative control. Error bars show the standard deviation calculated from the mean of 3 separate experiments.

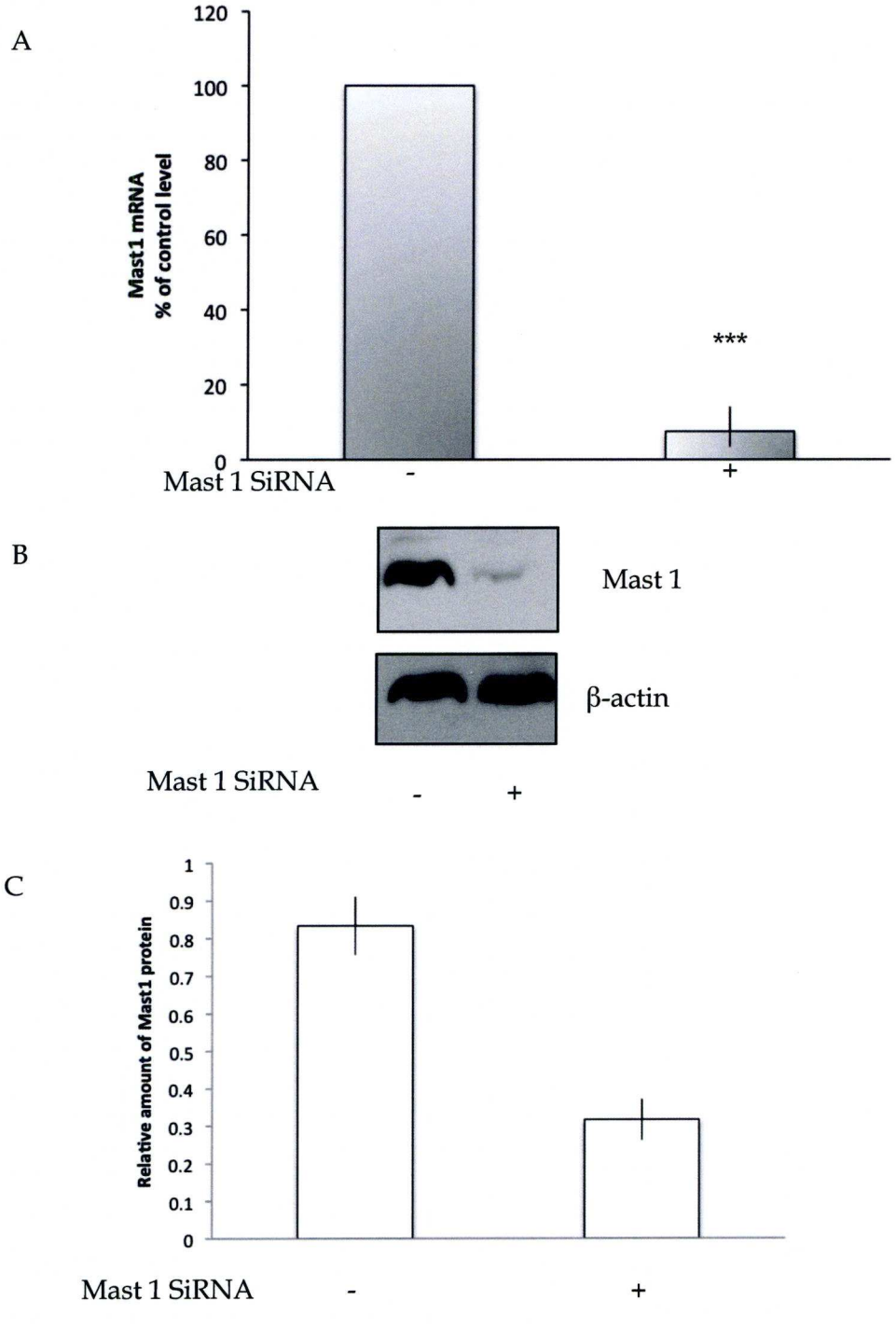

***Figure 4.4* MAST1 gene knockdown by SiRNA transfection in Rama 37 cells**

Pretreatment with SiRNA targeting Mast 1 inhibits mRNA and protein expression. Rama 37 cells grown in cultures were transfected with SiRNA targeting Mast1 for 48 h. Shown are quantitative qPCR and Western Blot analysis of Mast1 mRNA after 48 h of transfection with 10nM SiRNA. Data were normalised to β-actin

A. *Graph showing the mean percentage of Mast 1 mRNA in cells constitutively overexpressing intracellular S100P, treated with 10nM SiRNA probes (control and Mast 1). Data show the means +/- Standard Deviation (S.D.) from three separate experiments (*** $p < 0.001$).*
B. *Mast 1 protein detected by western blot of Rama 37 cells transfected with Control SiRNA (-) and Mast 1 SiRNA (+)*
C. *Histogram showing the amount of Mast1 protein relative to that of β-actin. Data show the mean +/- Standard Deviation (S.D.) of technical triplicates from three separate biological experiments.*

4.2.4. Effects of MAST1 mRNA knock-down on cell migration

These results were confirmed at the protein level by Western blotting for Mast1 which detected a protein at around 205 kDa (Figure 4.4). After SiRNA treatment for 48 h Mast1 expression was down-regulated with a decrease of 90% in gene expression observed by qPCR. (Figure 4.4 A). Mast1 gene was down-regulated at both mRNA and protein levels by transfection of Mast1 SiRNA probes in Rama 37 cells overexpressing high endogenous S100P levels (Figure 4.4 B). Similarly, Mast1 protein expression was reduced dramatically at 72 h post-transfection and persisted at 5 days (Figure 4.4 B).

To examine the effects of Mast1 on cell migration, Mast1 gene expression was suppressed and migration has been assayed in Boyden chambers between 24 and 48 h after addition of Mast1 SiRNA silencing (Figure 4.5). Percentage of migratory cells untransfected with SiRNA probes is similar to the level of cells transfected with SiRNA Allstar control with about 8% of cells migrating through the membrane (Figure 4.5 A). After silencing of Mast1 expression the number of cells significantly dropped to 3% despite the presence of S100P (Student's t-test, $p = 0.00532$). Results show that the presence of S100P alone was sufficient to stimulate cell migration but expression of both proteins was needed for the stimulated response in cell migration (Figure 4.5B).

A

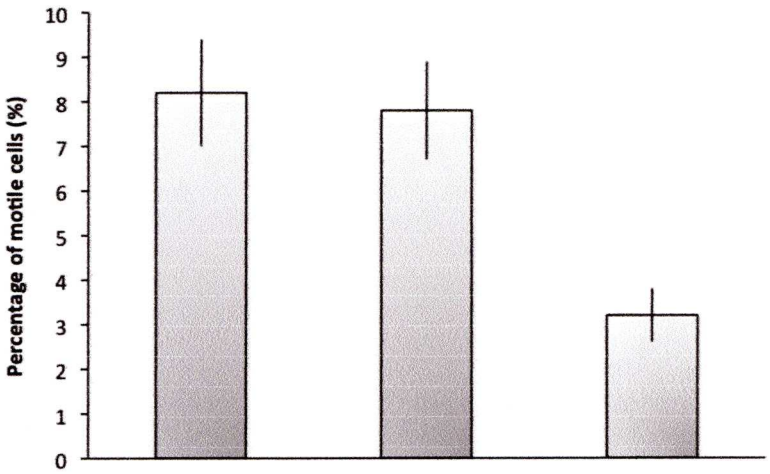

B

	No SiRNA	SiRNA Control	SiRNA Mast1
Mean of Motile cells (%)	8.6	7.8	3.2
S.D	1.2	1.1	0.5
p value		0.00532	

***Figure 4.5* Effect of MAST1 mRNA knockdown on cell migration**

Boyden chamber assay of Rama 37 constitutively expressing S100Pwas measured from cells pretreated with SiRNA probes for Mast 1 and controls. Results shown are from triplicate wells for each sample, performed three times.

A. *Bar chart showing the mean of percentage of cells treated with 10 nM of Mast 1 SiRNA probes (red bars) for 72h, and cells treated with SiRNA control, which does not target any gene product (white bars). Data show the means +/- S.D. from three separate experiments.*

B. *Table representing Student t-test results between Mast 1 SiRNA treated and SiRNA control treated cells (** $p = 0.00532$, Student's t-test comparison between cell transfected with Mast 1 SiRNA and transfected with control probes).*

4.3. Discussion

In order to examine the hypothesis that S100P affects the pattern of gene expression, I examined the differential gene expression influenced by S100P overexpression in the S100P inducible Rama 37 cell line by microarray. Five genes shown to be up-regulated by microarray have been confirmed to be differentially overexpressed in S100P constitutively overexpressed rat mammary cell lines (Rama 37) and in S100P inducible human cells (HeLa). Among these genes, some have been shown to be up-regulated previously in cancer and associated with cancer progression, namely, Folh1, CcnD2, and S100A7 (Mermelshtein et al., 2005; Perner et al., 2007; Takano et al., 1999; Tripathi et al., 2010). However, Akr7a2 and Mast1 confirmed by my own qPCR experiments to be up-regulated, have so far been indirectly associated with cancer or metastatic activity.

In my study, Mast1 SiRNAi resulted in potent silencing of Mast1 expression at the mRNA and protein level. My results suggest that Mast1 is necessary for rat mammary cell migration in cultured cells. The exact mechanism by which Mast1 stimulates migration is poorly understood. It has been speculated that Mast1 binding to PTEN, via the PDZ domain may be important in the control of PTEN's tumour suppressor function (Valiente et al., 2005). In my results knock down of MAST1 is strongly associated with reduced cell migration, and suggest direct involvement of S100P in Mast1 up-regulation. Thus Mast1 is probably positioned downstream of S100P in the pathway which leads to increased cell migration in S100P overexpressing cells.

Mast1 intracellular interactions or binding have not been analysed. Mast1 harbors a PDZ domain known to play several indispensable cellular and biological roles, such as in cell adhesion, growth, development and polarisation, suggesting Mast1 has several cellular applications. Mast1 activation by S100P induces cell migration. My results do not differentiate as to Mast1 up-regulation was caused by intracellular or extracellular S100P (Figure 4.7). Therefore since S100P overexpression led to Mast1 gene up-regulation and increase of cell motility. However, some S100 proteins occurs outside the cell (Schmidt-Hansen et al., 2004). Thus raising the possibility of an alternative mechanism for intracellular up-regulation of Mast1 gene expression by a nuclear transcriptional influence or extracellularly via a potential cell surface receptor (RAGE?) (Figure 4.7). Thus, to

explore the extracellular activity hypothesis, I analysed the extracellular activity of S100P.

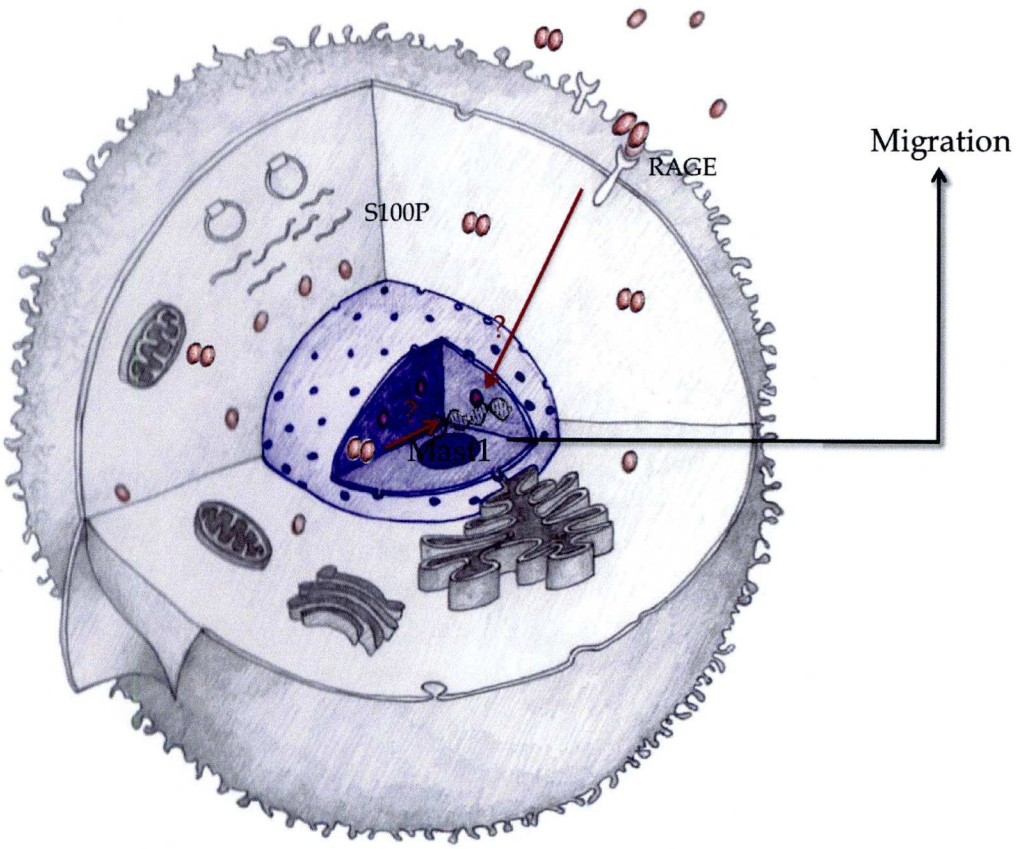

***Figure 4.7* Illustration of hypothesised S100P 's role in stimulating Rama 37 cell migration.**

S100P overexpression in Rama 37 cells up-regulates Mast1 gene expression, and induces cell migration. The mechanism of S100P in inducing Mast1 is totally unknown. One hypothesis is that S100P is secreted to the extracellularly and activate receptors, the second is that S100P is translocated into the nucleus and acts to stimulate Mast1 transcription.

Chapter 5

The Extracellular Role of S100P

5.1. Introduction

Several S100s proteins have been shown to be released from the cell and different extracellular functions have been described in recent years. For example S100A7, which was first observed as a protein highly upregulated in lesions of psoriatic skin (Madsen et al., 1991). It is excreted from cells during inflammation and acts as chemotactic factor for keratinocytes (Boniface et al., 2005) and leukocytes (Wolf et al., 2008) by activation of the RAGE receptor. S100A8 and S100A9 are also highly expressed in the extracellular matrix, and are associated with extracellular chemostatic stimulation of neutrophils to inflammatory sites (Ryckman et al., 2003; Wolf et al., 2008). Furthermore S100A13 is involved in the release of extracellular fibroblast growth factor-1 (FGF-1), interleukin-1-α, and to act as a cargo molecule by binding nuclear Prothymosin-α (ProTα) (Landriscina et al., 2001; Mandinova et al., 2003; Matsunaga and Ueda, 2008; Matsunaga and Ueda, 2010). The metastasis-inducing S100A4 protein has also been reported to be translocated outside the cell (Novitskaya et al., 2000) and to bind to the RAGE receptor (Yammani et al., 2006).

Although nothing is known about the excretion mechanism, S100P is found to be secreted to the extracellular compartment despite the lack of a conventional secretory signal sequence. Accumulation of extracellular S100P has been reported to have an influence on cell functions, such as cell proliferation and survival (Arumugam et al., 2004). The RAGE receptor has been identified as a target for several S100 proteins, including S100P (Arumugam et al., 2004; Schmidt et al., 2001). RAGE is 35 kDa protein of the immunoglobulin-like cell surface receptor superfamily. It is composed of three extracellular domains, a "V" (Variable) type immunoglobulin-like domain followed by two "C" (Constant) type domains, a single transmembrane-spanning helix, and a short cytosolic domain (Neeper et al., 1992) (Figure 5.1). Additional RAGE isoforms lacking the transmembrane and cytosolic regions (soluble RAGE (sRAGE)) (Park et al., 2004) or the "V" immunoglobulin domain (NtRAGE) (Yonekura et al., 2003) have been identified in human brain suggesting isoform-specific functions for the receptor (Figure 5.1). Structure-function studies have shown that the V-domain is critical for ligand binding and that the cytosolic tail is essential for RAGE-mediated intracellular signalling. A truncated form of RAGE, which lacks the cytosolic tail, but remains

embedded in the membrane, can bind ligands but it acts as a dominant negative ("DN-RAGE") receptor.

PI3K/AKT and extracellular signal-regulated kinase 1/2 (ERK1/2) signalling pathways are two important kinase cascades that have been reported to be activated by the RAGE receptor and to induce invasion and metastasis (Arumugam et al., 2004; Arumugam et al., 2005; Leclerc et al., 2007). S100P has been shown to be secreted from cancerous cells and to stimulate through the RAGE receptor ERK1/2 activation, which increased cell proliferation, migration survival and tumour growth (Arumugam et al., 2004; Arumugam et al., 2005). Activation of the PI3-K/AKT signalling pathway by S100P has never been described, but is associated with multiple human cancers. AKT (protein kinase B) is a serine/ threonine kinase, which was initially identified as a viral oncogene and is composed of three isoforms, AKT1, AKT2, and AKT3, with differing levels of tissue expression and function (Bellacosa et al., 1991). PI3K activation of AKT is a multistep process beginning with PI3K phosphorylating phosphatidylinositol-4,5-bisphosphate to phosphatidylinositol-3,4,5-triphosphate. AKT's binding to these phosphoinositides results in its relocation from the cytoplasm to the plasma membrane (Coffer et al., 1998). Phosphorylation of AKT at two distinct sites leads to its activation (Feng et al., 2004; Franke et al., 2003). Studies reported that direct PI3K activation was sufficient to disrupt epithelial polarisation and induce cell migration and invasion (Keely et al., 1997).

In the present project, a series of experiments were performed to determine whether extracellular S100P can affect cell migration and if so which receptor might be involved. I explored whether extracellular S100P was able to modulate Mitogen-activated protein kinase (MAPK) and Phosphoinositide 3-kinases (PI3K) activities in Rama 37 and HeLa cells, and analysed the their potential role on cell motility. Analysis consisted of the addition of extracellular S100P onto Rama 37 and HeLa cells, and examination of intracellular kinases phosphorylation.

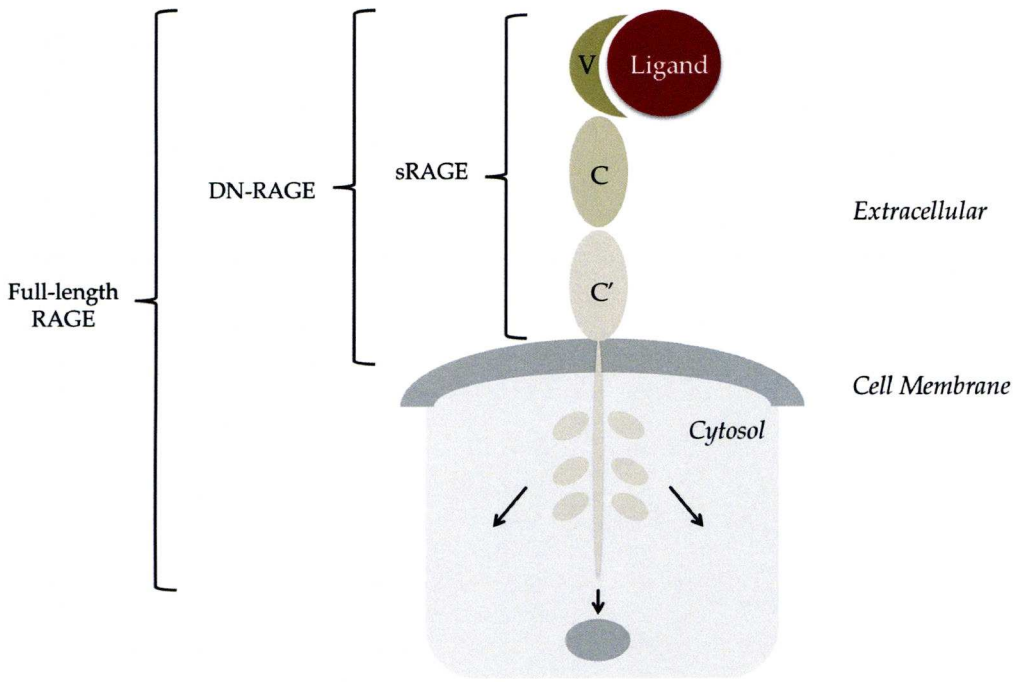

***Figure 5.1* Schematic representation of RAGE receptor structure and ligand interaction.**

RAGE is composed of an extracellular three immunoglobulin-like regions: One "V"-type followed by two "C"-type, a single transmembrane-spanning domain and a 43–amino acid cytosolic tail (not drawn to scale).

A truncated form of RAGE, which lacks the cytosolic tail and remains firmly embedded in the membrane is competent to bind the usual complement of RAGE ligands, but acts as a dominant negative receptor termed "DN-RAGE", and its expression strikingly suppresses RAGE-mediated signalling, even in cells bearing the full-length form.

The soluble RAGE (sRAGE) is a C-truncated form of full-length RAGE, which lacks a cytoplasmic tail and a transmembrane domain.

5.2. Results

5.2.1. S100P can translocate outside of cells

In order to find out whether the intracellular S100P finds its way into the medium, immunoblots were performed on medium from cultures of S100P expressing induced Rama 37 T-25 cells and HeLa A-9 cells. As shown in Figure 5.2, S100P was not detected in the culture medium of cell-free control plates, which only contained culture medium extracted from plates treated with (67.5 nM) or without doxycycline (Figure 5.2 a). Similar negative results were found in the medium from untreated Rama 37 T-25 and HeLa A-9 cells (Figure 5.2 b-c), which do not express S100P protein. However different sized S100P oligomers were detected in the culture media of doxycycline-treated Rama 37 T-25 (67.5 nM) and HeLa A-9 (112.5 nM) cells overexpressing intracellular S100P (Figure 5.2 d-e, respectively). Extracellular oligomers of S100P sized between 21 to 80 KDa in size were detected in the culture medium from the induced Rama 37 T-25 and HeLa A-9 cell lines. S100P octamers at around 80 kDa were the most prominent oligomers detected in induced Rama 37 T-25 cells (Figure 5.2 d), whilst S100P dimers (21 kDa) and tetramers (40 kDa) were the most abundant oligomers in the medium of induced heLa A-9 cells. A possible monomer band at 10 kDa was present in the medium from the human cells (lane e), but was absent in the medium from the rat cells (lane d). Although differences were found in the distribution of different sized oligomers between rat and human cells, nevertheless both cell lines produced larger S100P oligomers outside the cell and retained S100P in the form of monomers and dimers inside cells (Figure 5.3).

Within cells, most S100 family members exist in the form of antiparallel packed homodimers (sometimes heterodimers), capable of binding two homologous or heterologous target proteins in a Ca^{2+}- dependent manner (Donato, 2001). However S100 oligomers can form, under the non-reducing conditions found in the extracellular space (or within cells upon changes in the cells redox status) (Ilg et al., 1996) which may explain why I detect only S100P oligomers outside cells.

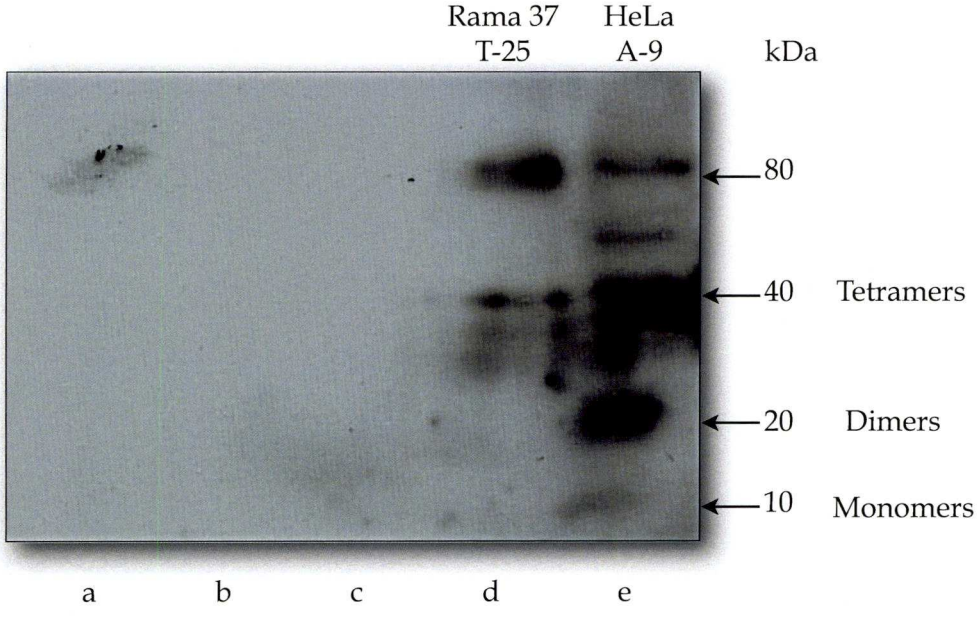

***Figure 5.2* Identification of S100P in the extracellular medium of S100P positive and negative cells.**

S100P oligomers were detected in the culture medium by immunoprecipitation 24 h after doxycycline treatment (67.5 nM).

a. *Detection of S100P by immunoprecipitation of 1 ml of culture medium treated with doxycycline (67.5 nM) extracted from a cell-free control plate.*

b. *Detection of S100P by immunoprecipitation of 1ml culture medium (67.5 nM) extracted from a plate growing untreated Rama 37 T-25 cells.*

c. *Detection of S100P by immunoprecipitation of 1ml culture medium treated with doxycycline (112.5 nM) extracted from untreated HeLa A-9 cells.*

d. *Detection of S100P by immunoprecipitation of 1ml culture medium treated with doxycycline (67.5 nM) extracted from Rama 37 T-25 cells overexpressing S100P.*

e. *Detection of S100P by immunoprecipitation of 1ml culture medium treated with doxycycline (112.5 nM) extracted from HeLa A-9 cells overexpressing S100P.*

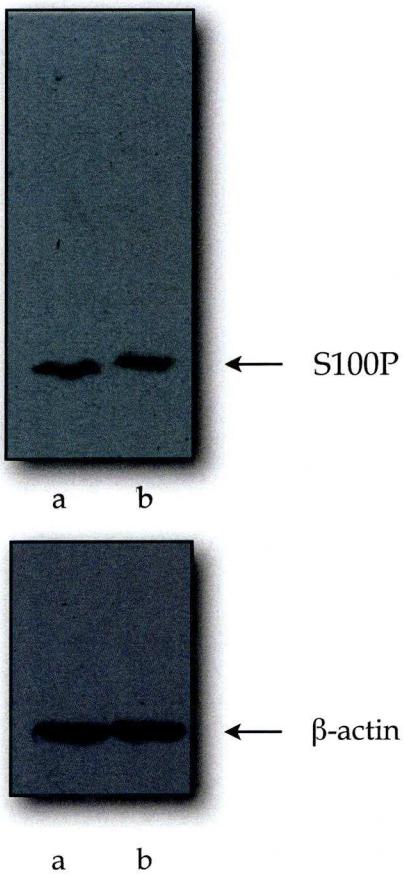

***Figure 5.3* S100P intracellular expression of cells overexpressing S100P**

a. *S100P-induced Rama 37 T-25 whole cell extract assessed by Western blotting for S100P using polyclonal anti-S100P.*

b. *S100P-induced HeLa A-9 cells whole cell extract S100P detection assessed by Western blotting analysis using polyclonal anti-S100P.*

5.2.2. Extracellular role of S100P

Purified recombinant S100P (rS100P) protein was added to the Rama 37 T-25 cell culture medium, and the resulting cellular responses to stimulation by extracellular S100P proteins, such as increased cell migration, and activation of receptor and signalling pathways were investigated.

5.2.2.1. Extracellular S100P can stimulate cell migration

Increasing concentrations of purified rS100P were added to the culture medium of S100P negative Rama 37 T-25 uninduced cells and cell migration was analysed over a 24 h period by in a Boyden chamber. After 24 h in control assays in which no S100P was added to the culture medium only 1.7 % of cells migrated through to the lower chamber (Figure 5.4 A). No significant differences were observed after addition of 5 nM S100P, since 1.8 % of cells were motile (p =0.7, Student's t-test). However when 10 nM exogenous S100P as added to the uninduced Rama 37 T-25 cells, this resulted in a significant increase in cell migration to 2.9% of motile cells (p = 0.0003, Student's t-test)(Figure 5.4 B). The optimal concentration of extracellular S100P protein required to stimulate uninduced Rama 37 T-25 cell migration was 100 nM, with a significant 7.5 % of cells passing to the lower chamber, (p = 0.0001, Student's t-test) (Figure 5.4 B). Addition of higher concentrations of exogenous S100P to uninduced Rama 37 T-25 cells still showed a significant increase in cell migration over no additions at all although the number of motile cells decreased to 6.1 % with 500 nM S100P (p = 0.002, Student's t-test) and to 4.5 % with 1000 nM of S100P addition (p= 0.006, Student's t-test) (Figure 5.4 B).

No significant difference in the proportion of migratory cells was observed between S100P added extracellularly to Rama 37 T-25 S100P uninduced cells and to induced intracellular S100P expressing (without addition of rS100P) Rama 37 cells (p = 0.051). This suggests that the extracellular effects of S100P on cell migration at these high concentrations may be similar to these produced by the induced Rama 37 T-25 cells.

A

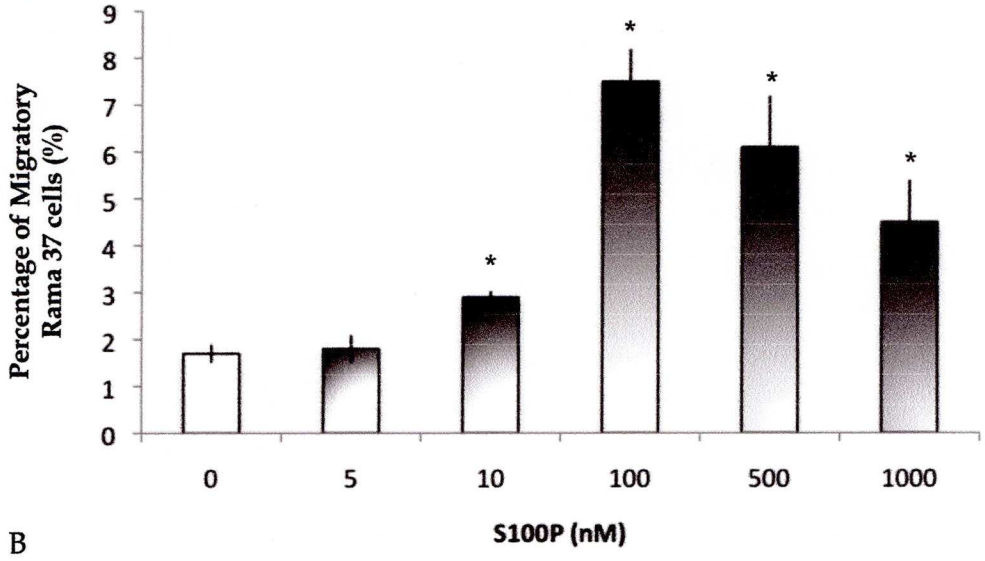

B

S100P (nM)	0	5	10	100	500	1000
Mean percentage of migratory cells (%)	1.7	1.8	2.9	7.5	6.1	4.5
S.D.	0.2	0.3	0.1	0.7	1.1	0.9
p values	/	0.7	0.0003	0.0001	0.002	0.006

***Figure 5.4* Stimulation of cell migration in the S100P negative, uninduced Rama 37 T-25 cell line.**

A. *Histogram of the percentage of migrating cells caused by increasing concentrations of S100P added to the extracellular medium.*

B. *Table showing Student's t-test between cells where no S100P was added and addition of S100P (0-1000 nM). Data show the mean +/- Standard Deviation (S.D.) from three separate experiments.*

($p < 0.05$) Data are from three independent experiments.*

Similar increasing concentrations of rS100P (0-1000 nM) were added to the culture medium of S100P negative HeLa A-9 uninduced cells and cell migration was analysed over a 24 h period in a Boyden chamber. After 24 h only 2.1 % of cells migrated through to the lower chamber in control assays (Figure 5.5 A). No significant differences were observed after addition of 5 nM S100P since only 2.1 % of cells were motile (p = 0.2, Student's t-test). However addition of 10 nM exogenous S100P resulted in a significant increase in migration to 3.7 % of motile cells (p = 0.002, Student's t-test)(Figure 5.5 B).

The optimal concentration of extracellular S100P protein required to stimulate uninduced HeLa A-9 cell migration was 100 nM, a concentration similar to that observed in Rama 37 T-25 cells, with a significant 8.3 % increase of cells passing to the lower chamber (Figure 5.5 A) (p = 0.0003, Student's t-test) (Figure 5.5 B). Addition of higher concentrations of rS100P (500-1000nM) showed a significant increase in cell migration stimulation over that without any additions; was 8.1 % with 500 nM (p = 0.0001, Student's t-test) 6 % with 1 mM of S100P addition (p = 0.0002, Student's t-test) (Figure 5.5 B).

A

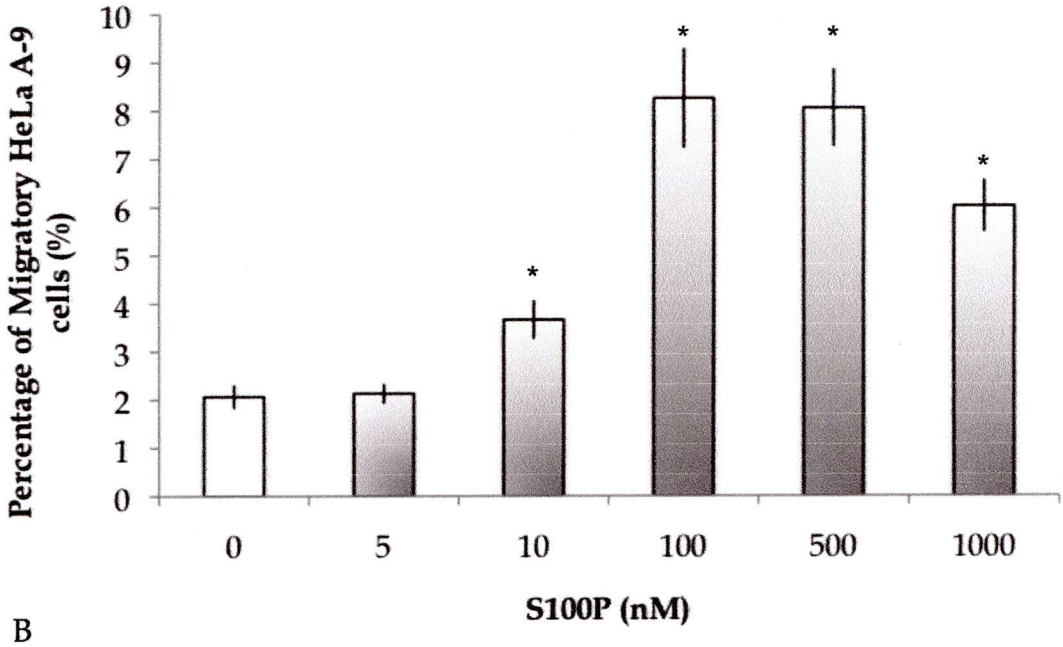

B

S100P (nM)	0	5	10	100	500	1000
Mean percentage of migratory cells (%)	2.1	2.1	3.7	8.3	8.1	6
S.D.	0.3	0.2	0.4	1	0	0.5
p values	/	0.4	0.002	0.0003	0.0001	0.0002

***Figure 5.5* Stimulation of cell migration in the S100P negative, uninduced HeLa A-9 cell line.**

A. *Histogram of the percentage of migrating produced by increasing concentrations of S100P added to the extracellular medium. Data shows the means +/- Standard Deviation (S.D.) from three separate experiments.*

B. *Table showing Student's t-test results between cells where no S100P was added and addition of S100P (0-1000 nM) (* $p < 0.05$, Student's t-test).*

5.2.2.2. Addition of Extracellular S100P stimulates the AKT signalling pathway

Previous experiments revealed that addition of extracellular S100P to the Rama 37 T-25 and HeLa A-9 uninduced cells significantly increased cell migration (Figures 5.4 and 5.5). I next examined the effect of similar concentrations of extracellular S100P on cell migration signalling pathways. The serine/threonine kinase AKT (also called protein kinase B) (Staal et al., 1977) is well known to be an important regulator of cell survival (Brunet et al., 1999) and growth and has also been shown to promote cell migration in different organisms (Kim et al., 2001) and to be activated by specific phosphorylations in breast cancer tissues (Bose et al., 2006).

In the present experiments, treatment of Rama 37 T-25 cells with extracellular S100P induced phosphorylation of AKT in a time-dependent manner (Figure 5.5 A). Addition of 100nM Extracellular S100P (shown previously to be the optimal concentration to stimulate significant cell migration), induced AKT phosphorylation within 20 min (p = 0.001), and a maximal increase over control levels was observed after 60 min (p = 0.000006) (Figure 5.5 B). AKT phosphorylation levels declined after 60 min (Figure 5.5 B).

The effects of S100P on phosphorylation of AKT were also concentration-dependent, with significant effects noted 60 min after addition of 10 nM rS100P with a 0.3 relative amount of pAKT (p = 0.0006, Student's t-test) and maximal effects noted with 200 nM S100P and a 0.8 relative amount of pAKT (p = 0.00001, Student's t-test) in the uninduced Rama 37 T-25 cells (Figure 5.6).

A

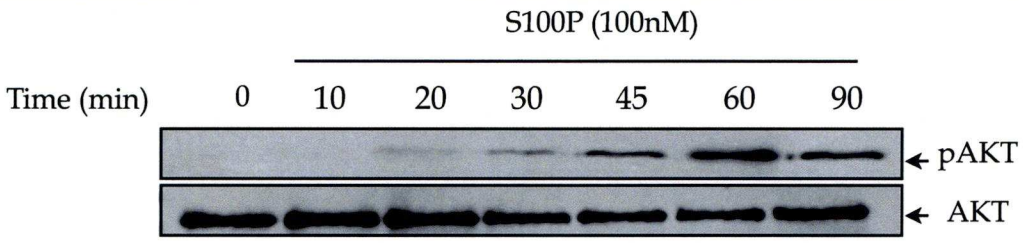

B

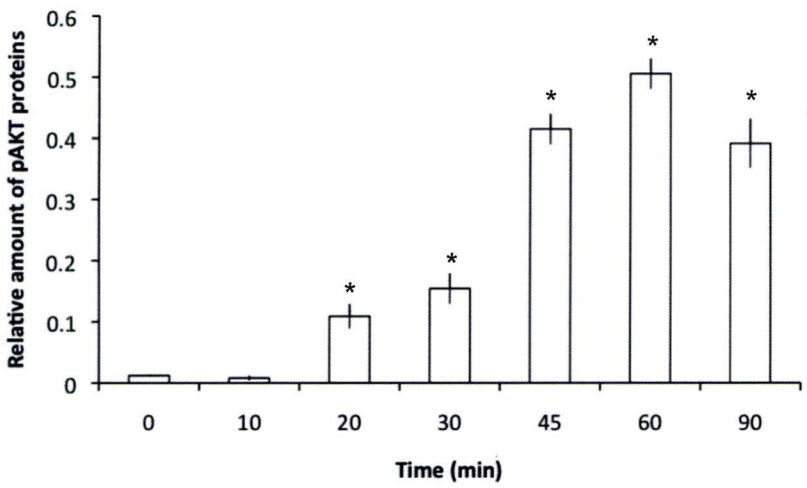

C

Time (min)	0	10	20	30	45	60	90
Relative amount of pAKT	0.01	0.008	0.1	0.15	0.4	0.5	0.35
S.D.	0.001	0.008	0.1	0.1	0	0.5	0.4
p values	/	0.164	0.001	0.0006	9E-06	6E-06	8E-05

***Figure 5.6* Addition of extracellular S100P stimulates AKT phosphorylation in a time-dependent-manner in uninduced Rama 37 T-25 cells.**

Purified S100P was added to the culture of Rama 37 T-25 cells. Cells were lysed and analysed for the presence of pAKT (Ser^{473}) by Western blotting.

A. *Western Blot showing the induction of AKT phosphorylation in uninduced Rama 37 T-25 cells treated with extracellular rS100P (100 nM) for the indicated times (0 –90 min).*

B. *Histogram showing the amount of pAKT related to AKT.*

C. *Table showing Student's t–test results between cells where no S100P was added and addition of S100P (100 nM). (Student's t-test, * $p < 0.05$). Data show mean ± S.D from three independent experiments.*

A

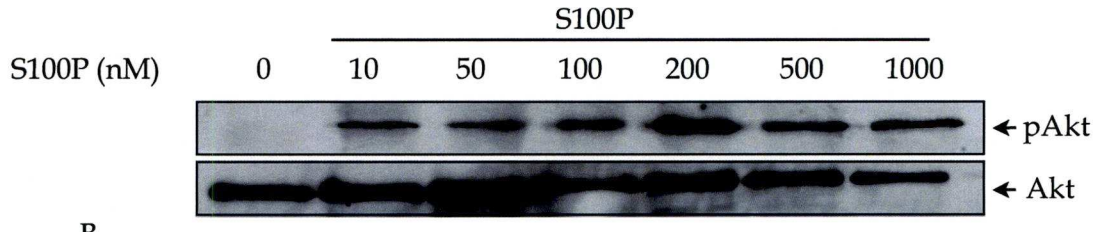

B

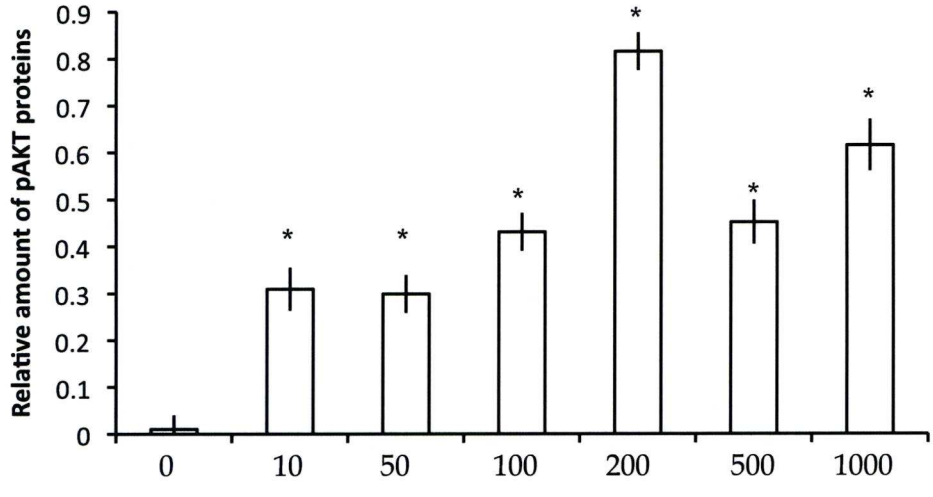

C

S100P (nM)	0	10	50	100	200	500	1000
Relative Amount of pAKT	0.01	0.3	0.3	0.4	0.8	0.4	0.6
S.D.	0.001	0.05	0.04	0.04	0.04	0.05	0.06
p values	/	0.0007	0.0006	0.0001	0.00001	0.0002	0.00008

***Figure 5.7* Addition of extracellular S100P stimulates AKT phosphorylation in a concentration-dependent-manner in uninduced Rama 37 T-25 cells.**

Purified S100P was added to culture medium of uninduced Rama 37 T-25 cells. Cells were lysed 60 min after addition of S100P and analysed for the presence of pAKT (Ser^{473}) by Western blotting.

A. *Western Blot showing the increase of AKT phosphorylation in uninduced Rama 37 T-25 cells after 60 min of treatment with extracellular rS100P for the indicated concentrations (0 –500 nM).*

B. *Histogram showing the amount of pAKT relative to AKT.*

C. *Table showing Student's t–test results between cells where no S100P was added and addition of S100P (0-1000 nM).*

*(Student's t-test, * $p < 0.05$) Data show mean ± S.D from three independent experiments.*

When extracellular rS100P (100 nM) was added to HeLa A-9 cells, it induced AKT phosphorylation within 10 min, and a maximal increase over control levels (0.7 pAKT/total AKT ratio) was observed after 45 min (Student's t-test, $p = 0.0001$). AKT phosphorylation levels declines after 60 min (Figure 5.7 B). Different concentrations of S100P were added to the culture medium of uninduced HeLa A-9 cells. There was a concentration-dependent phosphorylation of AKT with significant effects noted at 10 nM and maximal effects noted with 500 nM S100P 60 min after addition of S100P. Thus when extracellular rS100P was added to uninduced Rama 37 T-25 and HeLa A-9 show there was a time-dependent and concentration-related phosphorylation of AKT.

A

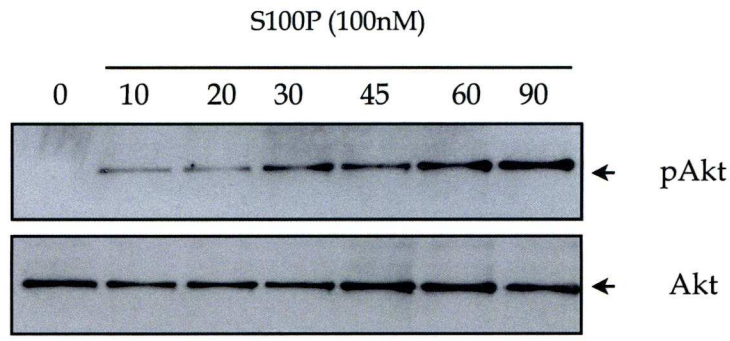

B

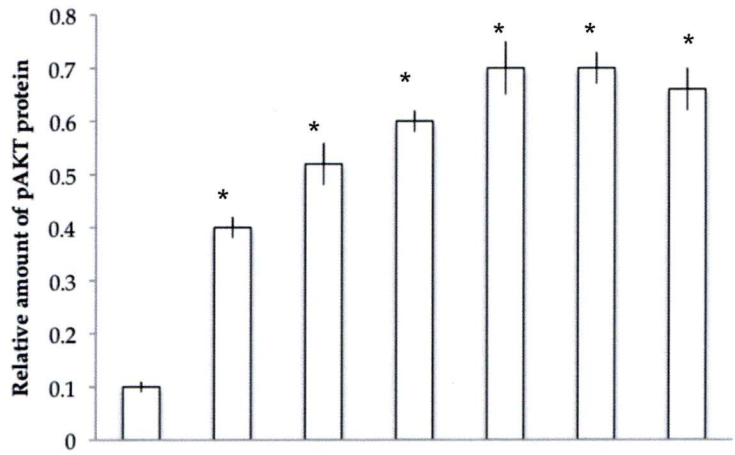

C

Time (min)	0	10	20	30	45	60	90
Relative Amount of pAKT	0.1	0.6	0.62	0.8	0.7	0.8	0.76
S.D.	0.01	0.02	0.04	0.02	0.05	0.03	0.04
p values	/	0.0003	0.0001	0.0001	0.0001	0.0002	0.0001

***Figure 5.8* Addition of extracellular S100P stimulates AKT phosphorylation in a time-dependent-manner in uninduced HeLa A-9 cells.**

Purified S100P was added to the culture of HeLa A-9 cells. Cells were lysed and analysed for the presence of pAKT (Ser^{473}) by Western blotting.

A. Western Blot showing the induction of AKT phosphorylation in uninduced HeLa A-9 cells treated with extracellular rS100P (100 nM) for the indicated times (0 –90 min).

B. Histogram showing the amount of pAKT related to AKT.

*C. Table showing Student's t–test results between cells where no S100P was added and addition of S100P (100 nM). (Student's t-test, * $p < 0.05$). Data show mean ± S.D from three independent experiments.*

A

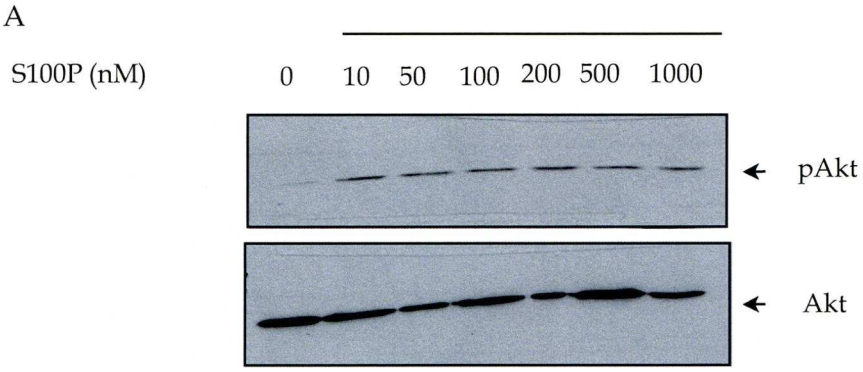

B

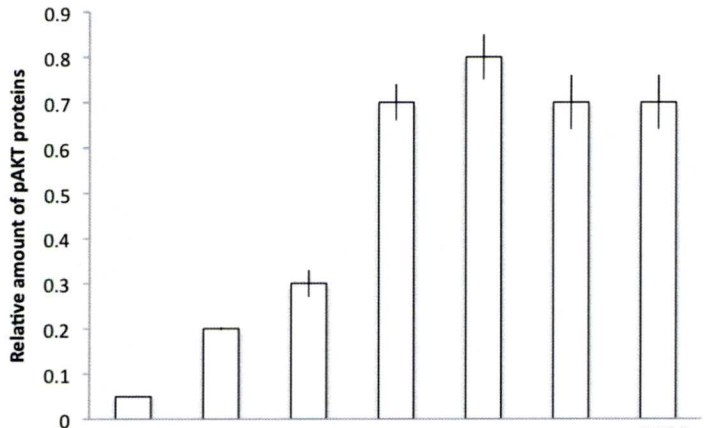

C

S100P (nM) 0 10 50 100 200 500 1000

S100P (nM)	0	10	50	100	200	500	1000
Relative Amount of pAKT	0.05	0.2	0.3	0.7	0.8	0.7	0.7
S.D.	0.001	0.003	0.03	0.04	0.05	0.06	0.06
p values	/	0.009	0.0003	0.0001	0.0001	0.0002	0.0007

***Figure 5.9* Addition of extracellular S100P stimulates AKT phosphorylation in a concentration-dependent-manner in uninduced HeLa A-9 cells.**

Purified S100P was added to culture medium of uninduced HeLa A-9 cells. Cells were lysed 60 min after addition of S100P and analysed for the presence of pAKT (Ser^{473}) by Western blotting.

A. *Western Blot showing the increase of AKT phosphorylation in uninduced Rama 37 T-25 cells after 60 min of treatment with extracellular rS100P for the indicated concentrations (0 –500 nM).*

B. *Histogram showing the amount of pAKT relative to AKT.*

C. *Table showing Student's t–test results between cells where no S100P was added and addition of S100P (0-1000 nM)*

*(Student's t-test, * $p < 0.05$) Data show mean ± S.D from three independent experiments.*

5.2.2.3. Addition of extracellular S100P stimulates the ERK 1/2 signalling pathway

Extracellular signal-regulated kinases (ERKs) are members of the mitogen-activated protein kinase (MAPK) family, which play pivotal roles in diverse cellular events such as regulating cell proliferation, survival (Kim et al., 2009), and migration (Jo et al., 2002). Furthermore S100P has been reported to stimulate ERKs in a mouse embryonic fibroblast cell line (NIH 3T3) through the RAGE Receptor (Arumugam et al., 2004), as well as in the SW480 colon cancer cell line (Fuentes et al., 2007). Activated ERKs phosphorylate numerous cytoplasmic, cytoskeletal proteins (Yoon and Seger, 2006), microtubule cytoskeleton (Reszka et al., 1995) and nuclear targets including transcription factors (Janknecht, 1996; Wang et al., 2004; Zhao et al., 2003). Therefore a pathological deregulation of ERKs signalling pathway can result in dramatic consequences to cell homeostasis. Thus different concentrations of exogenous S100P were added to the cell culture medium, and cell lysates were analysed for ERK (Thr202/Tyr204) phosphorylation by Western blotting.

When extracellular rS100P (100 nM) was added to uninduced Rama 37 T-25 cells, it induced ERK phosphorylation within 5 min (0.45 pERK 1/2 /β-actin ratio, p = 0.007, Student's t-test) and a maximal increase over control levels (0.8 pERK 1/2 / β-actin ratio) after 30 min (Figure 5.10). ERK 1/2 phosphorylation levels declined by 25 % at 45 min (0.6 pERK 1/2 /β-actin ratio). The Effect of S100P on ERK (Thr202/ Tyr204) phosphorylation is time-dependent (p = 0.002, Student's t-test).

Furthermore, extracellular rS100P (100 nM) was added to HeLa A-9 cells culture medium, and induced ERK phosphorylation within 5 min, with a 0.6 pERK/ β-actin ratio and a maximal increase over control levels (0.7 pERK/β-actin ratio) was observed after 45 min (Figure 5.11 B). ERK phosphorylation levels declines beyond 60 min. A time-dependant AKT phosphorylation was induced by extracellular S100P addition to non-expressing Rama 37 T-25 and HeLa A-9 cell lines

A

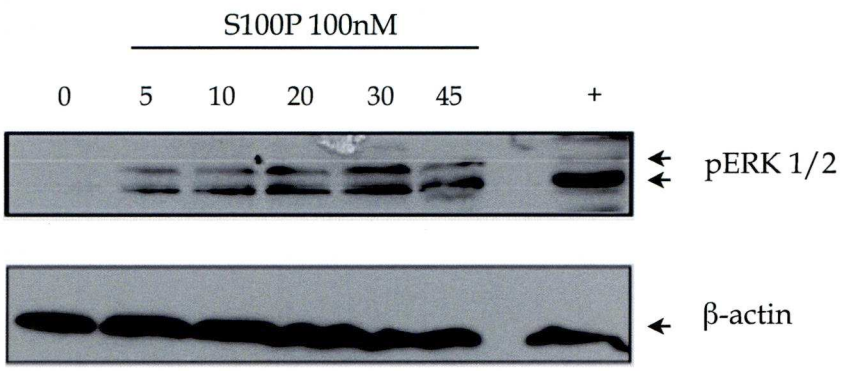

B

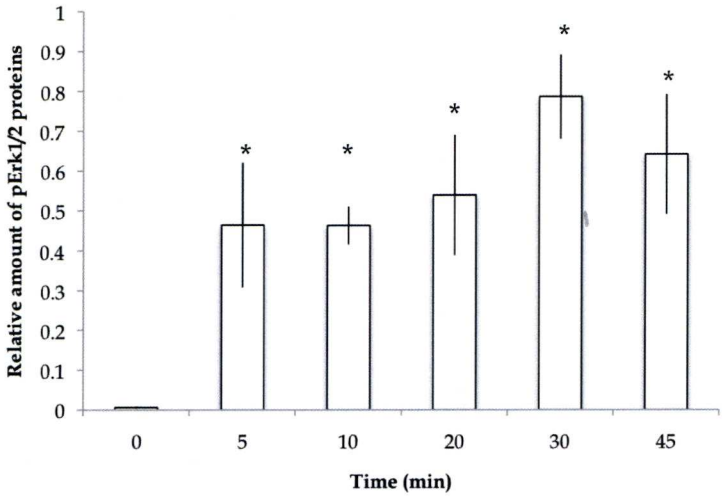

C

Time (min)	0	5	10	20	30	45
Relative amount of pAKT	0.006	0.45	0.46	0.55	0.8	0.6
S.D.	0.003	0.2	0.5	0.1	0.1	0.2
p values	/	0.007	0.00008	0.004	0.0001	0.002

***Figure 5.10* Addition of exogenous S100P stimulates phosphorylation of ERK in uninduced Rama T-25 cells**

Purified S100P (100 nM) was added to the culture medium of uninduced Rama37 T-25 cells for 45 min.

A. *Western Blot showing the increase of ERK (Thr202/Tyr204) phosphorylation in uninduced Rama 37 T-25 cells treated with extracellular rS100P (100 nM) for the indicated times (0 –90 min).*

B. *Histogram showing the amount of pERK 1/2 relative to that of β-actin.*

C. *Table showing Student's t–test results between cells where no S100P was added and addition of S100P (100 nM). (Student's t-test, * $p < 0.05$). Data show mean ± S.D from three independent experiments.*

A

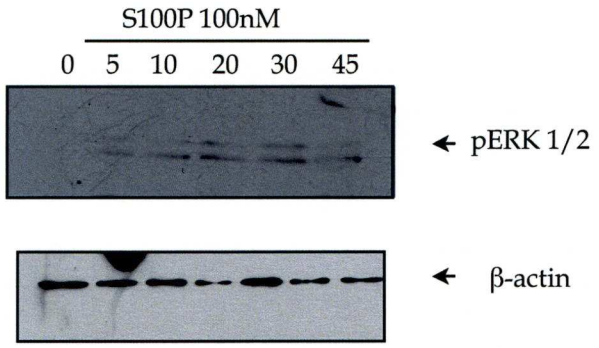

B

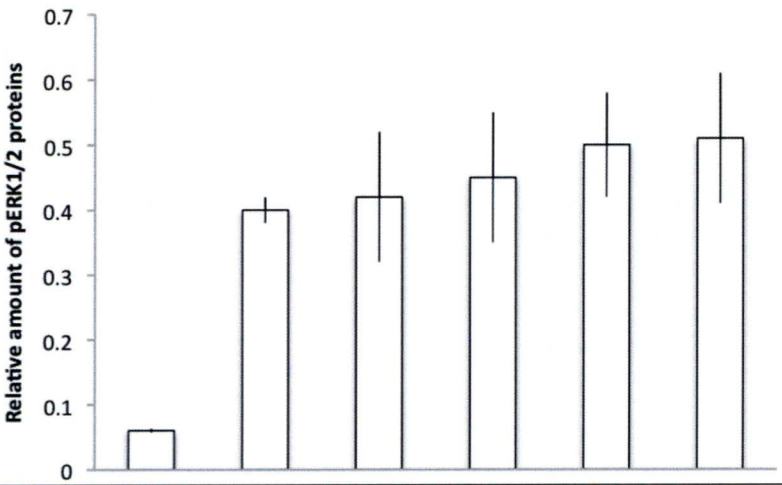

C

Time (min)	0	5	10	20	30	45
Relative amount of pAKT	0.06	0.4	0.42	0.45	0.5	0.51
S.D.	0.003	0.02	0.1	0.1	0.08	0.1
p values	/	0.003	0.007	0.003	0.001	0.002

***Figure 5.11* Addition of exogenous S100P stimulates phosphorylation of ERK in uninduced HeLa A-9 cells**

Purified S100P (100 nM) was added to the culture medium of uninduced HeLa A-9 cells for 45 min.

A. *Western Blot showing the increase of ERK (Thr202/Tyr204) phosphorylation in uninduced Rama 37 T-25 cells treated with extracellular rS100P (100 nM) for the indicated times (0 –90 min).*

B. *Histogram showing the amount of pERK 1/2 relative to that of β-actin.*

C. *Table showing Student's t–test results between cells where no S100P was added and addition of S100P (100 nM). (Student's t-test, * $p < 0.05$). Data show mean ± S.D from three independent experiments.*

5.2.2.4. S100P mediated PI3K/AKT and MEK/ERK activation is RAGE-dependent

Since exogenous S100P was added to the culture medium, it activated PI3K/AKT and MEK/ERK signalling pathways, this prompted us to investigate whether these pathways could be regulated by the RAGE receptor. To determine, whether the addition of extracellular S100P activates PI3K/AKT and MEK/ERK pathways through the RAGE receptor, anti-RAGE inhibitor was used to block the ligand-RAGE receptor binding (as described in the Material and Methods Chapter 2 Section 2.2.1.1.g.).

Thus uninduced Rama 37 T-25 cells were treated with Anti-RAGE (166μg/mL) for 30 min, before rS100P (100nM) was added to the cells, and enzyme in the signalling pathway analysed with time. When cells were treated with Anti-RAGE I observed an inhibition of the increase phosphorylation of both ERK (Thr202/Tyr204), at anytime up to 60 min (p = 0.302, Student's t-test) (Figure 5.9). The increase of phosphorylation of AKT (Ser^{473}) was also inhibited at anytime up to 60 min (p = 0.777, Student's t-test) (Figure 5.9). Presumably the blockage of S100P binding to RAGE by antagonists inhibited the phosphorylation and hence activation of the PI3K/AKT and MAPK/ERK signalling pathways (Figure 5.9). Thereafter phosphorylation of PI3K/AKT and ERK1/2 was observed after 60 min presumably because inhibition by the anti-RAGE receptor declined perhaps due to its degradation. The increase phosphorylation of AKT was still inhibited up to 1440 min (p = 0.119, Student's t-test) (Figure 5.9). Nevertheless, after 1440 min the increase of phosphorylation of ERK 1/2 was significant (p = 0.007, Student's t-test).

A

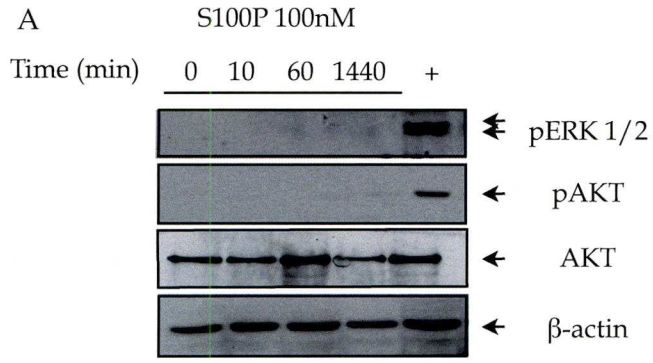

B

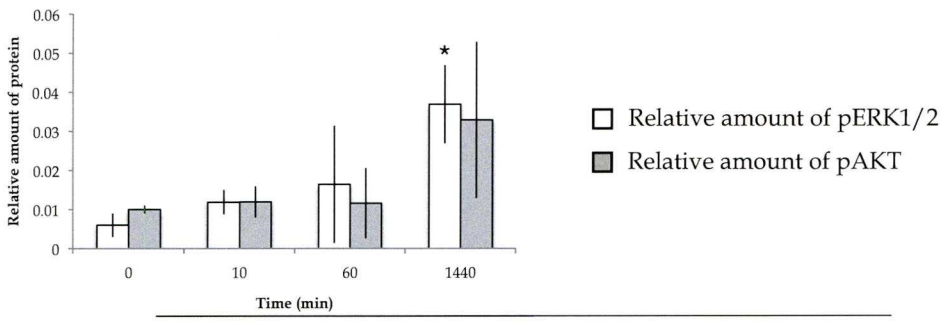

C

Time (min)	0	10	60	1440
Relative amount of pERK 1/2	0.006	0.01	0.017	0.04
S.D.	0.003	0.0031	0.015	0.01
p values	/	0.078	0.302	0.007
Relative amount of pAKT	0.01	0.01	0.01	0.03
S.D.	0.001	0.004	0.009	0.02
p values	/	0.468	0.777	0.119

***Figure 5.12* Effect of treating uninduced Rama 37 T-25 cells with Anti-RAGE inhibitor (166 µg/mL)**

Uninduced Rama 37 T-25 cells were treated with Anti-RAGE inhibitor (166 µg/mL) for 30 min prior addition of rS100P (100 nM) for 60 min

A. *Western Blot showing the induction of ERK (Thr202/Tyr204) and AKT (Ser^{473}) phosphorylation in uninduced Rama 37 T-25 cells treated with extracellular rS100P (100 nM) and Anti-RAGE for the indicated times (0 –1440 min).*

B. *Histogram showing the relative amount of pERK 1/2 relative to β-actin (white bars) and the amount of pAKT relative to AKT (grey bars).*

C. *Table showing Student's t–test results between Rama 37 T-25 cells treated with Anti-Rage (166 µg/mL) where no S100P was added and addition of S100P (100 nM). (Student's t-test, * $p < 0.05$). Data show mean ± S.D from three independent experiments.*

5.2.2.5. S100P stimulates cell migration through AKT and ERK 1/2 signalling pathway via the RAGE Receptor

To investigate whether the effects of extracellular S100P on cell migration were mediated via the RAGE receptor and the AKT and ERK pathways, I attempted to block its effect with the anti-RAGE antibody and a specific inhibitor of the AKT pathway, wortmannin and of the ERK pathway, PD98059. Wortmannin is a specific, covalent inhibitor of phosphatidylinositol 3-kinases (PI3Ks), which has been isolated as an antibiotic from a culture of the fungi *Penicillium wortmanni Klocker* (Brian et al., 1957). The fungal metabolite wortmannin is an inhibitor, which show a fairly high specificity for PI3K. Wortmannin binds to the p110 catalytic subunit of PI3K, noncompetitively and irreversibly inhibiting the enzyme (Powis et al., 1994).

A dose-response curve was assessed for wortmannin, in order to use the most efficient inhibitory concentration of the enzyme for my migration assay (Figure 5.10). The treatment of uninduced Rama 37 T-25 with 100nM wortmannin before the addition of rS100P (100 nM) to the culture medium decreased by 80 % the phosphorylation of pAKT, 60 min after addition of rS100P (Figure 5.10 A). Higher concentration of wortmannin inhibited the 90 % of AKT phosphorylation, but to limit cytotoxic effect that could be due to the use of high concentration of inhibitor, I used 100 nM wortmannin for my migration assay.

I also used PD98059, which is a synthetic non-competitive inhibitor of the ERK 1/2 MAP kinase cascade (Pang et al., 1995). A dose-response curve was assessed for PD98059 so that I could use use the most efficient inhibitory concentration of the enzyme for my cell migration assay (Figure 5.10 B).

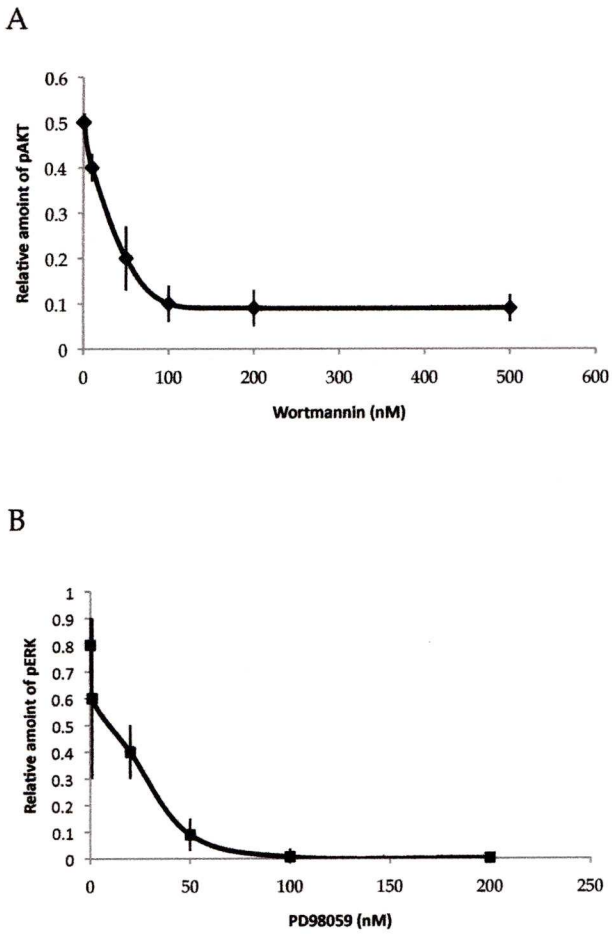

Figure 5.13 **Dose-response curve of Wortmannin and PD98059 concentration against Realtive amount of phosphorylation of pAKT and pERK**

A. *The inhibition activity of pAKT was monitored by increasing concentration of wortmannin inhibitor. pAKT levels were normalised to those of AKT.*

B. *The inhibition activity of pERK was monitored by increasing concentration of PD98059 inhibitor. pERK levels were normalised to those of* β-actin.

The migration assay was performed in the Boyden chambers, and migratory stimulation by extracellular S100P (100nM) with or without inhibitor treatment. After 24 h in control assays in which no S100P was added to the culture medium only 1.7 % of cells migrated through to the lower chamber. When 100 nM exogenous S100P protein was added to the uninduced Rama 37 T-25 cells, this resulted in a significant 7.5 % increase of cell motility passing to the lower chamber after addition of (p = 0.0001, Student's t-test) (Figure 5.11 A). Treatment of Rama 37 T-25 cells with wortmannin (100 nM) inhibited cell migration with no significant difference proportion of migratory cells observed with 1.7 % of motile cells before addition of 100 nM S100P and 2.3 % of motile cells after addition of 100nM (p = 0.2, Student's t-test). The inhibition of AKT phosphorylation significantly abolished the S100P extracellular induction of cell migration. No significant difference of motile cells (p = 0.8, Student's t-test) was observed after inhibition of phosphorylation of ERK1/2 with PD 98059 (50nM) treatment. Only 1.5 % of motile ininduced Rama 37 T-25 cells were observed before S100P was added to the cells, and 1.6 % motile ininduced Rama 37 T-25 cells after exogenous rS100P (100 nM) addition. Similar results were observed with treatment of uninduced Rama 37 T-25 cells with Anti-Rage when only 2.2 % of cells were motile prior addition of exogenous rS100P and no significant difference (p = 0.08, Student's t-test) of motile cells was observed with 3.2 % motile cells when S100P was added to the medium.

These results suggest that the extracellular effects of S100P on cell migration is RAGE-dependent and activates both MEK/ERK 1/2 and PI3K/AKT signalling pathways.

A

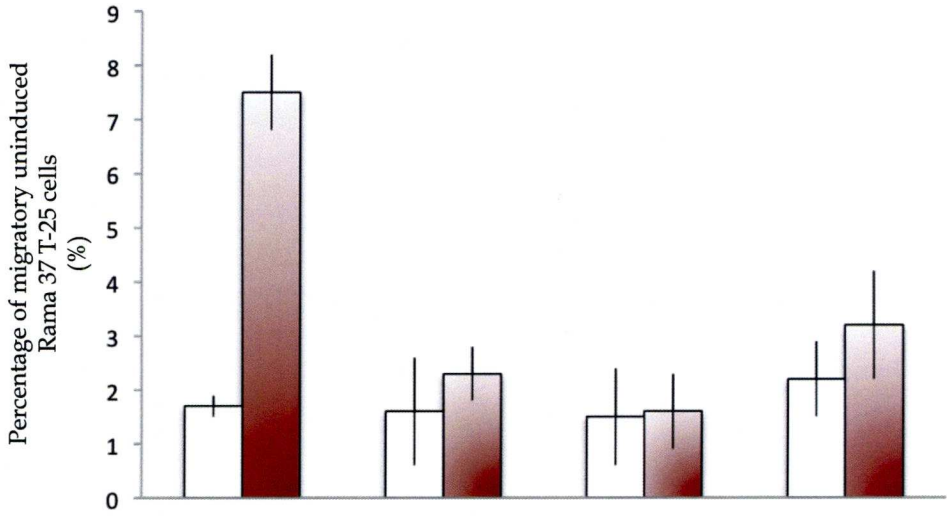

B

S100P (100 nM)	- +	- +	- +	- +
Wortmannin (100 nM)	- -	- +	- -	- -
PD 98059 (50 nM)	- -	- -	- +	- -
Anti-RAGE (166µg/mL)	- -	- -	- -	- +

Figure 5.14 **Effect of inhibitors wortmannin, PD98059 and RAGE anitibodies on extracellular S100P-induced migration in Rama 37 T-25 cell line.**

A. *Histogram of the percentage of migrating cells stimulated with (red bars) or without (white bars) extracellular rS100P (100 nM) in the presence (+) or absence (-) of an inhibitor treatment. Data show the mean +/- Standard Deviation (S.D.) from three separate experiments.*

B. *Table showing the presence (+) or absence (-) of inhibitor treatments*

5.3. Discussion

The extracellular appearance of S100P outside the cell as previously reported in the literature (Arumugam et al., 2004) has been confirmed in Rama 37 cells and HeLa cells. In this chapter, it is reported that the presence of S100P is correlated with cell migration through PI3K/AKT and MAPK/ERK 1/2 by the Rage receptor. Both pathways are critical for Rama 37 and HeLa cell migration, with significant decrease of migration when inhibited. Other member of the S100 protein family have been shown to stimulate AKT phosphorylation, such as S100A7, which has been correlated with phosphorylated AKT in breast invasive carcinomas (Emberley et al., 2005) via NF-κB regulation though IκB inhibition (Emberley et al., 2005). Moreover, in the previous chapter (Chapter 4) microarray results highlighted S100A7a, an isoform of S100A7, to be up-regulated by S100P, however in this study the cross-talks of the S100A7, AKT and NF-κB has not been investigated.

PI3K is activated downstream of extracellular signals and phosphorylates phosphatidylinositol-4,5-bisphosphate to generate phosphatidylinositol-3,4,5-trisphosphate (PIP3), which is a lipid second messenger, which activates the phosphorylation of AKT. A tumour suppressor is known to play an important role pAKT phosphorylation regulation: Pten (phosphatase and tensin homologue deleted on chromosome 10) (Tokunaga et al., 2007). The tumour suppressor PTEN catalyses the opposite reaction by reducing the pool of PIP3. The PI3K/AKT pathway alteration is commonly associated with the tumour-suppressor Pten deregulation in human malignancy (Marty et al., 2008). Abnormal PI3K and PTEN regulation is a strong indicator of metastasis and poor patient survival in breast carcinomas (Marty et al., 2008; Saal et al., 2007). I have not investigated the implication of PTEN in the S100P cell migration inducing process.

Furthermore I have shown that the knock-down of Mastl gene in Rama 37 pcDNA-S100P cells overexpressing S100P significantly decreased cell migration (Chapter 4), and despite the extracellular addition of S100P, no cell migration was activated, showing an important combination of S100P-Mastl regulator activity direct role of Mastl on the extracellular. The hypothesis of a downstream regulation of the RAGE receptor on cell migration, such as the inactivation of AKT and/or ERK downstream pathways via MAST1 up-regulation S100P, as represented in the illustration Figure 5.13.

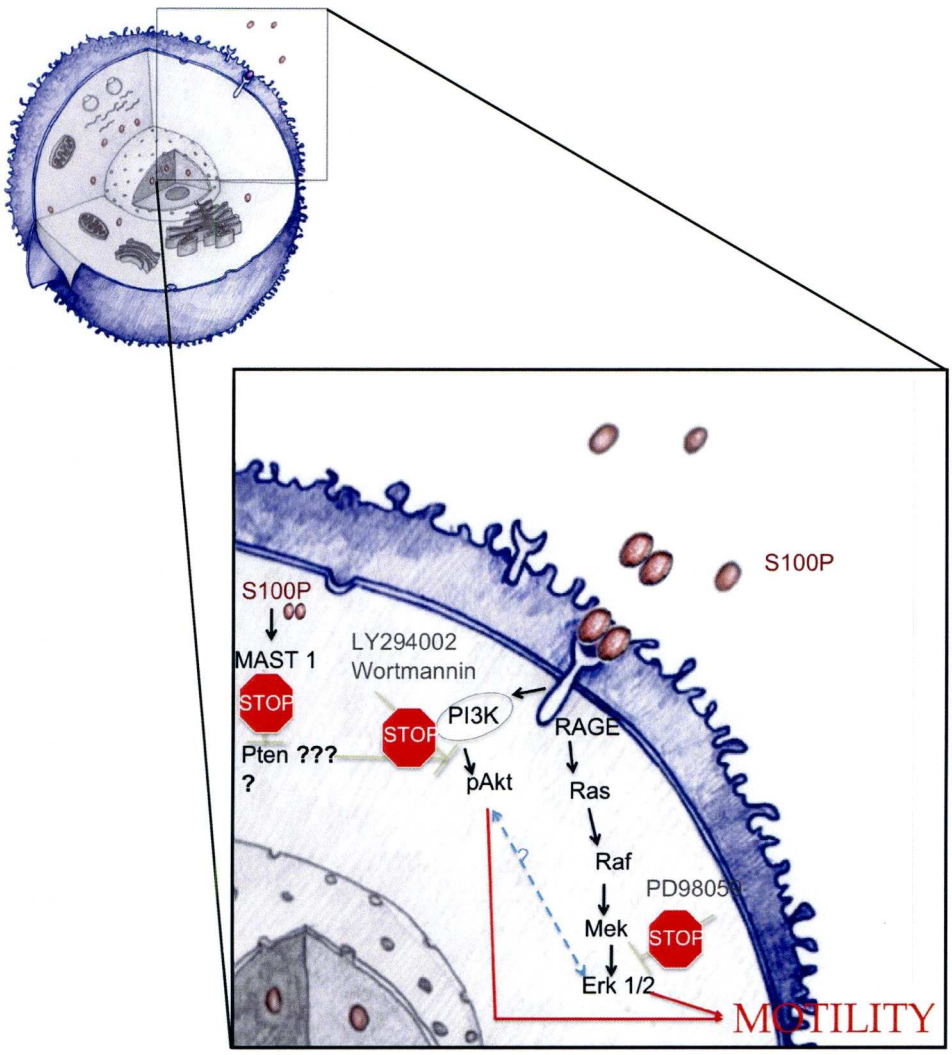

Figure 5.13 **Illustration of the role of extracellular S100P in Rama 37 T-25 stimulated cell migration**

It's suggested that extracellular S100P activates cell migration via PI3K/AKT and ERK 1/2 / MAPK signalling pathways through the RAGE receptor. The stimulated migration was abolished after treatments of induced Rama 37 T-25 cells with inhibitor that blocked RAGE receptor and AKT and ERK 1/2. Intracellular S100P up-regulates Mast1 expression, which is also involved in cell migration (Results Chapter 4), and knock-down of Mast1 gene expression, despite addition of extracellular S100P significantly decreases cell migration.

Chapter 6

General Discussion

GENERAL DISCUSSION

The ultimate goal of this study has been to identify new molecular markers associated with cell migration induced by up-regulation of S100P and further verify experimentally, the role of these markers. To characterise the role of the metastatis-inducible calcium-binding protein S100P's role on cell activity I used cells transfected with a single inducible transgene vector that confers site-specific expression after induction with doxycycline. This approach of the use of a single cell-type specific doxycycline-inducible construct for *in vitro* studies over the conventional knock-out or overexpression of a specific gene has several advantages, including ability to turn S100P on or off as desired, giving more accuracy in the detection of potential targets for S100P. For further investigations in rats, administration of oral doxycycline is easy to perform compared to the intra-peritoneal administration of other inducers such as tamoxifen and it also generates less side effects. Some disadvantages of doxycycline-inducible strategies have been reported, such as possible leakiness in un-induced cells, or when the cDNA was used instead of the genomic sequence, normal post-transcriptional modifications such as alternative splicing may not take place due to lack of introns in the sequence (Meyer-Ficca et al., 2004; Pham et al., 2008). Doxycycline is 6-deoxy-5-oxy tetracycline antibiotic, synthesized from oxytetracycline by a series of sequential steps that produce methacycline and eventually doxycycline (Nelson, 1998). It has been reported to have effects on cancer cells *in vitro* and *in vivo* (Fife and Sledge, 1995; Fife and Sledge, 1998). At higher (42 mM) concentrations it inhibited cell proliferation, induction of apoptosis and growth of tumours in breast carcinoma cells (Fife et al., 1994), but low concentration used here (62.5 - 112.5 nM) have been reported to have no effect on cancer cells (Onoda et al., 2006; Sourdeval et al., 2006).

Our investigations using the S100P inducible cell line developed in our laboratory by Dr G.Wang, demonstrates that intracellular overexpression of intracellular S100P significantly stimulates cell migration in our rat mammary (Rama 37) and human derived cervical cancer cell lines (HeLa). The results demonstrated a direct role for S100P in cell migration.

Despite the fact that overexpression of S100P has been well documented in numerous cancers, associated with tumour progression (Arumugam et al., 2005; Bartling et al., 2007; Basu et al., 2008; Fuentes et al., 2007; Mousses et al., 2002), poor

patient prognosis (Diederichs et al., 2004; Fuentes et al., 2007; Guerreiro Da Silva et al., 2000; Logsdon et al., 2003; Mousses et al., 2002; Wang et al., 2006) and more recently with induction of metastasis (Wang et al., 2006), the underlying cellular mechanisms are obscure. The subcellular localisation of the protein in our cell models was in agreement with previously reported results i.e. it occurred in the cell cytoplasm, nucleus and extracellular compartments (Parkkila, 2008; Sato and Hitomi, 2002; Wang et al., 2006). S100P is naturally expressed in trophoblastic cells, with a stronger expression in nuclei than in the cytoplasm (Parkkila et al., 2008), and a similar nucleo-cytoplamic localisation has been detected in overexpression of S100P in malignant tumour cells (Nakata et al., 2010; Parkkila et al., 2008; Rehbein et al., 2008; Sato and Hitomi, 2002; Wang et al., 2006). The majority of normal cells do not or only weakly express S100P, but after malignant transformation cells are often found overexpressing intracellular S100P with a strong nuclear localisation. In one study it is the nuclear S100P which is associated with a poor prognosis for breast cancer patients. The association of patient death with nuclear S100P has been observed for another S100 metastasis-inducing protein, S100A4 , with a poor patient prognosis and poor response to chemotherapy diagnosis in advanced-stage ovarian carcinoma (Maelandsmo et al., 2009). Wang et al. (2006) observed that in tumours overexpressing S100P, it was principally localised in the nucleus, and the presence of S100P expression has been strongly associated with a decrease of patient survival.

Nuclear localisation has been reported for several other S100 proteins: S100A1 (Baudier et al., 1995), S100A4 (Flatmark et al., 2003), S100A5 , S100A6 (Deloulme et al., 2000), S100A11 (Davey et al., 2000; Sakaguchi et al., 2000) and S100B (Deloulme et al., 2000), but the translocation mechanism is poorly understood. Since S100P is a small molecule of only 10.4 kDa (Becker et al., 1992), and does not contain any classical consensus sequences that could target the protein to the nucleus, it could possibly pass through the nuclear pores without any active transport mechanism being involved.

A number of microarray-based analyses have identified up-regulation of S100P in various tumoral tissues. Our inducible system has allowed us to use cDNA chip microarrays, to compare gene expression between migratory cells overexpressing S100P and non-migratory cells not expressing S100P. This list of differentially expressed genes contains 5 up-regulated genes and 3 down-regulated genes. The up-regulated genes include Folate Hydrolase (Folh1), Cyclin D2 (CcnD2), S100A7, aldo-keto reductase family 7 member A2 (Akr7a2) and a microtubule-

associated serine/threonine kinase 1 (Mastl). The upregulations have been confirmed by qPCR in our inducible rat mammary (Rama 37 T-25) and human cell lines (HeLa A-9) and these results support the role of S100P in up-regulation of these genes. All five up-regulated genes have been correlated with cancer progression, invasion, poor prognostic or chemotherapy resistance. Folh1 (previously known as the prostate specific-membrane antigen (PSMA)) is a type II metallo-peptidase glycoprotein (Murphy et al., 1998; Pinto et al., 1996) commonly found to be overexpressed in prostate (Sweat et al., 1998), including metastatic prostate cancer (Chang et al., 2001), gastric colorectal (Haffner et al., 2009), bladder (Gala et al., 2000), and renal cancers (Dumas et al., 1999), and has been associated with poor patient prognosis in patients suffering from endometrial carcinomas (Mhawech-Fauceglia et al., 2008).

Studies have shown that the cyclin-dependent kinases D2, is overexpressed in 20 breast carcinoma-derived cell lines (Buckley et al., 1993), in colon tumours, where overexpression of Cyclin D2 is correlated with a higher TNM stage of the cancer (Mermelshtein et al., 2005), and is also considered as a proto-oncogene due to transcriptional activation of cyclin D2 in immortalisation of primary B lymphocytes by the Epstein-Barr virus (Sinclair et al., 1994).

S100A7a is an isoform of the S100A7 protein (Kulski et al., 2003). S100A7 was originally named psoriasin because it was first identified as a pathophysiologically active element of psoriasis (Madsen et al., 1991). Studies have since found S100A7 to be expressed in several tumoral tissues such as skin (Alowami et al., 2003), bladder (Celis et al., 1996), stomach (El-Rifai et al., 2002) and breast (Al-Haddad et al., 1999; Leygue et al., 1996; Moog-Lutz et al., 1995). S100A7 has also been associated with poor prognosis of breast cancer patients (Emberley et al., 2003). Akr7a2 is an aflatoxin B aldehyde reductase, which is involved in the detoxification of aldehydes and ketones in phase I metabolism. It is also involved in metabolism of γ-amino-butyric acid by converting the succinic semi-aldehyde to γ-hydroxybutyrate (Jez et al., 1997; Jez and Penning, 2001). Akr7a2 has recently been reported to be highly up-regulated in pancreatic cancer, but is not expressed in normal pancreas or benign tumours.This result suggests a potential role for Akr7a2 in pancreatic tumour pathological processes (Cui et al., 2009).

Finally, Mastl is a cytoskeletal-associated kinase, which has been discovered in the granule cells of the brain's hippocampal dentate gyrus. These stem cells proliferate to produce neuronal granule in the adult (Yano et al., 2003). Mastl is

highly expressed in the brain and also in multiple tissues (Garland et al., 2008). It binds syntrophin adapter proteins by PDZ-PDZ domain interactions. It have also been reported that the Mast1 protein binds the tumour suppressor PTEN by PDZ-PDZ interaction. It facilitates PTEN inactivation by phosphorylation (Valiente et al., 2005). Up-regulation of these genes follows S100P up-regulation, and they are therefore candidates for the S100P induction mechanism for increased cell migration in our inducible systems. Thus I have shown that up-regulation of S100P in two cancer cell lines increases the expression of 5 genes described in the literature to be active in tumorigenesis.

The up-regulation by S100P of a gene coding for a protein binding to the microtubules, the microtubule-associated serine-threonine kinase 1 (Mast1), suggests a potential role for Mast1 in cell migration. Thus it was of interest to characterise its role further. So far Mast1 has not been associated directly with cancer or metastatic activity and its functions are largely unknown. In this thesis knock-out using SiRNA technology has been performed and our results demonstrate a significant drop in cell migration when Mast1 expression is silenced in rat mammary cells. Since there are no differences in levels of expression of S100P mRNA after knock-out of Mast1, this result suggests that there is no effect of Mast1 on S100P gene expression. Thus Mast1 is located downstream of S100P in the induction of increased cell migration in our cellular systems. Our results demonstrates a crucial involvement of Mast1 in S100P induced cell migration, with a significant 5-fold decrease in S100P induced cell migration despite the presence of S100P.

The data shows that addition of extracellular S100P to the culture medium also increased cell motility. S100P has been reported to interact with one commonly described receptor, the Receptor for Advanced Glycation End-product (RAGE) (Arumugam et al., 2004; Fuentes et al., 2007). Activation of the RAGE receptor has been shown to stimulate cell growth, tumour progression and invasion via the PI3K/MAPK intracellular signalling pathways (Arumugam et al., 2005). Our results corroborated these observations, since I observed enhanced Erk1/2 phosphorylation after addition of 100 nM exogenous S100P to the culture medium. This addition also caused a significant increase (8 fold) in cell migration. I also described for the first time the activation of the Akt pathway presumably by the same RAGE receptor. Thus addition of extracellular S100P activated Erk1/2 and Akt phosphorylation, and their phosphorylation were inhibited by prior treatment of the cells with RAGE

inhibitors and/or PD 98059. Cell migration stimulated by exogenous S100P was also significantly decreased by 60% when cells were treated with Akt, Erk1/2 or RAGE inhibitors. Thus extracellular S100P can stimulate cell migration *in vitro* though the RAGE receptor activation of the PI3K/Akt signalling pathways.

Akt phosphorylation is an important initiator of a variety of oncogenic processes, such as cell growth, proliferation, cell motility and invasion (Mitsiades et al., 2004). Akt activation has been correlated with the loss or inactivation of the PTEN tumour-suppressor in human patients and, in animal models, with increased tumorigenicity and metastasis (Stiles et al., 2002). These results raise a possible connection between the reduced functions of PTEN and its binding to Mast1 via PDZ domains. This result could lead to AKT activation by the RAGE receptor.

This hypothesis is supported by our results, which shows a decrease of AKT phosphorylation after Mast1 gene knockdown, despite the extracellular stimulation of RAGE by exogenous S100P (Chapter 5). The present study clearly advances our knowledge of potential molecules and pathways with which S100P can interact, but presumably, some other unknown co-activators, such as non muscle skeletal myosin, microtubules or tumour-suppressor, may also be involved in cell migration. However it is clear that overexpression of S100P then increases cell migration.

Further investigation of S100P regulation of cell migration requires multidisciplinary approaches to examine specific molecular interactions *in vitro* and translate this information to S100P functions *in vivo*. Our microarray results revealed an induction of transcription of 5 genes following intracellular stimulation of S100P expression. I have targeted Mast1's influence on cell migration, but more analysis is required to clarify how this gene is regulated and potential S100P microtubule and/or tumour suppressor binding partners. Investigations are also warranted to determine, whether S100P nuclear localisation is due to the promoter or other regulatory region of the binding Mast1 gene and acting as a transcription factor to activate Mast1 gene expression. Lastly, investigation to determine whether other S100 proteins, which are structurally similar, are acting the same way to widen patients presenting the same pathological features for potential targets against S100 metastasis-inducing proteins.

Appendix

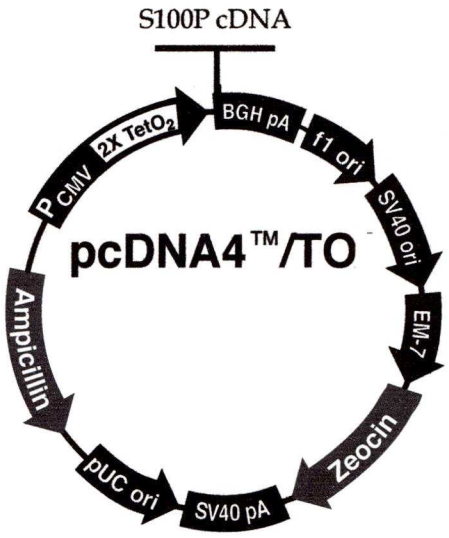

Comments for pcDNA4™/TO

5078 nucleotides

CMV promoter: bases 232-958
TATA box: bases 804-810
Tetracycline operator 2 (2X $TetO_2$) sequences: bases 820-859
CMV Forward priming site: bases 769-789
Multiple cloning site: bases 968-1069
c-myc epitope: bases 1073-1102
Polyhistidine (6xHis) tag: bases 1118-1135
BGH reverse priming site: bases 1158-1175
BGH polyadenylation sequence: bases 1164-1388
f1 origin: bases 1434-1862
SV40 promoter and origin: bases 1867-2211
EM-7 promoter: bases 2253-2319
Zeocin™ resistance gene: bases 2320-2694
SV40 early polyadenylation sequence: bases 2824-2954
pUC origin: bases 3337-4010 (complementary strand)
bla promoter: bases 5016-5114 (complementary strand)
Ampicillin (*bla*) resistance gene: bases 4155-5015 (complementary strand)

***Figure A.1* pcDNA4/TO inducible vector**

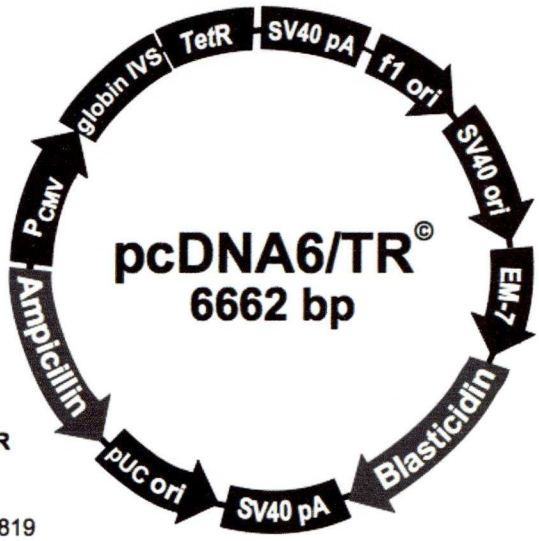

Comments for pcDNA6/TR
6662 nucleotides

CMV promoter: bases 232-819
Rabbit β-globin intron II: bases 1028-1600
*Tet*R gene: bases 1684-2304
SV40 early polyadenylation sequence: bases 2346-2477
f1 origin: bases 2897-3325
SV40 promoter and origin: bases 3335-3675
EM-7 promoter: bases 3715-3781
Blasticidin resistance gene: bases 3782-4180
SV40 early polyadenylation sequence: bases 4338-4468
pUC-derived origin: bases 4851-5521
bla promoter: bases 6521-6625 (C)
Ampicillin (*bla*) resistance gene: bases 5666-6526 (C)

Figure A.2 **pcDNA6/TR Regulatory plasmid**

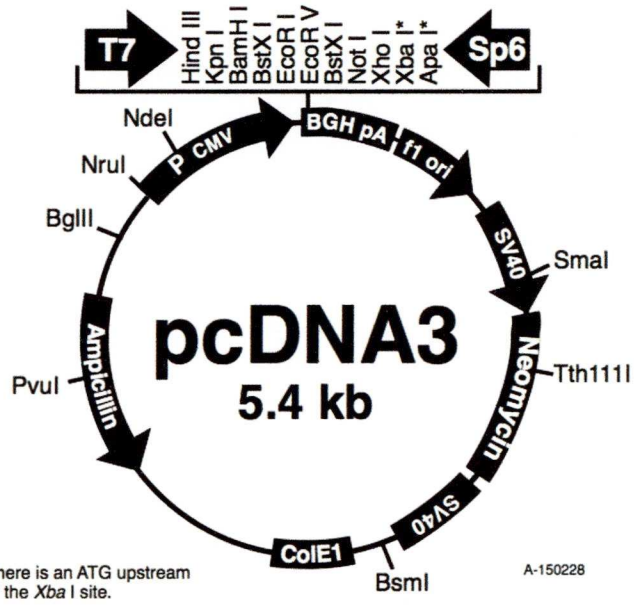

Comments for pcDNA3:
5446 nucleotides

CMV promoter: bases 209-863
T7 promoter: bases 864-882
Polylinker: bases 889-994
Sp6 promoter: bases 999-1016
BGH poly A: bases 1018-1249
SV40 promoter: bases 1790-2115
SV40 origin of replication: bases 1984-2069
Neomycin ORF: bases 2151-2945
SV40 poly A: bases 3000-3372
ColE1 origin: bases 3632-4305
Ampicillin ORF: bases 4450-5310

Figure A.3. **pcDNA3 Expression plasmid**

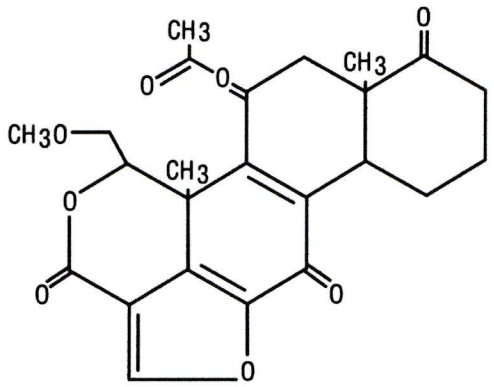

Figure A.4 **Chemical structure of wortmannin**

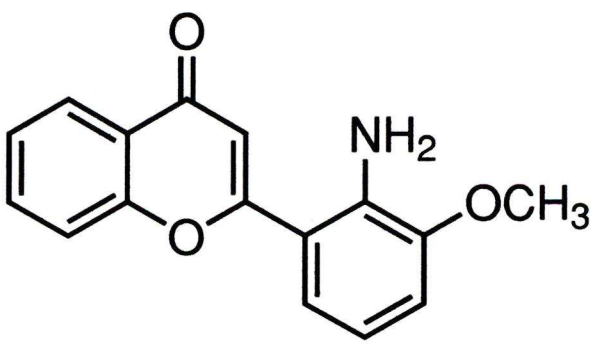

Figure A.5 **Chemical structure of PD 98059**

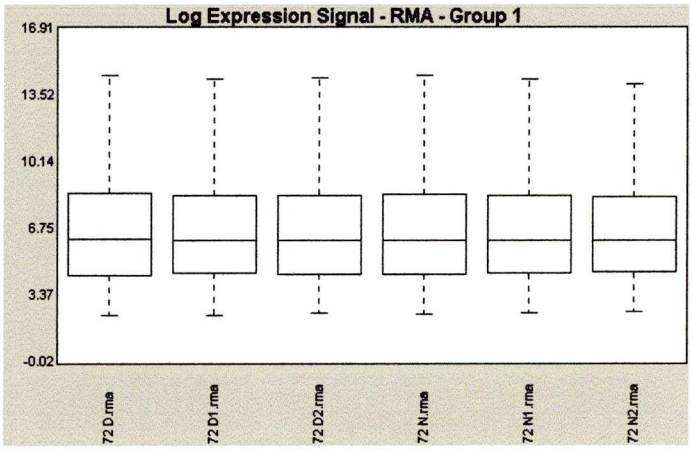

Figure A.6 **Boxplots showing log2 expression values < 0.01 to 0.01 of microarray Affymetrix analysis**

Each box plot shows the different log2 expression values < 0.01 to 0.01 of each RNA sample extracted from induced Rama 37 T-25 cells (72D, 72D1, 72D2) with doxycycline treatment (62.5 nM) for 72 h, and RNA from uninduced Rama 37 T-25 (72N, 72N1, 72N2).

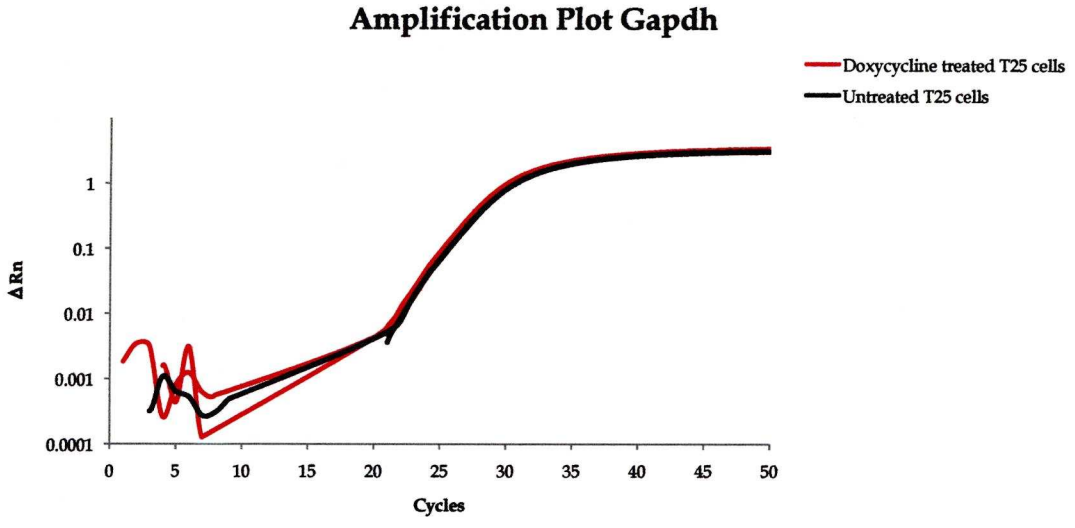
Amplification Plot Gapdh
Doxycycline treated T25 cells
Untreated T25 cells
ΔRn
1
0.1
0.01
0.001
0.0001
0
5
10
15
20
25
30
35
40
45
50
Cycles

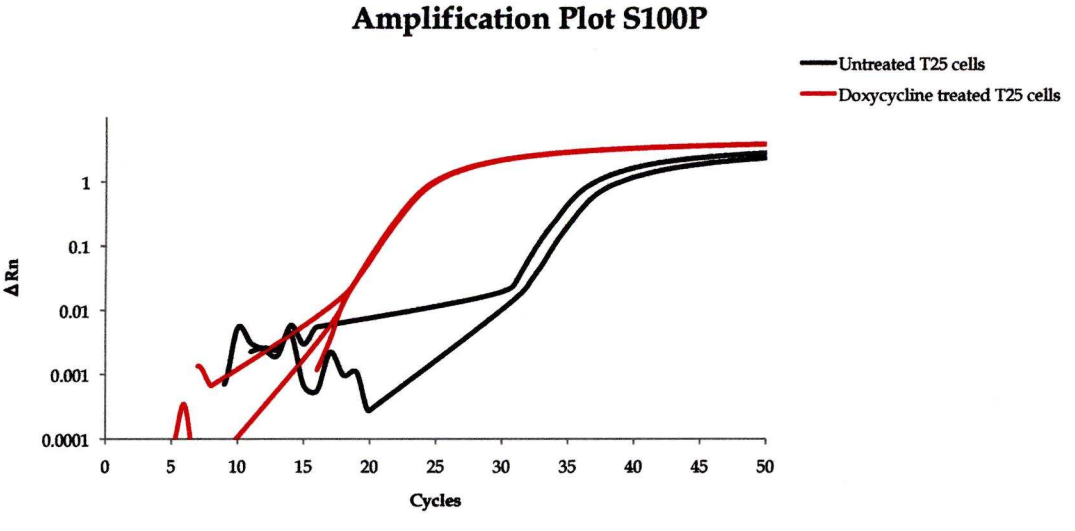
Amplification Plot S100P
Untreated T25 cells
Doxycycline treated T25 cells
ΔRn
1
0.1
0.01
0.001
0.0001
0
5
10
15
20
25
30
35
40
45
50
Cycles

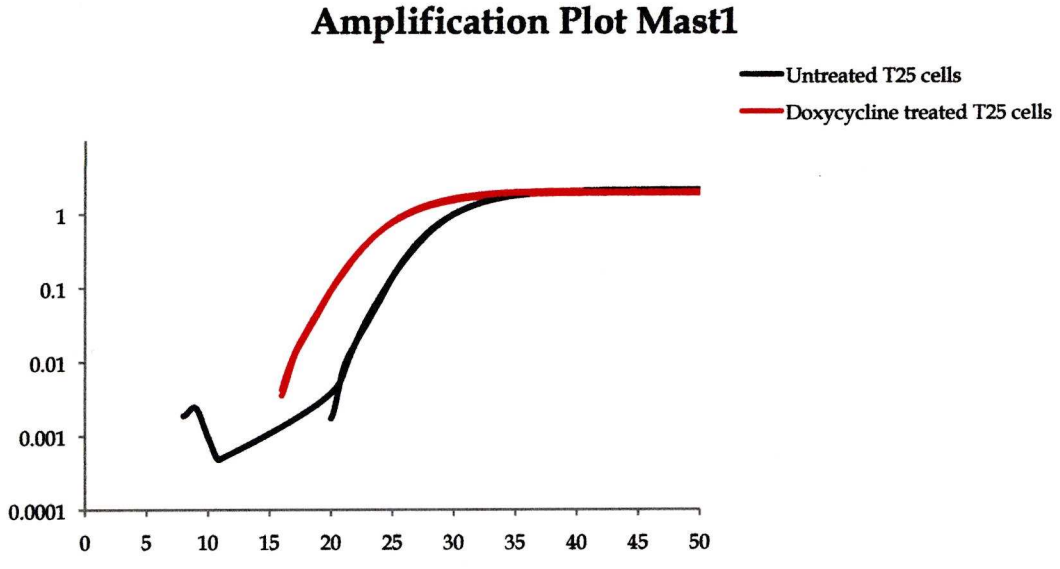
Amplification Plot Mast1
Untreated T25 cells
Doxycycline treated T25 cells
1
0.1
0.01
0.001
0.0001
0
5
10
15
20
25
30
35
40
45
50

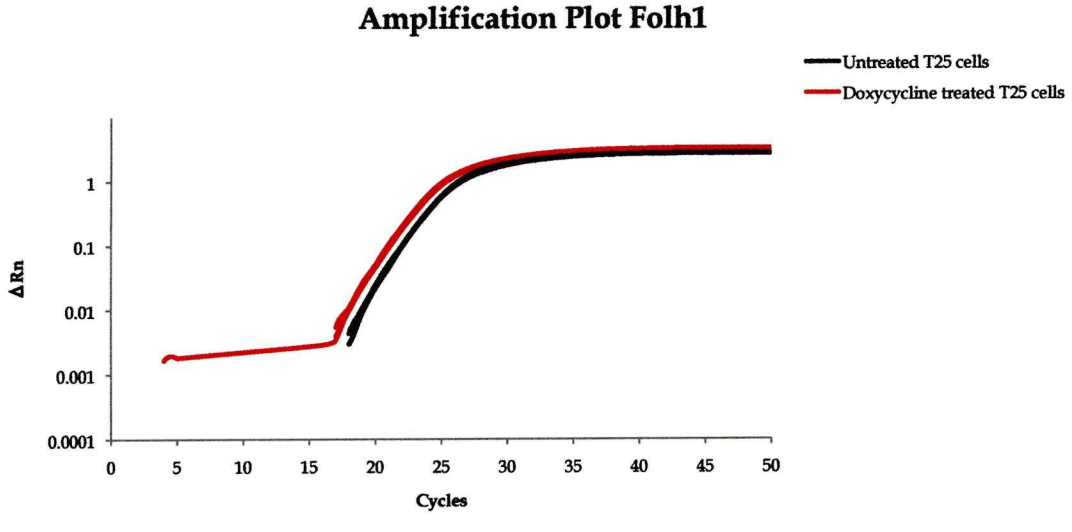
Amplification Plot Folh1
Untreated T25 cells
Doxycycline treated T25 cells
ΔRn
1
0.1
0.01
0.001
0.0001
0
5
10
15
20
25
30
35
40
45
50
Cycles

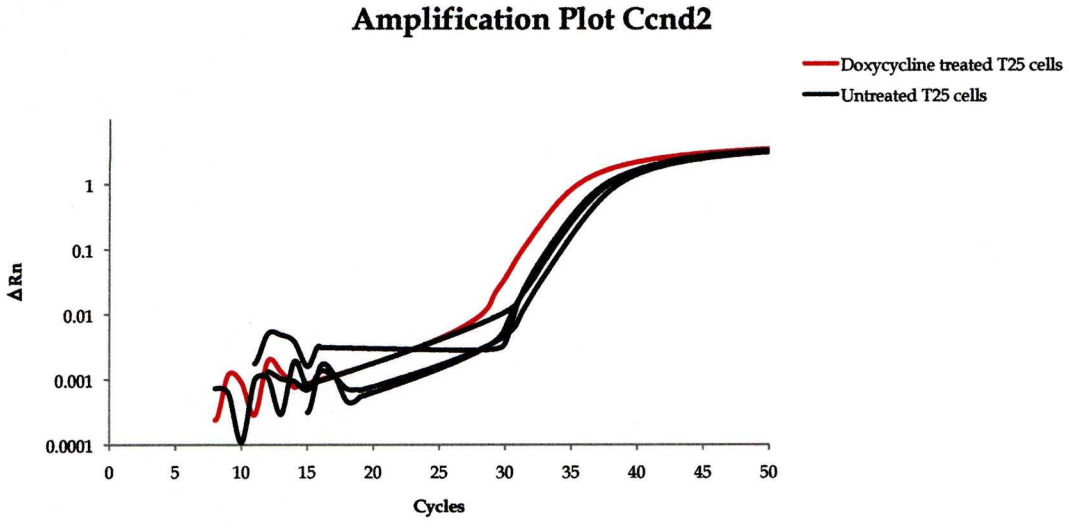
Amplification Plot Ccnd2
Doxycycline treated T25 cells
Untreated T25 cells
ΔRn
1
0.1
0.01
0.001
0.0001
0
5
10
15
20
25
30
35
40
45
50
Cycles

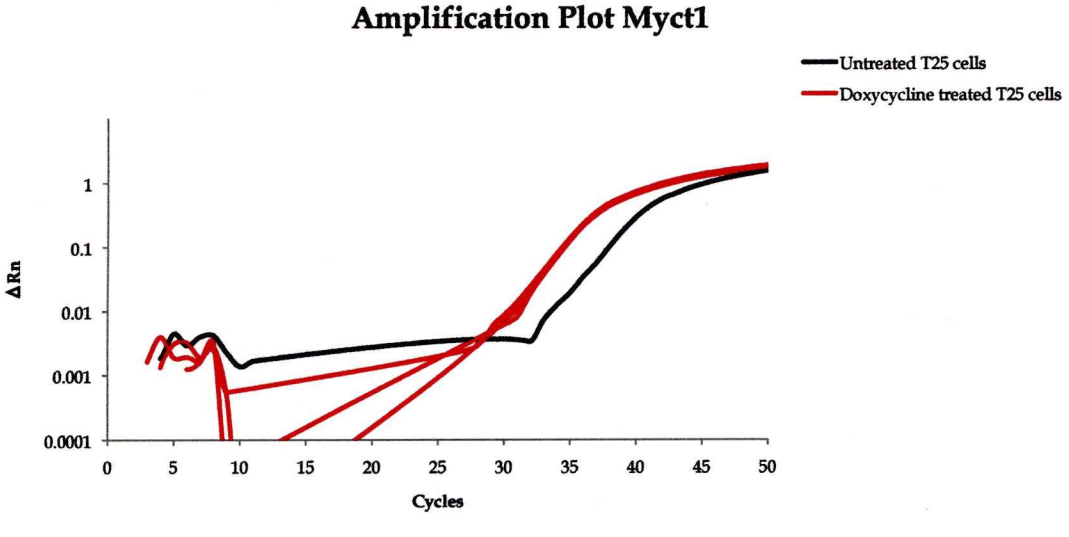
Amplification Plot Myct1
Untreated T25 cells
Doxycycline treated T25 cells
ΔRn
1
0.1
0.01
0.001
0.0001
0
5
10
15
20
25
30
35
40
45
50
Cycles

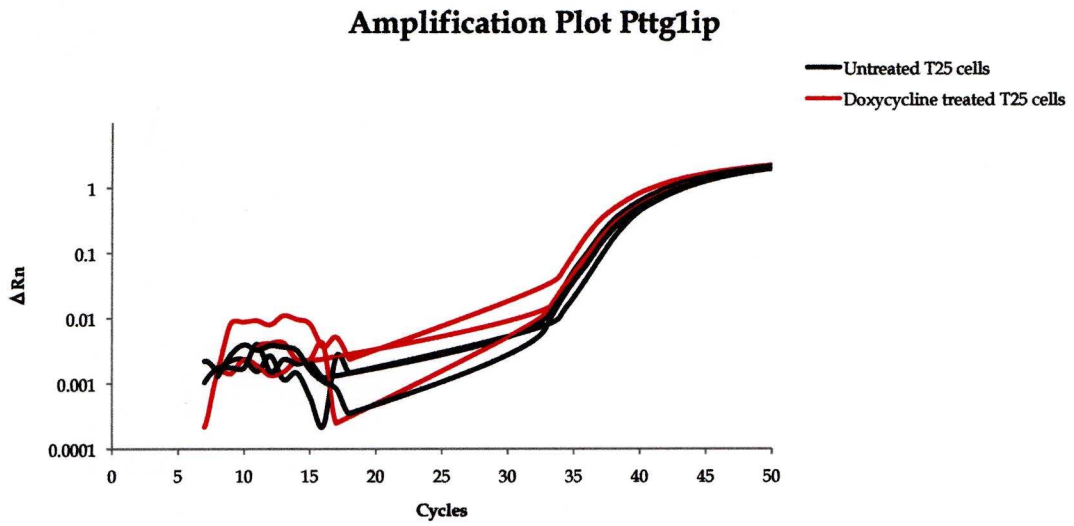

Figure A.7 **Amplification plots for qPCR targeted genes in induced and uninduced Rama 37 T-25 cells**

Target gene	Average Relative quantity (Rq)
S100P	13.42 ± 1.8
Mast1	4.56 ± 0.98
Akr7a2	3.79 ± 0.64
CcnD2	4.2 ± 1.12
Folh1	1.28 ± 0.38
S100A7a	5.52 ± 0.81
Pttg1ip	1.12 ± 0.2
Myct1	1.28 ± 0.38

Table A.1 **QPCR relative quantification data for targeted genes in induced and uninduced Rama 37 T-25 cells for S100P expression**

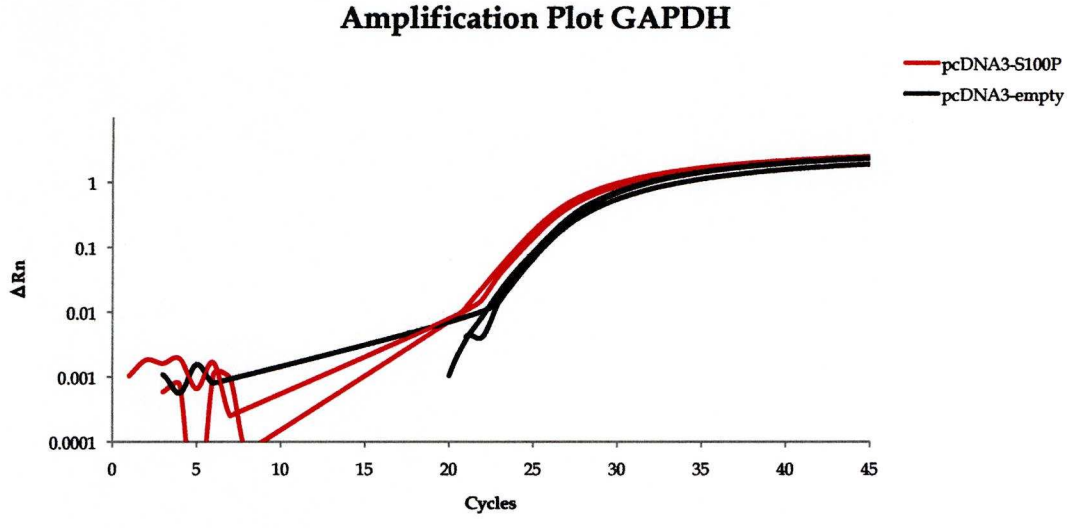
Amplification Plot GAPDH
pcDNA3-S100P
pcDNA3-empty
ΔRn
1
0.1
0.01
0.001
0.0001
0
5
10
15
20
25
30
35
40
45
Cycles

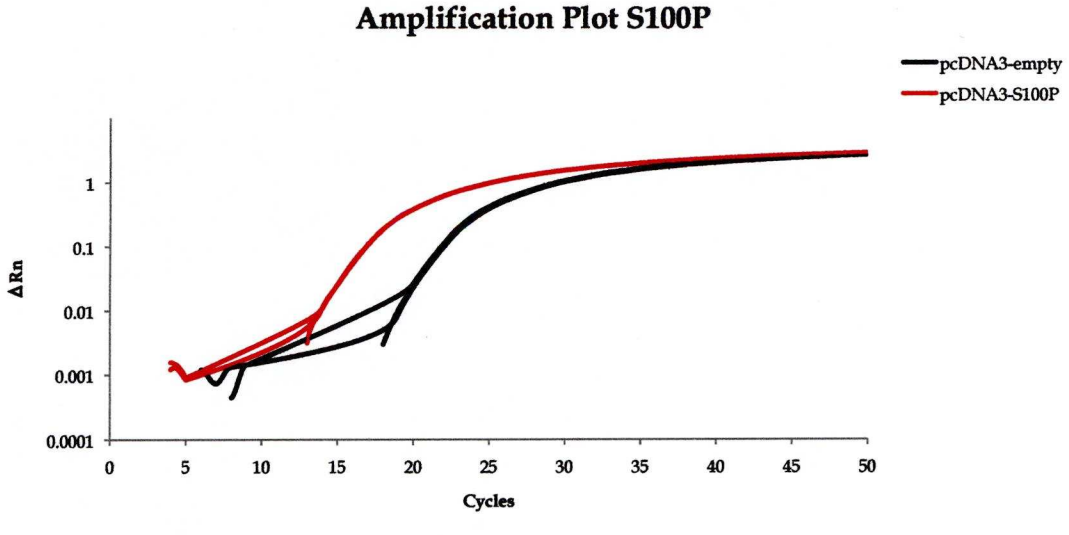
Amplification Plot S100P
pcDNA3-empty
pcDNA3-S100P
ΔRn
1
0.1
0.01
0.001
0.0001
0
5
10
15
20
25
30
35
40
45
50
Cycles

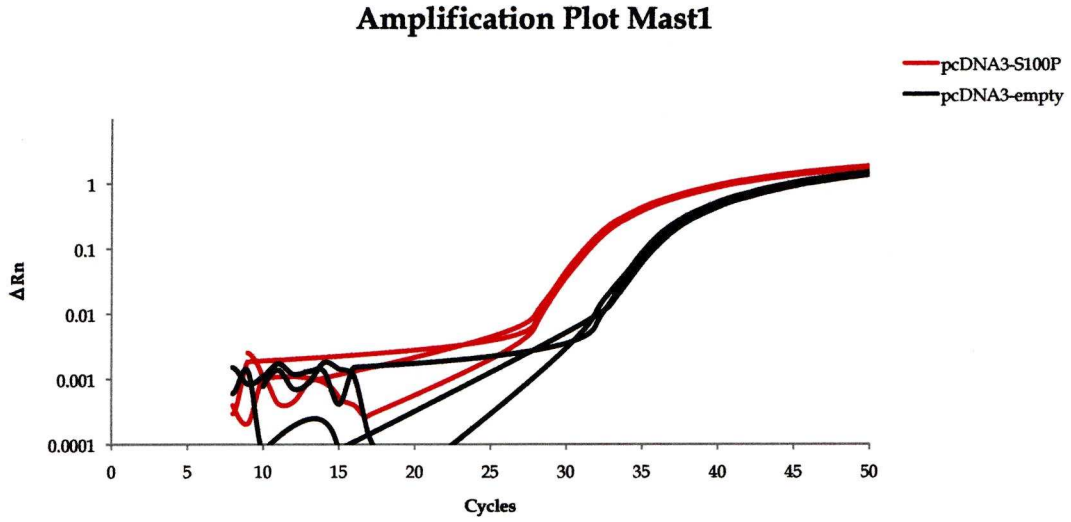
Amplification Plot Mast1
pcDNA3-S100P
pcDNA3-empty
ΔRn
1
0.1
0.01
0.001
0.0001
0
5
10
15
20
25
30
35
40
45
50
Cycles

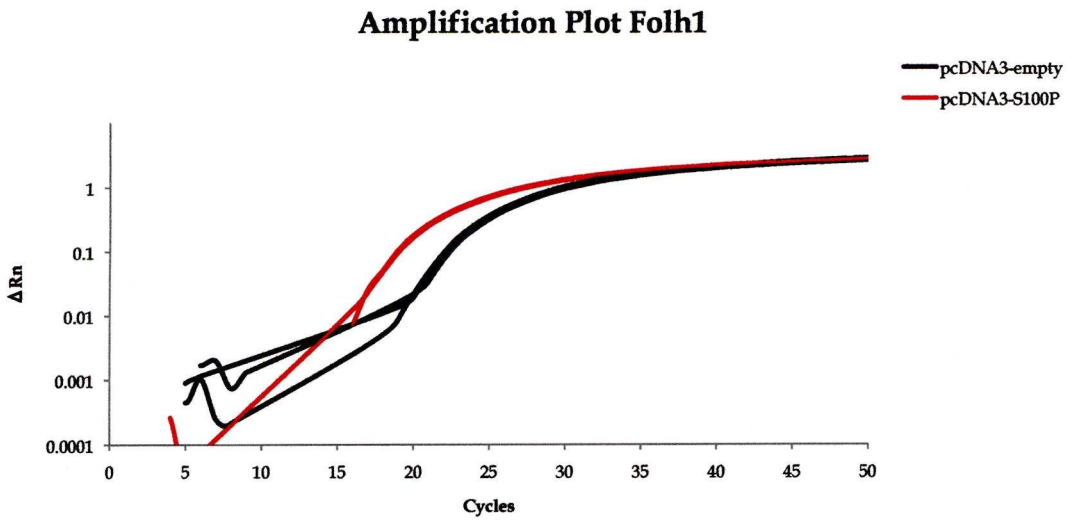
Amplification Plot Folh1
pcDNA3-empty
pcDNA3-S100P
ΔRn
1
0.1
0.01
0.001
0.0001
0
5
10
15
20
25
30
35
40
45
50
Cycles

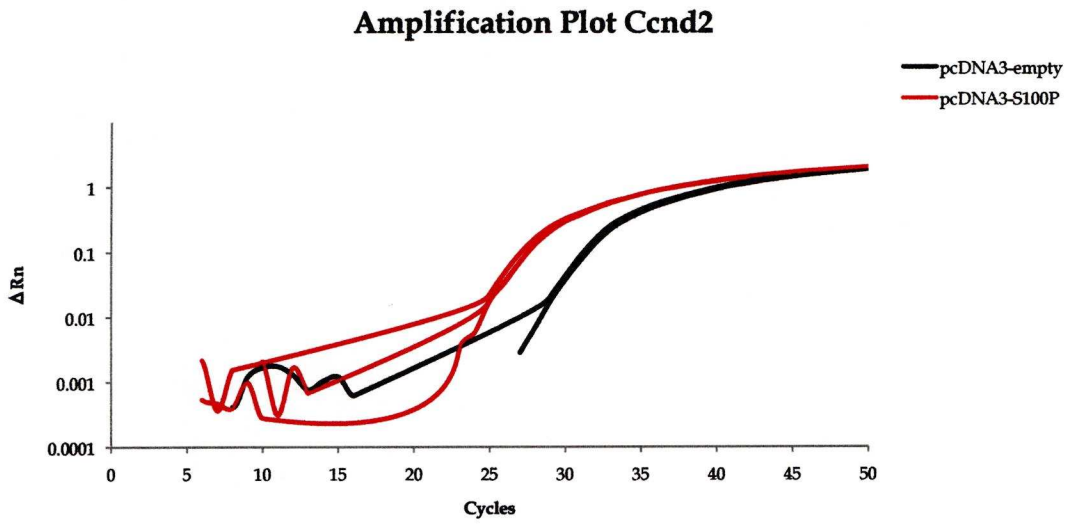
Amplification Plot Ccnd2
pcDNA3-empty
pcDNA3-S100P
ΔRn
1
0.1
0.01
0.001
0.0001
0
5
10
15
20
25
30
35
40
45
50
Cycles

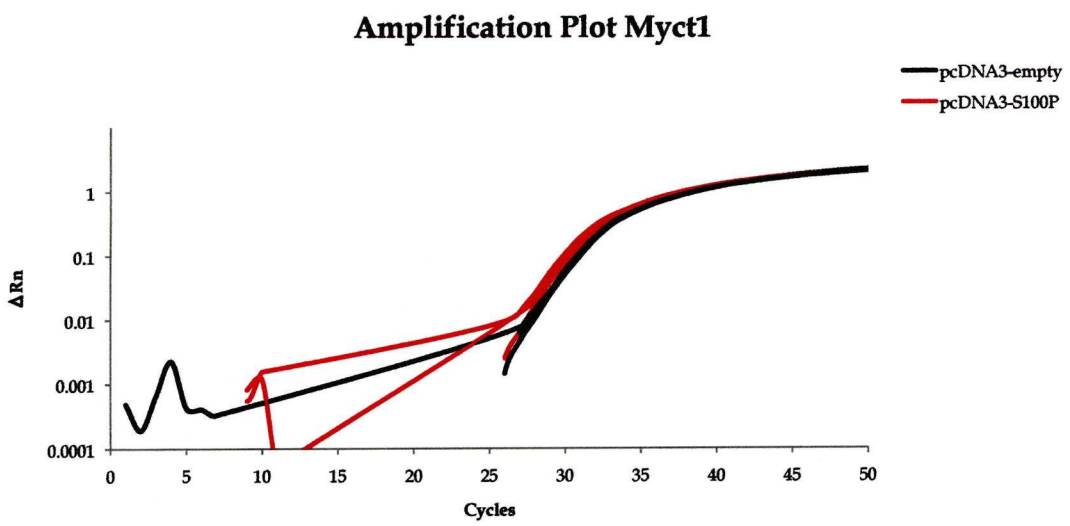
Amplification Plot Myct1
pcDNA3-empty
pcDNA3-S100P
ΔRn
1
0.1
0.01
0.001
0.0001
0
5
10
15
20
25
30
35
40
45
50
Cycles

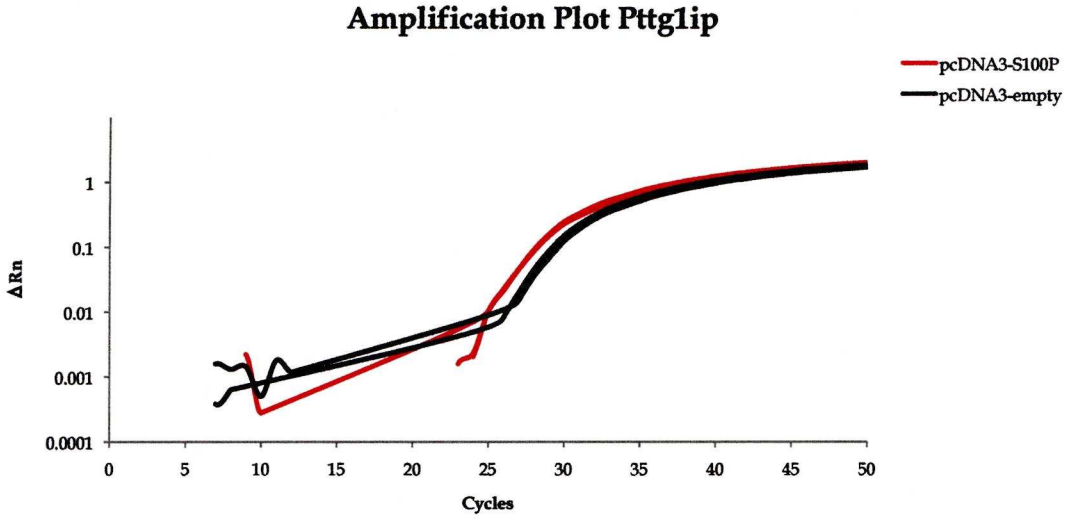

Figure A.8 **Amplification plots for qPCR targeted genes in pcDNA3-empty and pcDNA3-S100P Rama 37 cells**

Target gene	Average Rq
S100P	17.6 ± 2.4
Mast1	3.7 ± 0.4
Akr7a2	4.5 ± 1.2
CcnD2	3.8 ± 1.4
Folh1	1.6 ± 0.4
S100A7a	3.2 ± 0.7
Pttg1ip	0.98 ±
Myct1	1.1 ±

***Table A.2* QPCR relative quantification data for targeted genes between Rama 37 pcDNA3-S100P and pcDNA3-empty cells**

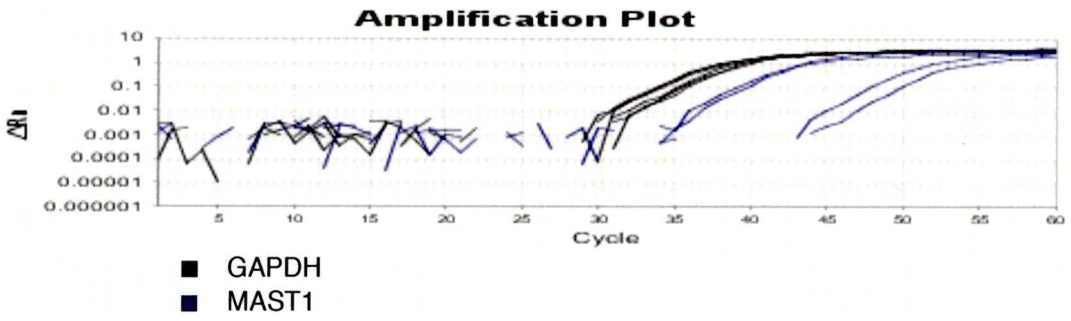

Figure A.9 **Amplification plots for qPCR targeted genes in induced and uninduced Rama 37 T-25 cells**

	Target	Average Ct	Average ΔCt	Average ΔΔCt	Average Rq	Average Rq min	Average Rq max
SiRNA control	MAST1	40.37494	8.542105	0	1	0.468387	2.134985
	GAPDH	31.83283					
SiRNA Mast1	MAST1	49.90142	16.49419	7.952084	0.004038	4.50E-04	0.036261
	GAPDH	33.40723					

Calculation of the percentage of Knock-down:

(% KD) = $[1-2^{-\Delta\Delta Ct}] \times 100$

Table A.3 **Mast 1 SiRNA quantitative real-time PCR raw datas**

identification of S100A4 (Mts1) gene overexpression as a poor prognostic marker for thyroid carcinoma." J Clin Endocrinol Metab **89**(12): 6146-6154.

References

Akisawa, N., I. Nishimori, T. Iwamura, S. Onishi and M. A. Hollingsworth (1999). "High levels of ezrin expressed by human pancreatic adenocarcinoma cell lines with high metastatic potential." Biochem Biophys Res Commun **258**(2): 395-400.

Al-Haddad, S., Z. Zhang, E. Leygue, L. Snell, A. Huang, Y. Niu, T. Hiller-Hitchcock, K. Hole, L. C. Murphy and P. H. Watson (1999). "Psoriasin (S100A7) expression and invasive breast cancer." Am J Pathol **155**(6): 2057-2066.

Alowami, S., G. Qing, E. Emberley, L. Snell and P. H. Watson (2003). "Psoriasin (S100A7) expression is altered during skin tumorigenesis." BMC Dermatol **3**: 1.

Altschul, S. F., W. Gish, W. Miller, E. W. Myers and D. J. Lipman (1990). "Basic local alignment search tool." J Mol Biol **215**(3): 403-410.

Ambartsumian, N. S., M. S. Grigorian, I. F. Larsen, O. Karlstrom, N. Sidenius, J. Rygaard, G. Georgiev and E. Lukanidin (1996). "Metastasis of mammary carcinomas in GRS/A hybrid mice transgenic for the mts1 gene." Oncogene **13**(8): 1621-1630.

Andersen, K., J. M. Nesland, R. Holm, V. A. Florenes, O. Fodstad and G. M. Maelandsmo (2004). "Expression of S100A4 combined with reduced E-cadherin expression predicts patient outcome in malignant melanoma." Mod Pathol **17**(8): 990-997.

Ando, K., F. Ajchenbaum-Cymbalista and J. D. Griffin (1993). "Regulation of G1/S transition by cyclins D2 and D3 in hematopoietic cells." Proc Natl Acad Sci U S A **90**(20): 9571-9575.

Arumugam, T., D. M. Simeone, A. M. Schmidt and C. D. Logsdon (2004). "S100P stimulates cell proliferation and survival via receptor for activated glycation end products (RAGE)." J Biol Chem **279**(7): 5059-5065.

Arumugam, T., D. M. Simeone, K. Van Golen and C. D. Logsdon (2005). "S100P promotes pancreatic cancer growth, survival, and invasion." Clin Cancer Res **11**(15): 5356-5364.

Averboukh, L., P. Liang, P. W. Kantoff and A. B. Pardee (1996). "Regulation of S100P expression by androgen." Prostate **29**(6): 350-355.

Bailly, M., L. Yan, G. M. Whitesides, J. S. Condeelis and J. E. Segall (1998). "Regulation of protrusion shape and adhesion to the substratum during

chemotactic responses of mammalian carcinoma cells." Exp Cell Res **241**(2): 285-299.

Bartling, B., G. Rehbein, W. D. Schmitt, H. S. Hofmann, R. E. Silber and A. Simm (2007). "S100A2-S100P expression profile and diagnosis of non-small cell lung carcinoma: impairment by advanced tumour stages and neoadjuvant chemotherapy." Eur J Cancer **43**(13): 1935-1943.

Basu, G. D., D. O. Azorsa, J. A. Kiefer, A. M. Rojas, S. Tuzmen, M. T. Barrett, J. M. Trent, O. Kallioniemi and S. Mousses (2008). "Functional evidence implicating S100P in prostate cancer progression." Int J Cancer **123**(2): 330-339.

Baudier, J., E. Bergeret, N. Bertacchi, H. Weintraub, J. Gagnon and J. Garin (1995). "Interactions of myogenic bHLH transcription factors with calcium-binding calmodulin and S100a (alpha alpha) proteins." Biochemistry **34**(24): 7834-7846.

Baudier, J. and D. Gerard (1983). "Ions binding to S100 proteins: structural changes induced by calcium and zinc on S100a and S100b proteins." Biochemistry **22**(14): 3360-3369.

Baudier, J., N. Glasser, K. Haglid and D. Gerard (1984). "Purification, characterization and ion binding properties of human brain S100b protein." Biochim Biophys Acta **790**(2): 164-173.

Baylin, S. B., S. A. Belinsky and J. G. Herman (2000). "Aberrant methylation of gene promoters in cancer---concepts, misconcepts, and promise." J Natl Cancer Inst **92**(18): 1460-1461.

Becker, T., V. Gerke, E. Kube and K. Weber (1992). "S100P, a novel Ca(2+)-binding protein from human placenta. cDNA cloning, recombinant protein expression and Ca2+ binding properties." Eur J Biochem **207**(2): 541-547.

Beer, D. G., S. L. Kardia, C. C. Huang, T. J. Giordano, A. M. Levin, D. E. Misek, L. Lin, G. Chen, T. G. Gharib, D. G. Thomas, M. L. Lizyness, R. Kuick, S. Hayasaka, J. M. Taylor, M. D. Iannettoni, M. B. Orringer and S. Hanash (2002). "Gene-expression profiles predict survival of patients with lung adenocarcinoma." Nat Med **8**(8): 816-824.

Bellacosa, A., J. R. Testa, S. P. Staal and P. N. Tsichlis (1991). "A retroviral oncogene, akt, encoding a serine-threonine kinase containing an SH2-like region." Science **254**(5029): 274-277.

Berman, B. A., M. M. Fenton, L. S. Girsch, Z. H. Haddad, W. A. Sellars, E. L. Strem, H. C. Thompson and L. E. Wall (1975). "Cromolyn sodium in the treatment of children with severe, perennial asthma." Pediatrics **55**(5): 621-629.

Bertram, J., K. Palfner, W. Hiddemann and M. Kneba (1998). "Elevated expression of S100P, CAPL and MAGE 3 in doxorubicin-resistant cell lines: comparison of mRNA differential display reverse transcription-polymerase chain reaction and subtractive suppressive hybridization for the analysis of differential gene expression." Anticancer Drugs **9**(4): 311-317.

Bird, A. (2002). "DNA methylation patterns and epigenetic memory." Genes Dev **16**(1): 6-21.

Birkenkamp-Demtroder, K., S. H. Olesen, F. B. Sorensen, S. Laurberg, P. Laiho, L. A. Aaltonen and T. F. Orntoft (2005). "Differential gene expression in colon cancer of the caecum versus the sigmoid and rectosigmoid." Gut **54**(3): 374-384.

Bjornland, K., J. O. Winberg, O. T. Odegaard, E. Hovig, T. Loennechen, A. O. Aasen, O. Fodstad and G. M. Maelandsmo (1999). "S100A4 involvement in metastasis: deregulation of matrix metalloproteinases and tissue inhibitors of matrix metalloproteinases in osteosarcoma cells transfected with an anti-S100A4 ribozyme." Cancer Res **59**(18): 4702-4708.

Bolstad, B. M., R. A. Irizarry, M. Astrand and T. P. Speed (2003). "A comparison of normalization methods for high density oligonucleotide array data based on variance and bias." Bioinformatics **19**(2): 185-193.

Bonfrer, J. M., C. M. Korse, O. E. Nieweg and E. M. Rankin (1998). "The luminescence immunoassay S-100: a sensitive test to measure circulating S-100B: its prognostic value in malignant melanoma." Br J Cancer **77**(12): 2210-2214.

Boniface, K., F. X. Bernard, M. Garcia, A. L. Gurney, J. C. Lecron and F. Morel (2005). "IL-22 inhibits epidermal differentiation and induces proinflammatory gene expression and migration of human keratinocytes." J Immunol **174**(6): 3695-3702.

Bose, S., S. Chandran, J. M. Mirocha and N. Bose (2006). "The Akt pathway in human breast cancer: a tissue-array-based analysis." Mod Pathol **19**(2): 238-245.

Boyden, S. (1962). "The chemotactic effect of mixtures of antibody and antigen on polymorphonuclear leucocytes." J Exp Med **115**: 453-466.

Bretscher, A., K. Edwards and R. G. Fehon (2002). "ERM proteins and merlin: integrators at the cell cortex." Nat Rev Mol Cell Biol **3**(8): 586-599.

Brian, P. W., P. J. Curtis, H. G. Hemming and G. L. F. Norris (1957). "Wortmannin, an antibiotic produced by Penicillium wortmanni." Transactions of the British Mycological Society **40**(3): 365-368, IN363.

Brunet, A., A. Bonni, M. J. Zigmond, M. Z. Lin, P. Juo, L. S. Hu, M. J. Anderson, K. C. Arden, J. Blenis and M. E. Greenberg (1999). "Akt promotes cell survival by phosphorylating and inhibiting a Forkhead transcription factor." Cell **96**(6): 857-868.

Buckley, M. F., K. J. Sweeney, J. A. Hamilton, R. L. Sini, D. L. Manning, R. I. Nicholson, A. deFazio, C. K. Watts, E. A. Musgrove and R. L. Sutherland (1993). "Expression and amplification of cyclin genes in human breast cancer." Oncogene **8**(8): 2127-2133.

Burnette, W. N. (1981). ""Western blotting": electrophoretic transfer of proteins from sodium dodecyl sulfate--polyacrylamide gels to unmodified nitrocellulose and radiographic detection with antibody and radioiodinated protein A." Anal Biochem **112**(2): 195-203.

Celis, J. E., H. H. Rasmussen, H. Vorum, P. Madsen, B. Honore, H. Wolf and T. F. Orntoft (1996). "Bladder squamous cell carcinomas express psoriasin and externalize it to the urine." J Urol **155**(6): 2105-2112.

Chang, S. S., V. E. Reuter, W. D. Heston and P. B. Gaudin (2001). "Comparison of anti-prostate-specific membrane antigen antibodies and other immunomarkers in metastatic prostate carcinoma." Urology **57**(6): 1179-1183.

Chien, W. and L. Pei (2000). "A novel binding factor facilitates nuclear translocation and transcriptional activation function of the pituitary tumor-transforming gene product." J Biol Chem **275**(25): 19422-19427.

Chomczynski, P. and N. Sacchi (1987). "Single-step method of RNA isolation by acid guanidinium thiocyanate-phenol-chloroform extraction." Anal Biochem **162**(1): 156-159.

Coffer, P. J., J. Jin and J. R. Woodgett (1998). "Protein kinase B (c-Akt): a multifunctional mediator of phosphatidylinositol 3-kinase activation." Biochem J **335 (Pt 1)**: 1-13.

Conway, R. E., N. Petrovic, Z. Li, W. Heston, D. Wu and L. H. Shapiro (2006). "Prostate-specific membrane antigen regulates angiogenesis by modulating integrin signal transduction." Mol Cell Biol **26**(14): 5310-5324.

Cornish, C. J., J. M. Devery, P. Poronnik, M. Lackmann, D. I. Cook and C. L. Geczy (1996). "S100 protein CP-10 stimulates myeloid cell chemotaxis without activation." J Cell Physiol **166**(2): 427-437.

Crnogorac-Jurcevic, T., E. Missiaglia, E. Blaveri, R. Gangeswaran, M. Jones, B. Terris, E. Costello, J. P. Neoptolemos and N. R. Lemoine (2003). "Molecular alterations in pancreatic carcinoma: expression profiling shows that dysregulated expression of S100 genes is highly prevalent." J Pathol **201**(1): 63-74.

Cui, Y., M. Tian, M. Zong, M. Teng, Y. Chen, J. Lu, J. Jiang, X. Liu and J. Han (2009). "Proteomic analysis of pancreatic ductal adenocarcinoma compared with normal adjacent pancreatic tissue and pancreatic benign cystadenoma." Pancreatology **9**(1-2): 89-98.

Davey, G. E., P. Murmann, M. Hoechli, T. Tanaka and C. W. Heizmann (2000). "Calcium-dependent translocation of S100A11 requires tubulin filaments." Biochim Biophys Acta **1498**(2-3): 220-232.

Davies, B. R., M. P. Davies, F. E. Gibbs, R. Barraclough and P. S. Rudland (1993). "Induction of the metastatic phenotype by transfection of a benign rat mammary epithelial cell line with the gene for p9Ka, a rat calcium-binding protein, but not with the oncogene EJ-ras-1." Oncogene **8**(4): 999-1008.

Davies, B. R., M. O'Donnell, G. C. Durkan, P. S. Rudland, R. Barraclough, D. E. Neal and J. K. Mellon (2002). "Expression of S100A4 protein is associated with metastasis and reduced survival in human bladder cancer." J Pathol **196**(3): 292-299.

Davies, M. P., P. S. Rudland, L. Robertson, E. W. Parry, P. Jolicoeur and R. Barraclough (1996). "Expression of the calcium-binding protein S100A4 (p9Ka) in MMTV-neu transgenic mice induces metastasis of mammary tumours." Oncogene **13**(8): 1631-1637.

Deloulme, J. C., N. Assard, G. O. Mbele, C. Mangin, R. Kuwano and J. Baudier (2000). "S100A6 and S100A11 are specific targets of the calcium- and zinc-binding S100B protein in vivo." J Biol Chem **275**(45): 35302-35310.

Deng, H., J. Shi, M. Wilkerson, S. Meschter, W. Dupree and F. Lin (2008). "Usefulness of S100P in diagnosis of adenocarcinoma of pancreas on fine-needle aspiration biopsy specimens." Am J Clin Pathol **129**(1): 81-88.

Devery, J. M., N. J. King and C. L. Geczy (1994). "Acute inflammatory activity of the S100 protein CP-10. Activation of neutrophils in vivo and in vitro." J Immunol **152**(4): 1888-1897.

Diederichs, S., E. Bulk, B. Steffen, P. Ji, L. Tickenbrock, K. Lang, K. S. Zanker, R. Metzger, P. M. Schneider, V. Gerke, M. Thomas, W. E. Berdel, H. Serve and C. Muller-Tidow (2004). "S100 family members and trypsinogens are predictors of distant metastasis and survival in early-stage non-small cell lung cancer." Cancer Res **64**(16): 5564-5569.

Doerfler, W. (1983). "DNA methylation and gene activity." Annu Rev Biochem **52**: 93-124.

Donato, R. (1999). "Functional roles of S100 proteins, calcium-binding proteins of the EF-hand type." Biochim Biophys Acta **1450**(3): 191-231.

Donato, R. (2001). "S100: a multigenic family of calcium-modulated proteins of the EF-hand type with intracellular and extracellular functional roles." Int J Biochem Cell Biol **33**(7): 637-668.

Donato, R. (2003). "Intracellular and extracellular roles of S100 proteins." Microsc Res Tech **60**(6): 540-551.

Dowen, S. E., T. Crnogorac-Jurcevic, R. Gangeswaran, M. Hansen, J. J. Eloranta, V. Bhakta, T. A. Brentnall, J. Luttges, G. Kloppel and N. R. Lemoine (2005). "Expression of S100P and its novel binding partner S100PBPR in early pancreatic cancer." Am J Pathol **166**(1): 81-92.

Dudley, D. T., L. Pang, S. J. Decker, A. J. Bridges and A. R. Saltiel (1995). "A synthetic inhibitor of the mitogen-activated protein kinase cascade." Proc Natl Acad Sci U S A **92**(17): 7686-7689.

Dukhanina, E. A., A. S. Dukhanin, M. Y. Lomonosov, E. M. Lukanidin and G. P. Georgiev (1997). "Spectral studies on the calcium-binding properties of Mts1 protein and its interaction with target protein." FEBS Lett **410**(2-3): 403-406.

Dumas, F., J. L. Gala, P. Berteau, F. Brasseur, P. Eschwege, V. Paradis, B. Lacour, M. Philippe and S. Loric (1999). "Molecular expression of PSMA mRNA and protein in primary renal tumors." Int J Cancer **80**(6): 799-803.

Dunnington, D. J., C. M. Hughes, P. Monaghan and P. S. Rudland (1983). "Phenotypic instability of rat mammary tumor epithelial cells." J Natl Cancer Inst **71**(6): 1227-1240.

Ebralidze, A., E. Tulchinsky, M. Grigorian, A. Afanasyeva, V. Senin, E. Revazova and E. Lukanidin (1989). "Isolation and characterization of a gene specifically expressed in different metastatic cells and whose deduced gene product has a high degree of homology to a Ca2+-binding protein family." Genes Dev **3**(7): 1086-1093.

Ehlermann, P., K. Eggers, A. Bierhaus, P. Most, D. Weichenhan, J. Greten, P. P. Nawroth, H. A. Katus and A. Remppis (2006). "Increased proinflammatory endothelial response to S100A8/A9 after preactivation through advanced glycation end products." Cardiovasc Diabetol **5**: 6.

El-Rifai, W., C. A. Moskaluk, M. K. Abdrabbo, J. Harper, C. Yoshida, G. J. Riggins, H. F. Frierson, Jr. and S. M. Powell (2002). "Gastric cancers overexpress S100A calcium-binding proteins." Cancer Res **62**(23): 6823-6826.

Emberley, E. D., Y. Niu, L. Curtis, S. Troup, S. K. Mandal, J. N. Myers, S. B. Gibson, L. C. Murphy and P. H. Watson (2005). "The S100A7-c-Jun activation domain binding protein 1 pathway enhances prosurvival pathways in breast cancer." Cancer Res **65**(13): 5696-5702.

Emberley, E. D., Y. Niu, C. Njue, E. V. Kliewer, L. C. Murphy and P. H. Watson (2003). "Psoriasin (S100A7) expression is associated with poor outcome in estrogen receptor-negative invasive breast cancer." Clin Cancer Res **9**(7): 2627-2631.

Emoto, Y., R. Kobayashi, H. Akatsuka and H. Hidaka (1992). "Purification and characterization of a new member of the S-100 protein family from human placenta." Biochem Biophys Res Commun **182**(3): 1246-1253.

Endo, H., K. Takenaga, T. Kanno, H. Satoh and S. Mori (2002). "Methionine aminopeptidase 2 is a new target for the metastasis-associated protein, S100A4." J Biol Chem **277**(29): 26396-26402.

Fano, G., P. Angelella, D. Mariggio, M. C. Aisa, I. Giambanco and R. Donato (1989). "S-100a0 protein stimulates the basal (Mg2+-activated) adenylate cyclase activity associated with skeletal muscle membranes." FEBS Lett **248**(1-2): 9-12.

Feng, J., J. Park, P. Cron, D. Hess and B. A. Hemmings (2004). "Identification of a PKB/Akt hydrophobic motif Ser-473 kinase as DNA-dependent protein kinase." J Biol Chem **279**(39): 41189-41196.

Fernandez-Fernandez, M. R., D. B. Veprintsev and A. R. Fersht (2005). "Proteins of the S100 family regulate the oligomerization of p53 tumor suppressor." Proc Natl Acad Sci U S A **102**(13): 4735-4740.

Fife, K. H., C. S. Crumpacker, G. J. Mertz, E. L. Hill and G. S. Boone (1994). "Recurrence and resistance patterns of herpes simplex virus following cessation of > or = 6 years of chronic suppression with acyclovir. Acyclovir Study Group." J Infect Dis **169**(6): 1338-1341.

Fife, R. S. and G. W. Sledge, Jr. (1995). "Effects of doxycycline on in vitro growth, migration, and gelatinase activity of breast carcinoma cells." J Lab Clin Med **125**(3): 407-411.

Fife, R. S. and G. W. Sledge, Jr. (1998). "Effects of doxycycline on cancer cells in vitro and in vivo." Adv Dent Res **12**(2): 94-96.

Finley, K. D., P. T. Edeen, R. C. Cumming, M. D. Mardahl-Dumesnil, B. J. Taylor, M. H. Rodriguez, C. E. Hwang, M. Benedetti and M. McKeown (2003). "blue cheese mutations define a novel, conserved gene involved in progressive neural degeneration." J Neurosci **23**(4): 1254-1264.

Flatmark, K., K. B. Pedersen, J. M. Nesland, H. Rasmussen, G. Aamodt, S. O. Mikalsen, K. Bjornland, O. Fodstad and G. M. Maelandsmo (2003). "Nuclear localization of the metastasis-related protein S100A4 correlates with tumour stage in colorectal cancer." J Pathol **200**(5): 589-595.

Ford, H. L. and S. B. Zain (1995). "Interaction of metastasis associated Mts1 protein with nonmuscle myosin." Oncogene **10**(8): 1597-1605.

Franke, T. F., C. P. Hornik, L. Segev, G. A. Shostak and C. Sugimoto (2003). "PI3K/Akt and apoptosis: size matters." Oncogene **22**(56): 8983-8998.

Freeman, W. M., S. J. Walker and K. E. Vrana (1999). "Quantitative RT-PCR: pitfalls and potential." Biotechniques **26**(1): 112-122, 124-115.

Freshney, R. I. (2005). Culture of animal cells : a manual of basic technique. Hoboken, N.J., Wiley-Liss, Chichester : John Wiley [distributor].

Fuentes, M. K., S. S. Nigavekar, T. Arumugam, C. D. Logsdon, A. M. Schmidt, J. C. Park and E. H. Huang (2007). "RAGE activation by S100P in colon cancer

stimulates growth, migration, and cell signaling pathways." Dis Colon Rectum **50**(8): 1230-1240.

Gabriel, J. (2007). The biology of cancer. Hoboken, N.J., Wiley ; Chichester : John Wiley [distributor].

Gala, J. L., S. Loric, Y. Guiot, S. R. Denmeade, A. Gady, F. Brasseur, M. Heusterspreute, P. Eschwege, P. De Nayer, P. Van Cangh and B. Tombal (2000). "Expression of prostate-specific membrane antigen in transitional cell carcinoma of the bladder: prognostic value?" Clin Cancer Res **6**(10): 4049-4054.

Garland, P., S. Quraishe, P. French and V. O'Connor (2008). "Expression of the MAST family of serine/threonine kinases." Brain Res **1195**: 12-19.

Gautier, L., L. Cope, B. M. Bolstad and R. A. Irizarry (2004). "affy--analysis of Affymetrix GeneChip data at the probe level." Bioinformatics **20**(3): 307-315.

Gentleman, R. C., V. J. Carey, D. M. Bates, B. Bolstad, M. Dettling, S. Dudoit, B. Ellis, L. Gautier, Y. Ge, J. Gentry, K. Hornik, T. Hothorn, W. Huber, S. Iacus, R. Irizarry, F. Leisch, C. Li, M. Maechler, A. J. Rossini, G. Sawitzki, C. Smith, G. Smyth, L. Tierney, J. Y. Yang and J. Zhang (2004). "Bioconductor: open software development for computational biology and bioinformatics." Genome Biol **5**(10): R80.

Goode, B. L., D. G. Drubin and G. Barnes (2000). "Functional cooperation between the microtubule and actin cytoskeletons." Curr Opin Cell Biol **12**(1): 63-71.

Gribenko, A., M. M. Lopez, J. M. Richardson, 3rd and G. I. Makhatadze (1998). "Cloning, overexpression, purification, and spectroscopic characterization of human S100P." Protein Sci **7**(1): 211-215.

Gribenko, A. V., M. Guzman-Casado, M. M. Lopez and G. I. Makhatadze (2002). "Conformational and thermodynamic properties of peptide binding to the human S100P protein." Protein Sci **11**(6): 1367-1375.

Gribenko, A. V., J. E. Hopper and G. I. Makhatadze (2001). "Molecular characterization and tissue distribution of a novel member of the S100 family of EF-hand proteins." Biochemistry **40**(51): 15538-15548.

Gribenko, A. V. and G. I. Makhatadze (1998). "Oligomerization and divalent ion binding properties of the S100P protein: a Ca2+/Mg2+-switch model." J Mol Biol **283**(3): 679-694.

Grigorian, M., N. Ambartsumian, A. E. Lykkesfeldt, L. Bastholm, F. Elling, G. Georgiev and E. Lukanidin (1996). "Effect of mts1 (S100A4) expression on the progression of human breast cancer cells." Int J Cancer **67**(6): 831-841.

Grigorian, M., S. Andresen, E. Tulchinsky, M. Kriajevska, C. Carlberg, C. Kruse, M. Cohn, N. Ambartsumian, A. Christensen, G. Selivanova and E. Lukanidin (2001). "Tumor suppressor p53 protein is a new target for the metastasis-associated Mts1/S100A4 protein: functional consequences of their interaction." J Biol Chem **276**(25): 22699-22708.

Guerreiro Da Silva, I. D., Y. F. Hu, I. H. Russo, X. Ao, A. M. Salicioni, X. Yang and J. Russo (2000). "S100P calcium-binding protein overexpression is associated with immortalization of human breast epithelial cells in vitro and early stages of breast cancer development in vivo." Int J Oncol **16**(2): 231-240.

Haffner, M. C., I. E. Kronberger, J. S. Ross, C. E. Sheehan, M. Zitt, G. Muhlmann, D. Ofner, B. Zelger, C. Ensinger, X. J. Yang, S. Geley, R. Margreiter and N. H. Bander (2009). "Prostate-specific membrane antigen expression in the neovasculature of gastric and colorectal cancers." Hum Pathol **40**(12): 1754-1761.

Hamada, S., K. Satoh, M. Hirota, W. Fujibuchi, A. Kanno, J. Umino, H. Ito, A. Satoh, K. Kikuta, K. Kume, A. Masamune and T. Shimosegawa (2009). "Expression of the calcium-binding protein S100P is regulated by bone morphogenetic protein in pancreatic duct epithelial cell lines." Cancer Sci **100**(1): 103-110.

Hammacher, A., E. W. Thompson and E. D. Williams (2005). "Interleukin-6 is a potent inducer of S100P, which is up-regulated in androgen-refractory and metastatic prostate cancer." Int J Biochem Cell Biol **37**(2): 442-450.

Hanahan, D. and R. A. Weinberg (2000). "The hallmarks of cancer." Cell **100**(1): 57-70.

Hauschild, A., G. Engel, W. Brenner, R. Glaser, H. Monig, E. Henze and E. Christophers (1999). "S100B protein detection in serum is a significant prognostic factor in metastatic melanoma." Oncology **56**(4): 338-344.

Hauschild, A., J. Michaelsen, W. Brenner, P. Rudolph, R. Glaser, E. Henze and E. Christophers (1999). "Prognostic significance of serum S100B detection compared with routine blood parameters in advanced metastatic melanoma patients." Melanoma Res **9**(2): 155-161.

Hazeki, O., K. Hazeki, T. Katada and M. Ui (1996). "Inhibitory effect of wortmannin on phosphatidylinositol 3-kinase-mediated cellular events." J Lipid Mediat Cell Signal **14**(1-3): 259-261.

Heizmann, C. W. (2004). "S100B protein in clinical diagnostics: assay specificity." Clin Chem **50**(1): 249-251.

Heizmann, C. W., G. Fritz and B. W. Schafer (2002). "S100 proteins: structure, functions and pathology." Front Biosci **7**: d1356-1368.

Heras, A., R. CM and K. ME (1995). Enhanced labelled-polymer system for immunohistochemistry. XVth European Congress of Pathology. Copenhagen, Denmark.

Hermani, A., B. De Servi, S. Medunjanin, P. A. Tessier and D. Mayer (2006). "S100A8 and S100A9 activate MAP kinase and NF-kappaB signaling pathways and trigger translocation of RAGE in human prostate cancer cells." Exp Cell Res **312**(2): 184-197.

Hiratsuka, S., A. Watanabe, H. Aburatani and Y. Maru (2006). "Tumour-mediated upregulation of chemoattractants and recruitment of myeloid cells predetermines lung metastasis." Nat Cell Biol **8**(12): 1369-1375.

Hofmann, M. A., S. Drury, C. Fu, W. Qu, A. Taguchi, Y. Lu, C. Avila, N. Kambham, A. Bierhaus, P. Nawroth, M. F. Neurath, T. Slattery, D. Beach, J. McClary, M. Nagashima, J. Morser, D. Stern and A. M. Schmidt (1999). "RAGE mediates a novel proinflammatory axis: a central cell surface receptor for S100/ calgranulin polypeptides." Cell **97**(7): 889-901.

Huttunen, H. J., J. Kuja-Panula, G. Sorci, A. L. Agneletti, R. Donato and H. Rauvala (2000). "Coregulation of neurite outgrowth and cell survival by amphoterin and S100 proteins through receptor for advanced glycation end products (RAGE) activation." J Biol Chem **275**(51): 40096-40105.

Iacobuzio-Donahue, C. A., A. Maitra, G. L. Shen-Ong, T. van Heek, R. Ashfaq, R. Meyer, K. Walter, K. Berg, M. A. Hollingsworth, J. L. Cameron, C. J. Yeo, S. E. Kern, M. Goggins and R. H. Hruban (2002). "Discovery of novel tumor markers of pancreatic cancer using global gene expression technology." Am J Pathol **160**(4): 1239-1249.

IARC (2010). Globocan 2008. World Health Organisation.

Ilg, E. C., B. W. Schafer and C. W. Heizmann (1996). "Expression pattern of S100 calcium-binding proteins in human tumors." Int J Cancer **68**(3): 325-332.

Jakubickova, L., M. Barathova, S. Pastorekova, J. Pastorek and A. Gibadulinova (2005). "Expression of S100P gene in cervical carcinoma cells is independent of E7 human papillomavirus oncogene." Acta Virol **49**(2): 133-137.

Janknecht, R. (1996). "Analysis of the ERK-stimulated ETS transcription factor ER81." Mol Cell Biol **16**(4): 1550-1556.

Jenkinson, S. R., R. Barraclough, C. R. West and P. S. Rudland (2004). "S100A4 regulates cell motility and invasion in an in vitro model for breast cancer metastasis." Br J Cancer **90**(1): 253-262.

Jez, J. M., T. G. Flynn and T. M. Penning (1997). "A new nomenclature for the aldo-keto reductase superfamily." Biochem Pharmacol **54**(6): 639-647.

Jez, J. M. and T. M. Penning (2001). "The aldo-keto reductase (AKR) superfamily: an update." Chem Biol Interact **130-132**(1-3): 499-525.

Jo, M., K. S. Thomas, A. V. Somlyo, A. P. Somlyo and S. L. Gonias (2002). "Cooperativity between the Ras-ERK and Rho-Rho kinase pathways in urokinase-type plasminogen activator-stimulated cell migration." J Biol Chem **277**(14): 12479-12485.

Johnson, G. D., R. S. Davidson, K. C. McNamee, G. Russell, D. Goodwin and E. J. Holborow (1982). "Fading of immunofluorescence during microscopy: a study of the phenomenon and its remedy." J Immunol Methods **55**(2): 231-242.

Keely, P. J., J. K. Westwick, I. P. Whitehead, C. J. Der and L. V. Parise (1997). "Cdc42 and Rac1 induce integrin-mediated cell motility and invasiveness through PI(3)K." Nature **390**(6660): 632-636.

Kim, D., S. Kim, H. Koh, S. O. Yoon, A. S. Chung, K. S. Cho and J. Chung (2001). "Akt/PKB promotes cancer cell invasion via increased motility and metalloproteinase production." FASEB J **15**(11): 1953-1962.

Kim, J. Y., Y. J. Kim, S. Lee and J. H. Park (2009). "The critical role of ERK in death resistance and invasiveness of hypoxia-selected glioblastoma cells." BMC Cancer **9**: 27.

Kimura, K., Y. Endo, Y. Yonemura, C. W. Heizmann, B. W. Schafer, Y. Watanabe and T. Sasaki (2000). "Clinical significance of S100A4 and E-cadherin-related adhesion molecules in non-small cell lung cancer." Int J Oncol **16**(6): 1125-1131.

Kita, H., Y. Hikichi, K. Hikami, K. Tsuneyama, Z. G. Cui, H. Osawa, H. Ohnishi, H. Mutoh, H. Hoshino, C. L. Bowlus, H. Yamamoto and K. Sugano (2006). "Differential gene expression between flat adenoma and normal mucosa in the colon in a microarray analysis." J Gastroenterol **41**(11): 1053-1063.

Kligman, D. and D. C. Hilt (1988). "The S100 protein family." Trends Biochem Sci **13**(11): 437-443.

Koltzscher, M., C. Neumann, S. Konig and V. Gerke (2003). "Ca2+-dependent binding and activation of dormant ezrin by dimeric S100P." Mol Biol Cell **14**(6): 2372-2384.

Kretsinger, R. H. and C. E. Nockolds (1973). "Carp muscle calcium-binding protein. II. Structure determination and general description." J Biol Chem **248**(9): 3313-3326.

Kriajevska, M., M. Fischer-Larsen, E. Moertz, O. Vorm, E. Tulchinsky, M. Grigorian, N. Ambartsumian and E. Lukanidin (2002). "Liprin beta 1, a member of the family of LAR transmembrane tyrosine phosphatase-interacting proteins, is a new target for the metastasis-associated protein S100A4 (Mts1)." J Biol Chem **277**(7): 5229-5235.

Kriajevska, M., S. Tarabykina, I. Bronstein, N. Maitland, M. Lomonosov, K. Hansen, G. Georgiev and E. Lukanidin (1998). "Metastasis-associated Mts1 (S100A4) protein modulates protein kinase C phosphorylation of the heavy chain of nonmuscle myosin." J Biol Chem **273**(16): 9852-9856.

Kriajevska, M. V., M. N. Cardenas, M. S. Grigorian, N. S. Ambartsumian, G. P. Georgiev and E. M. Lukanidin (1994). "Non-muscle myosin heavy chain as a possible target for protein encoded by metastasis-related mts-1 gene." J Biol Chem **269**(31): 19679-19682.

Kriajevska, M. V., L. G. Zakharova and A. D. Altstein (1994). "Genetic instability of vaccinia virus containing artificially duplicated genome regions." Virus Res **31**(1): 123-137.

Krop, I., A. Marz, H. Carlsson, X. Li, N. Bloushtain-Qimron, M. Hu, R. Gelman, M. S. Sabel, S. Schnitt, S. Ramaswamy, C. G. Kleer, C. Enerback and K. Polyak (2005). "A putative role for psoriasin in breast tumor progression." Cancer Res **65**(24): 11326-11334.

Kulski, J. K., C. P. Lim, D. S. Dunn and M. Bellgard (2003). "Genomic and phylogenetic analysis of the S100A7 (Psoriasin) gene duplications within the

region of the S100 gene cluster on human chromosome 1q21." J Mol Evol **56**(4): 397-406.

Lamartina, S., L. Silvi, G. Roscilli, D. Casimiro, A. J. Simon, M. E. Davies, J. W. Shiver, C. D. Rinaudo, I. Zampaglione, E. Fattori, S. Colloca, O. Gonzalez Paz, R. Laufer, H. Bujard, R. Cortese, G. Ciliberto and C. Toniatti (2003). "Construction of an rtTA2(s)-m2/tts(kid)-based transcription regulatory switch that displays no basal activity, good inducibility, and high responsiveness to doxycycline in mice and non-human primates." Mol Ther **7**(2): 271-280.

Landriscina, M., R. Soldi, C. Bagala, I. Micucci, S. Bellum, F. Tarantini, I. Prudovsky and T. Maciag (2001). "S100A13 participates in the release of fibroblast growth factor 1 in response to heat shock in vitro." J Biol Chem **276**(25): 22544-22552.

Lau, W., J. M. Devery and C. L. Geczy (1995). "A chemotactic S100 peptide enhances scavenger receptor and Mac-1 expression and cholesteryl ester accumulation in murine peritoneal macrophages in vivo." J Clin Invest **95**(5): 1957-1965.

Leclerc, E., G. Fritz, M. Weibel, C. W. Heizmann and A. Galichet (2007). "S100B and S100A6 differentially modulate cell survival by interacting with distinct RAGE (receptor for advanced glycation end products) immunoglobulin domains." J Biol Chem **282**(43): 31317-31331.

Lee, Y. C., D. E. Volk, V. Thiviyanathan, Q. Kleerekoper, A. V. Gribenko, S. Zhang, D. G. Gorenstein, G. I. Makhatadze and B. A. Luxon (2004). "NMR structure of the Apo-S100P protein." J Biomol NMR **29**(3): 399-402.

Leygue, E., L. Snell, T. Hiller, H. Dotzlaw, K. Hole, L. C. Murphy and P. H. Watson (1996). "Differential expression of psoriasin messenger RNA between in situ and invasive human breast carcinoma." Cancer Res **56**(20): 4606-4609.

Li, C. L., V. Martinez, B. He, A. Lombet and B. Perbal (2002). "A role for CCN3 (NOV) in calcium signalling." Mol Pathol **55**(4): 250-261.

Liang, J., G. Luo, X. Ning, Y. Shi, H. Zhai, S. Sun, H. Jin, Z. Liu, F. Zhang, Y. Lu, Y. Zhao, X. Chen, H. Zhang, X. Guo, K. Wu and D. Fan (2007). "Differential expression of calcium-related genes in gastric cancer cells transfected with cellular prion protein." Biochem Cell Biol **85**(3): 375-383.

Logsdon, C. D., D. M. Simeone, C. Binkley, T. Arumugam, J. K. Greenson, T. J. Giordano, D. E. Misek, R. Kuick and S. Hanash (2003). "Molecular profiling

of pancreatic adenocarcinoma and chronic pancreatitis identifies multiple genes differentially regulated in pancreatic cancer." Cancer Res **63**(10): 2649-2657.

Mackay, A., C. Jones, T. Dexter, R. L. Silva, K. Bulmer, A. Jones, P. Simpson, R. A. Harris, P. S. Jat, A. M. Neville, L. F. Reis, S. R. Lakhani and M. J. O'Hare (2003). "cDNA microarray analysis of genes associated with ERBB2 (HER2/neu) overexpression in human mammary luminal epithelial cells." Oncogene **22**(17): 2680-2688.

Maddox, P. H. and D. Jenkins (1987). "3-Aminopropyltriethoxysilane (APES): a new advance in section adhesion." J Clin Pathol **40**(10): 1256-1257.

Madsen, P., H. H. Rasmussen, H. Leffers, B. Honore, K. Dejgaard, E. Olsen, J. Kiil, E. Walbum, A. H. Andersen, B. Basse and et al. (1991). "Molecular cloning, occurrence, and expression of a novel partially secreted protein "psoriasin" that is highly up-regulated in psoriatic skin." J Invest Dermatol **97**(4): 701-712.

Maelandsmo, G. M., V. A. Florenes, M. T. Nguyen, K. Flatmark and B. Davidson (2009). "Different expression and clinical role of S100A4 in serous ovarian carcinoma at different anatomic sites." Tumour Biol **30**(1): 15-25.

Maelandsmo, G. M., E. Hovig, M. Skrede, O. Engebraaten, V. A. Florenes, O. Myklebost, M. Grigorian, E. Lukanidin, K. J. Scanlon and O. Fodstad (1996). "Reversal of the in vivo metastatic phenotype of human tumor cells by an anti-CAPL (mts1) ribozyme." Cancer Res **56**(23): 5490-5498.

Malashkevich, V. N., K. M. Varney, S. C. Garrett, P. T. Wilder, D. Knight, T. H. Charpentier, U. A. Ramagopal, S. C. Almo, D. J. Weber and A. R. Bresnick (2008). "Structure of Ca2+-bound S100A4 and its interaction with peptides derived from nonmuscle myosin-IIA." Biochemistry **47**(18): 5111-5126.

Mandinova, A., D. Atar, B. W. Schafer, M. Spiess, U. Aebi and C. W. Heizmann (1998). "Distinct subcellular localization of calcium binding S100 proteins in human smooth muscle cells and their relocation in response to rises in intracellular calcium." J Cell Sci **111 (Pt 14)**: 2043-2054.

Mandinova, A., R. Soldi, I. Graziani, C. Bagala, S. Bellum, M. Landriscina, F. Tarantini, I. Prudovsky and T. Maciag (2003). "S100A13 mediates the copper-dependent stress-induced release of IL-1alpha from both human U937 and murine NIH 3T3 cells." J Cell Sci **116**(Pt 13): 2687-2696.

Marty, B., V. Maire, E. Gravier, G. Rigaill, A. Vincent-Salomon, M. Kappler, I. Lebigot, F. Djelti, A. Tourdes, P. Gestraud, P. Hupe, E. Barillot, F. Cruzalegui, G. C. Tucker, M. H. Stern, J. P. Thiery, J. A. Hickman and T. Dubois (2008). "Frequent PTEN genomic alterations and activated phosphatidylinositol 3-kinase pathway in basal-like breast cancer cells." Breast Cancer Res **10**(6): R101.

Matsunaga, H. and H. Ueda (2008). "Synergistic Ca2+ and Cu2+ requirements of the FGF1-S100A13 interaction measured by quartz crystal microbalance: an initial step in amlexanox-reversible non-classical release of FGF1." Neurochem Int **52**(6): 1076-1085.

Matsunaga, H. and H. Ueda (2010). "Stress-induced non-vesicular release of prothymosin-alpha initiated by an interaction with S100A13, and its blockade by caspase-3 cleavage." Cell Death Differ.

McLellan, M. R. and J. G. Day (1995). "Cryopreservation and freeze-drying protocols. Introduction." Methods Mol Biol **38**: 1-5.

Mermelshtein, A., A. Gerson, S. Walfisch, B. Delgado, G. Shechter-Maor, J. Delgado, A. Fich and L. Gheber (2005). "Expression of D-type cyclins in colon cancer and in cell lines from colon carcinomas." Br J Cancer **93**(3): 338-345.

Meyer-Ficca, M. L., R. G. Meyer, H. Kaiser, A. R. Brack, R. Kandolf and J. H. Kupper (2004). "Comparative analysis of inducible expression systems in transient transfection studies." Anal Biochem **334**(1): 9-19.

Mhawech-Fauceglia, P., D. J. Smiraglia, W. Bshara, C. Andrews, J. Schwaller, S. South, D. Higgs, S. Lele, F. Herrmann and K. Odunsi (2008). "Prostate-specific membrane antigen expression is a potential prognostic marker in endometrial adenocarcinoma." Cancer Epidemiol Biomarkers Prev **17**(3): 571-577.

Missiaglia, E., E. Blaveri, B. Terris, Y. H. Wang, E. Costello, J. P. Neoptolemos, T. Crnogorac-Jurcevic and N. R. Lemoine (2004). "Analysis of gene expression in cancer cell lines identifies candidate markers for pancreatic tumorigenesis and metastasis." Int J Cancer **112**(1): 100-112.

Mitsiades, C. S., N. Mitsiades and M. Koutsilieris (2004). "The Akt pathway: molecular targets for anti-cancer drug development." Curr Cancer Drug Targets **4**(3): 235-256.

Moog-Lutz, C., P. Bouillet, C. H. Regnier, C. Tomasetto, M. G. Mattei, M. P. Chenard, P. Anglard, M. C. Rio and P. Basset (1995). "Comparative expression of the psoriasin (S100A7) and S100C genes in breast carcinoma and co-localization to human chromosome 1q21-q22." Int J Cancer **63**(2): 297-303.

Moore, B. W. (1965). "A soluble protein characteristic of the nervous system." Biochem Biophys Res Commun **19**(6): 739-744.

Morgan, D. O. (1997). "Cyclin-dependent kinases: engines, clocks, and microprocessors." Annu Rev Cell Dev Biol **13**: 261-291.

Mousses, S., L. Bubendorf, U. Wagner, G. Hostetter, J. Kononen, R. Cornelison, N. Goldberger, A. G. Elkahloun, N. Willi, P. Koivisto, W. Ferhle, M. Raffeld, G. Sauter and O. P. Kallioniemi (2002). "Clinical validation of candidate genes associated with prostate cancer progression in the CWR22 model system using tissue microarrays." Cancer Res **62**(5): 1256-1260.

Murphy, G. P., T. G. Greene, W. T. Tino, A. L. Boynton and E. H. Holmes (1998). "Isolation and characterization of monoclonal antibodies specific for the extracellular domain of prostate specific membrane antigen." J Urol **160**(6 Pt 2): 2396-2401.

Nakata, K., E. Nagai, K. Ohuchida, A. Hayashi, Y. Miyasaka, S. Aishima, Y. Oda, K. Mizumoto, M. Tanaka and M. Tsuneyoshi (2010). "S100P is a novel marker to identify intraductal papillary mucinous neoplasms." Hum Pathol **41**(6): 824-831.

Neeper, M., A. M. Schmidt, J. Brett, S. D. Yan, F. Wang, Y. C. Pan, K. Elliston, D. Stern and A. Shaw (1992). "Cloning and expression of a cell surface receptor for advanced glycosylation end products of proteins." J Biol Chem **267**(21): 14998-15004.

Nelson, M. L. (1998). "Chemical and biological dynamics of tetracyclines." Adv Dent Res **12**(2): 5-11.

Ninomiya, I., T. Ohta, S. Fushida, Y. Endo, T. Hashimoto, M. Yagi, T. Fujimura, G. Nishimura, T. Tani, K. Shimizu, Y. Yonemura, C. W. Heizmann, B. W. Schafer, T. Sasaki and K. Miwa (2001). "Increased expression of S100A4 and its prognostic significance in esophageal squamous cell carcinoma." Int J Oncol **18**(4): 715-720.

Noss, K. R., R. Singal and S. R. Grimes (2002). "Methylation state of the prostate specific membrane antigen (PSMA) CpG island in prostate cancer cell lines." Anticancer Res **22**(3): 1505-1511.

Novitskaya, V., M. Grigorian, M. Kriajevska, S. Tarabykina, I. Bronstein, V. Berezin, E. Bock and E. Lukanidin (2000). "Oligomeric forms of the metastasis-related Mts1 (S100A4) protein stimulate neuronal differentiation in cultures of rat hippocampal neurons." J Biol Chem **275**(52): 41278-41286.

O'Connor, T., L. S. Ireland, D. J. Harrison and J. D. Hayes (1999). "Major differences exist in the function and tissue-specific expression of human aflatoxin B1 aldehyde reductase and the principal human aldo-keto reductase AKR1 family members." Biochem J **343 Pt 2**: 487-504.

Ohuchida, K., K. Mizumoto, T. Egami, H. Yamaguchi, K. Fujii, H. Konomi, E. Nagai, K. Yamaguchi, M. Tsuneyoshi and M. Tanaka (2006). "S100P is an early developmental marker of pancreatic carcinogenesis." Clin Cancer Res **12**(18): 5411-5416.

Okada, M., H. Tokumitsu, Y. Kubota and R. Kobayashi (2002). "Interaction of S100 proteins with the antiallergic drugs, olopatadine, amlexanox, and cromolyn: identification of putative drug binding sites on S100A1 protein." Biochem Biophys Res Commun **292**(4): 1023-1030.

Onoda, T., T. Ono, D. K. Dhar, A. Yamanoi and N. Nagasue (2006). "Tetracycline analogues (doxycycline and COL-3) induce caspase-dependent and -independent apoptosis in human colon cancer cells." Int J Cancer **118**(5): 1309-1315.

Oyama, Y., T. Shishibori, K. Yamashita, T. Naya, S. Nakagiri, H. Maeta and R. Kobayashi (1997). "Two distinct anti-allergic drugs, amlexanox and cromolyn, bind to the same kinds of calcium binding proteins, except calmodulin, in bovine lung extract." Biochem Biophys Res Commun **240**(2): 341-347.

Pang, L., T. Sawada, S. J. Decker and A. R. Saltiel (1995). "Inhibition of MAP kinase kinase blocks the differentiation of PC-12 cells induced by nerve growth factor." J Biol Chem **270**(23): 13585-13588.

Park, I. H., S. I. Yeon, J. H. Youn, J. E. Choi, N. Sasaki, I. H. Choi and J. S. Shin (2004). "Expression of a novel secreted splice variant of the receptor for advanced

glycation end products (RAGE) in human brain astrocytes and peripheral blood mononuclear cells." Mol Immunol **40**(16): 1203-1211.

Parkkila, S. (2008). "Significance of pH regulation and carbonic anhydrases in tumour progression and implications for diagnostic and therapeutic approaches." BJU Int **101 Suppl 4**: 16-21.

Parkkila, S., P. W. Pan, A. Ward, A. Gibadulinova, I. Oveckova, S. Pastorekova, J. Pastorek, A. R. Martinez, H. O. Helin and J. Isola (2008). "The calcium-binding protein S100P in normal and malignant human tissues." BMC Clin Pathol **8**: 2.

Perner, S., M. D. Hofer, R. Kim, R. B. Shah, H. Li, P. Moller, R. E. Hautmann, J. E. Gschwend, R. Kuefer and M. A. Rubin (2007). "Prostate-specific membrane antigen expression as a predictor of prostate cancer progression." Hum Pathol **38**(5): 696-701.

Pham, D. H., P. A. Moretti, G. J. Goodall and S. M. Pitson (2008). "Attenuation of leakiness in doxycycline-inducible expression via incorporation of 3' AU-rich mRNA destabilizing elements." Biotechniques **45**(2): 155-156, 158, 160 passim.

Pinto, J. T., B. P. Suffoletto, T. M. Berzin, C. H. Qiao, S. Lin, W. P. Tong, F. May, B. Mukherjee and W. D. Heston (1996). "Prostate-specific membrane antigen: a novel folate hydrolase in human prostatic carcinoma cells." Clin Cancer Res **2**(9): 1445-1451.

Platt-Higgins, A. M., C. A. Renshaw, C. R. West, J. H. Winstanley, S. De Silva Rudland, R. Barraclough and P. S. Rudland (2000). "Comparison of the metastasis-inducing protein S100A4 (p9ka) with other prognostic markers in human breast cancer." Int J Cancer **89**(2): 198-208.

Powis, G., R. Bonjouklian, M. M. Berggren, A. Gallegos, R. Abraham, C. Ashendel, L. Zalkow, W. F. Matter, J. Dodge, G. Grindey and et al. (1994). "Wortmannin, a potent and selective inhibitor of phosphatidylinositol-3-kinase." Cancer Res **54**(9): 2419-2423.

Ravasi, T., K. Hsu, J. Goyette, K. Schroder, Z. Yang, F. Rahimi, L. P. Miranda, P. F. Alewood, D. A. Hume and C. Geczy (2004). "Probing the S100 protein family through genomic and functional analysis." Genomics **84**(1): 10-22.

Rehbein, G., A. Simm, H. S. Hofmann, R. E. Silber and B. Bartling (2008). "Molecular regulation of S100P in human lung adenocarcinomas." Int J Mol Med **22**(1): 69-77.

Reszka, A. A., R. Seger, C. D. Diltz, E. G. Krebs and E. H. Fischer (1995). "Association of mitogen-activated protein kinase with the microtubule cytoskeleton." Proc Natl Acad Sci U S A **92**(19): 8881-8885.

Richter, H., P. Slezak, A. Walch, M. Werner, H. Braselmann, E. Jaramillo, A. Ost, I. Hirata, K. Takahama and H. Zitzelsberger (2003). "Distinct chromosomal imbalances in nonpolypoid and polypoid colorectal adenomas indicate different genetic pathways in the development of colorectal neoplasms." Am J Pathol **163**(1): 287-294.

Rodriguez, O. C., A. W. Schaefer, C. A. Mandato, P. Forscher, W. M. Bement and C. M. Waterman-Storer (2003). "Conserved microtubule-actin interactions in cell movement and morphogenesis." Nat Cell Biol **5**(7): 599-609.

Rosty, C., T. Ueki, P. Argani, M. Jansen, C. J. Yeo, J. L. Cameron, R. H. Hruban and M. Goggins (2002). "Overexpression of S100A4 in pancreatic ductal adenocarcinomas is associated with poor differentiation and DNA hypomethylation." Am J Pathol **160**(1): 45-50.

Rudland, P. S., C. M. Hughes, S. A. Ferns and M. J. Warburton (1989). "Characterization of human mammary cell types in primary culture: immunofluorescent and immunocytochemical indicators of cellular heterogeneity." In Vitro Cell Dev Biol **25**(1): 23-36.

Rudland, P. S., A. Platt-Higgins, M. El-Tanani, S. De Silva Rudland, R. Barraclough, J. H. Winstanley, R. Howitt and C. R. West (2002). "Prognostic significance of the metastasis-associated protein osteopontin in human breast cancer." Cancer Res **62**(12): 3417-3427.

Rudland, P. S., A. Platt-Higgins, C. Renshaw, C. R. West, J. H. Winstanley, L. Robertson and R. Barraclough (2000). "Prognostic significance of the metastasis-inducing protein S100A4 (p9Ka) in human breast cancer." Cancer Res **60**(6): 1595-1603.

Ryckman, C., K. Vandal, P. Rouleau, M. Talbot and P. A. Tessier (2003). "Proinflammatory activities of S100: proteins S100A8, S100A9, and S100A8/A9 induce neutrophil chemotaxis and adhesion." J Immunol **170**(6): 3233-3242.

Saal, L. H., P. Johansson, K. Holm, S. K. Gruvberger-Saal, Q. B. She, M. Maurer, S. Koujak, A. A. Ferrando, P. Malmstrom, L. Memeo, J. Isola, P. O. Bendahl, N. Rosen, H. Hibshoosh, M. Ringner, A. Borg and R. Parsons (2007). "Poor prognosis in carcinoma is associated with a gene expression signature of aberrant PTEN tumor suppressor pathway activity." Proc Natl Acad Sci U S A **104**(18): 7564-7569.

Sakaguchi, M., M. Miyazaki, Y. Inoue, T. Tsuji, H. Kouchi, T. Tanaka, H. Yamada and M. Namba (2000). "Relationship between contact inhibition and intranuclear S100C of normal human fibroblasts." J Cell Biol **149**(6): 1193-1206.

Sakaushi, S., K. Inoue, H. Zushi, K. Senda-Murata, T. Fukada, S. Oka and K. Sugimoto (2007). "Dynamic behavior of FCHO1 revealed by live-cell imaging microscopy: its possible involvement in clathrin-coated vesicle formation." Biosci Biotechnol Biochem **71**(7): 1764-1768.

Salama, I., P. S. Malone, F. Mihaimeed and J. L. Jones (2008). "A review of the S100 proteins in cancer." Eur J Surg Oncol **34**(4): 357-364.

Saleem, M., V. M. Adhami, N. Ahmad, S. Gupta and H. Mukhtar (2005). "Prognostic significance of metastasis-associated protein S100A4 (Mts1) in prostate cancer progression and chemoprevention regimens in an autochthonous mouse model." Clin Cancer Res **11**(1): 147-153.

Sambrook, J. and D. W. Russell (2001). Molecular cloning : a laboratory manual. Cold Spring Harbor, N.Y., Cold Spring Harbor Laboratory Press.

Santamaria-Kisiel, L., A. C. Rintala-Dempsey and G. S. Shaw (2006). "Calcium-dependent and -independent interactions of the S100 protein family." Biochem J **396**(2): 201-214.

Sato, N., N. Fukushima, H. Matsubayashi and M. Goggins (2004). "Identification of maspin and S100P as novel hypomethylation targets in pancreatic cancer using global gene expression profiling." Oncogene **23**(8): 1531-1538.

Sato, N. and J. Hitomi (2002). "S100P expression in human esophageal epithelial cells: Human esophageal epithelial cells sequentially produce different S100 proteins in the process of differentiation." Anat Rec **267**(1): 60-69.

Sato, N., T. Ueki, N. Fukushima, C. A. Iacobuzio-Donahue, C. J. Yeo, J. L. Cameron, R. H. Hruban and M. Goggins (2002). "Aberrant methylation of CpG islands in intraductal papillary mucinous neoplasms of the pancreas." Gastroenterology **123**(1): 365-372.

Schafer, B. W. and C. W. Heizmann (1996). "The S100 family of EF-hand calcium-binding proteins: functions and pathology." Trends Biochem Sci **21**(4): 134-140.

Schaller, M., M. Schaffhauser, N. Sans and B. Wermuth (1999). "Cloning and expression of succinic semialdehyde reductase from human brain. Identity with aflatoxin B1 aldehyde reductase." Eur J Biochem **265**(3): 1056-1060.

Scherer, W. F., J. T. Syverton and G. O. Gey (1953). "Studies on the propagation in vitro of poliomyelitis viruses. IV. Viral multiplication in a stable strain of human malignant epithelial cells (strain HeLa) derived from an epidermoid carcinoma of the cervix." J Exp Med **97**(5): 695-710.

Schmidt, A. M., S. D. Yan, S. F. Yan and D. M. Stern (2001). "The multiligand receptor RAGE as a progression factor amplifying immune and inflammatory responses." J Clin Invest **108**(7): 949-955.

Schmidt-Hansen, B., D. Ornas, M. Grigorian, J. Klingelhofer, E. Tulchinsky, E. Lukanidin and N. Ambartsumian (2004). "Extracellular S100A4(mts1) stimulates invasive growth of mouse endothelial cells and modulates MMP-13 matrix metalloproteinase activity." Oncogene **23**(32): 5487-5495.

Schor, A. P., F. M. Carvalho, C. Kemp, I. D. Silva and J. Russo (2006). "S100P calcium-binding protein expression is associated with high-risk proliferative lesions of the breast." Oncol Rep **15**(1): 3-6.

Schultz, E. S., T. L. Diepgen and P. Von Den Driesch (1998). "Clinical and prognostic relevance of serum S-100 beta protein in malignant melanoma." Br J Dermatol **138**(3): 426-430.

Shishibori, T., Y. Oyama, O. Matsushita, K. Yamashita, H. Furuichi, A. Okabe, H. Maeta, Y. Hata and R. Kobayashi (1999). "Three distinct anti-allergic drugs, amlexanox, cromolyn and tranilast, bind to S100A12 and S100A13 of the S100 protein family." Biochem J **338 (Pt 3)**: 583-589.

Shyu, R. Y., S. L. Huang and S. Y. Jiang (2003). "Retinoic acid increases expression of the calcium-binding protein S100P in human gastric cancer cells." J Biomed Sci **10**(3): 313-319.

Sinclair, A. J., I. Palmero, G. Peters and P. J. Farrell (1994). "EBNA-2 and EBNA-LP cooperate to cause G0 to G1 transition during immortalization of resting human B lymphocytes by Epstein-Barr virus." EMBO J **13**(14): 3321-3328.

Slamon, D. J., G. M. Clark, S. G. Wong, W. J. Levin, A. Ullrich and W. L. McGuire (1987). "Human breast cancer: correlation of relapse and survival with amplification of the HER-2/neu oncogene." Science **235**(4785): 177-182.

Sorci, G., A. L. Agneletti and R. Donato (2000). "Effects of S100A1 and S100B on microtubule stability. An in vitro study using triton-cytoskeletons from astrocyte and myoblast cell lines." Neuroscience **99**(4): 773-783.

Sourdeval, M., C. Lemaire, C. Brenner, E. Boisvieux-Ulrich and F. Marano (2006). "Mechanisms of doxycycline-induced cytotoxicity on human bronchial epithelial cells." Front Biosci **11**: 3036-3048.

Staal, S. P., J. W. Hartley and W. P. Rowe (1977). "Isolation of transforming murine leukemia viruses from mice with a high incidence of spontaneous lymphoma." Proc Natl Acad Sci U S A **74**(7): 3065-3067.

Stiles, B., V. Gilman, N. Khanzenzon, R. Lesche, A. Li, R. Qiao, X. Liu and H. Wu (2002). "Essential role of AKT-1/protein kinase B alpha in PTEN-controlled tumorigenesis." Mol Cell Biol **22**(11): 3842-3851.

Storey, J. D. and R. Tibshirani (2003). "Statistical methods for identifying differentially expressed genes in DNA microarrays." Methods Mol Biol **224**: 149-157.

Strynadka, N. C. and M. N. James (1989). "Crystal structures of the helix-loop-helix calcium-binding proteins." Annu Rev Biochem **58**: 951-998.

Surowiak, P., A. Maciejczyk, V. Materna, M. Drag-Zalesinska, A. Wojnar, M. Pudelko, W. Kedzia, M. Spaczynski, M. Dietel, M. Zabel and H. Lage (2007). "Unfavourable prognostic significance of S100P expression in ovarian cancers." Histopathology **51**(1): 125-128.

Sweat, S. D., A. Pacelli, G. P. Murphy and D. G. Bostwick (1998). "Prostate-specific membrane antigen expression is greatest in prostate adenocarcinoma and lymph node metastases." Urology **52**(4): 637-640.

Takano, Y., Y. Kato, M. Masuda, Y. Ohshima and I. Okayasu (1999). "Cyclin D2, but not cyclin D1, overexpression closely correlates with gastric cancer progression and prognosis." J Pathol **189**(2): 194-200.

Takenaga, K., Y. Nakamura, H. Endo and S. Sakiyama (1994). "Involvement of S100-related calcium-binding protein pEL98 (or mts1) in cell motility and tumor cell invasion." Jpn J Cancer Res **85**(8): 831-839.

Takenaga, K., Y. Nakamura, S. Sakiyama, Y. Hasegawa, K. Sato and H. Endo (1994). "Binding of pEL98 protein, an S100-related calcium-binding protein, to nonmuscle tropomyosin." J Cell Biol **124**(5): 757-768.

Tarabykina, S., M. Kriajevska, D. J. Scott, T. J. Hill, D. Lafitte, P. J. Derrick, G. G. Dodson, E. Lukanidin and I. Bronstein (2000). "Heterocomplex formation between metastasis-related protein S100A4 (Mts1) and S100A1 as revealed by the yeast two-hybrid system." FEBS Lett **475**(3): 187-191.

Tokunaga, E., E. Oki, Y. Kimura, T. Yamanaka, A. Egashira, K. Nishida, T. Koga, M. Morita, Y. Kakeji and Y. Maehara (2007). "Coexistence of the loss of heterozygosity at the PTEN locus and HER2 overexpression enhances the Akt activity thus leading to a negative progesterone receptor expression in breast carcinoma." Breast Cancer Res Treat **101**(3): 249-257.

Tong, X. M., X. N. Lin, T. Song, L. Liu and S. Y. Zhang (2010). "Calcium-binding protein S100P is highly expressed during the implantation window in human endometrium." Fertil Steril **94**(4): 1510-1518.

Tripathi, S. C., A. Matta, J. Kaur, J. Grigull, S. S. Chauhan, A. Thakar, N. K. Shukla, R. Duggal, S. DattaGupta, R. Ralhan and K. W. Siu (2010). "Nuclear S100A7 is associated with poor prognosis in head and neck cancer." PLoS One **5**(8): e11939.

Tsuneoka, M., Y. Koda, M. Soejima, K. Teye and H. Kimura (2002). "A novel myc target gene, mina53, that is involved in cell proliferation." J Biol Chem **277**(38): 35450-35459.

Valiente, M., A. Andres-Pons, B. Gomar, J. Torres, A. Gil, C. Tapparel, S. E. Antonarakis and R. Pulido (2005). "Binding of PTEN to specific PDZ domains contributes to PTEN protein stability and phosphorylation by microtubule-associated serine/threonine kinases." J Biol Chem **280**(32): 28936-28943.

van Dieck, J., M. R. Fernandez-Fernandez, D. B. Veprintsev and A. R. Fersht (2009). "Modulation of the oligomerization state of p53 by differential binding of proteins of the S100 family to p53 monomers and tetramers." J Biol Chem **284**(20): 13804-13811.

Vlahos, C. J., W. F. Matter, K. Y. Hui and R. F. Brown (1994). "A specific inhibitor of phosphatidylinositol 3-kinase, 2-(4-morpholinyl)-8-phenyl-4H-1-benzopyran-4-one (LY294002)." J Biol Chem **269**(7): 5241-5248.

von Schoultz, E., L. O. Hansson, E. Djureen, J. Hansson, R. Karnell, B. Nilsson, T. Stigbrand and U. Ringborg (1996). "Prognostic value of serum analyses of S-100 beta protein in malignant melanoma." Melanoma Res **6**(2): 133-137.

Walden, P. D. and N. J. Cowan (1993). "A novel 205-kilodalton testis-specific serine/threonine protein kinase associated with microtubules of the spermatid manchette." Mol Cell Biol **13**(12): 7625-7635.

Wang, F. S., C. J. Wang, Y. J. Chen, P. R. Chang, Y. T. Huang, Y. C. Sun, H. C. Huang, Y. J. Yang and K. D. Yang (2004). "Ras induction of superoxide activates ERK-dependent angiogenic transcription factor HIF-1alpha and VEGF-A expression in shock wave-stimulated osteoblasts." J Biol Chem **279**(11): 10331-10337.

Wang, G., A. Platt-Higgins, J. Carroll, S. de Silva Rudland, J. Winstanley, R. Barraclough and P. S. Rudland (2006). "Induction of metastasis by S100P in a rat mammary model and its association with poor survival of breast cancer patients." Cancer Res **66**(2): 1199-1207.

Wang, G., P. S. Rudland, M. R. White and R. Barraclough (2000). "Interaction in vivo and in vitro of the metastasis-inducing S100 protein, S100A4 (p9Ka) with S100A1." J Biol Chem **275**(15): 11141-11146.

Wang, G., S. Zhang, D. G. Fernig, D. Spiller, M. Martin-Fernandez, H. Zhang, Y. Ding, Z. Rao, P. S. Rudland and R. Barraclough (2004). "Heterodimeric interaction and interfaces of S100A1 and S100P." Biochem J **382**(Pt 1): 375-383.

Wang, Q., M. Williamson, S. Bott, N. Brookman-Amissah, A. Freeman, J. Nariculam, M. J. Hubank, A. Ahmed and J. R. Masters (2007). "Hypomethylation of WNT5A, CRIP1 and S100P in prostate cancer." Oncogene **26**(45): 6560-6565.

Wang, W., J. L. Abbruzzese, D. B. Evans, L. Larry, K. R. Cleary and P. J. Chiao (1999). "The nuclear factor-kappa B RelA transcription factor is constitutively activated in human pancreatic adenocarcinoma cells." Clin Cancer Res **5**(1): 119-127.

Warburton, M. J., S. A. Ferns and P. S. Rudland (1982). "Enhanced synthesis of basement membrane proteins during the differentiation of rat mammary tumour epithelial cells into myoepithelial-like cells in vitro." Exp Cell Res **137**(2): 373-380.

Warburton, M. J., D. Mitchell, E. J. Ormerod and P. Rudland (1982). "Distribution of myoepithelial cells and basement membrane proteins in the resting,

pregnant, lactating, and involuting rat mammary gland." J Histochem Cytochem **30**(7): 667-676.

Wettenhall, J. M. and G. K. Smyth (2004). "limmaGUI: a graphical user interface for linear modeling of microarray data." Bioinformatics **20**(18): 3705-3706.

Whiteman, H. J., M. E. Weeks, S. E. Dowen, S. Barry, J. F. Timms, N. R. Lemoine and T. Crnogorac-Jurcevic (2007). "The role of S100P in the invasion of pancreatic cancer cells is mediated through cytoskeletal changes and regulation of cathepsin D." Cancer Res **67**(18): 8633-8642.

Wolf, R., O. M. Howard, H. F. Dong, C. Voscopoulos, K. Boeshans, J. Winston, R. Divi, M. Gunsior, P. Goldsmith, B. Ahvazi, T. Chavakis, J. J. Oppenheim and S. H. Yuspa (2008). "Chemotactic activity of S100A7 (Psoriasin) is mediated by the receptor for advanced glycation end products and potentiates inflammation with highly homologous but functionally distinct S100A15." J Immunol **181**(2): 1499-1506.

Wolf, R., A. Mirmohammadsadegh, M. Walz, B. Lysa, U. Tartler, R. Remus, U. Hengge, G. Michel and T. Ruzicka (2003). "Molecular cloning and characterization of alternatively spliced mRNA isoforms from psoriatic skin encoding a novel member of the S100 family." FASEB J **17**(13): 1969-1971.

Wozney, J. M., V. Rosen, A. J. Celeste, L. M. Mitsock, M. J. Whitters, R. W. Kriz, R. M. Hewick and E. A. Wang (1988). "Novel regulators of bone formation: molecular clones and activities." Science **242**(4885): 1528-1534.

Wu, J., C. Lee, D. Yokom, H. Jiang, M. C. Cheang, E. Yorida, D. Turbin, I. M. Berquin, P. R. Mertens, T. Iftner, C. B. Gilks and S. E. Dunn (2006). "Disruption of the Y-box binding protein-1 results in suppression of the epidermal growth factor receptor and HER-2." Cancer Res **66**(9): 4872-4879.

Wyckoff, J. B., J. G. Jones, J. S. Condeelis and J. E. Segall (2000). "A critical step in metastasis: in vivo analysis of intravasation at the primary tumor." Cancer Res **60**(9): 2504-2511.

Yammani, R. R., C. S. Carlson, A. R. Bresnick and R. F. Loeser (2006). "Increase in production of matrix metalloproteinase 13 by human articular chondrocytes due to stimulation with S100A4: Role of the receptor for advanced glycation end products." Arthritis Rheum **54**(9): 2901-2911.

Yano, R., C. C. Yap, Y. Yamazaki, Y. Muto, H. Kishida, D. Okada and T. Hashikawa (2003). "Sast124, a novel splice variant of syntrophin-associated serine/

threonine kinase (SAST), is specifically localized in the restricted brain regions." Neuroscience **117**(2): 373-381.

Yen, T., C. A. Harrison, J. M. Devery, S. Leong, S. E. Iismaa, T. Yoshimura and C. L. Geczy (1997). "Induction of the S100 chemotactic protein, CP-10, in murine microvascular endothelial cells by proinflammatory stimuli." Blood **90**(12): 4812-4821.

Yonekura, H., Y. Yamamoto, S. Sakurai, R. G. Petrova, M. J. Abedin, H. Li, K. Yasui, M. Takeuchi, Z. Makita, S. Takasawa, H. Okamoto, T. Watanabe and H. Yamamoto (2003). "Novel splice variants of the receptor for advanced glycation end-products expressed in human vascular endothelial cells and pericytes, and their putative roles in diabetes-induced vascular injury." Biochem J **370**(Pt 3): 1097-1109.

Yonemura, Y., Y. Endou, K. Kimura, S. Fushida, E. Bandou, K. Taniguchi, K. Kinoshita, I. Ninomiya, K. Sugiyama, C. W. Heizmann, B. W. Schafer and T. Sasaki (2000). "Inverse expression of S100A4 and E-cadherin is associated with metastatic potential in gastric cancer." Clin Cancer Res **6**(11): 4234-4242.

Yoon, S. and R. Seger (2006). "The extracellular signal-regulated kinase: multiple substrates regulate diverse cellular functions." Growth Factors **24**(1): 21-44.

Zhang, H., G. Wang, Y. Ding, Z. Wang, R. Barraclough, P. S. Rudland, D. G. Fernig and Z. Rao (2003). "The crystal structure at 2A resolution of the Ca2+ - binding protein S100P." J Mol Biol **325**(4): 785-794.

Zhao, J., X. Yuan, M. Frodin and I. Grummt (2003). "ERK-dependent phosphorylation of the transcription initiation factor TIF-IA is required for RNA polymerase I transcription and cell growth." Mol Cell **11**(2): 405-413.

Zhou, Y., W. Yang, M. Kirberger, H. W. Lee, G. Ayalasomayajula and J. J. Yang (2006). "Prediction of EF-hand calcium-binding proteins and analysis of bacterial EF-hand proteins." Proteins **65**(3): 643-655.

Zimmer, D. B., E. H. Cornwall, P. D. Reynolds and C. M. Donald (1998). "S100A1 regulates neurite organization, tubulin levels, and proliferation in PC12 cells." J Biol Chem **273**(8): 4705-4711.

Zou, M., K. S. Famulski, R. S. Parhar, E. Baitei, F. A. Al-Mohanna, N. R. Farid and Y. Shi (2004). "Microarray analysis of metastasis-associated gene expression profiling in a murine model of thyroid carcinoma pulmonary metastasis: